

## Transition-Metal-Catalyzed Silylation and Borylation of C–H Bonds for the Synthesis and Functionalization of Complex Molecules

Published as part of the Chemical Reviews *virtual special issue* “Remote and Late Stage Functionalization”.

Isaac F. Yu, Jake W. Wilson, and John F. Hartwig\*



Cite This: <https://doi.org/10.1021/acs.chemrev.3c00207>



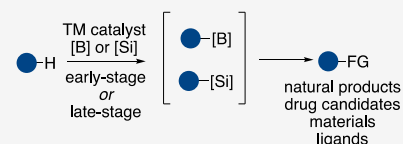
Read Online

ACCESS |

Metrics & More

Article Recommendations

**ABSTRACT:** The functionalization of C–H bonds in organic molecules containing functional groups has been one of the holy grails of catalysis. One synthetically important approach to the diverse functionalization of C–H bonds is the catalytic silylation or borylation of C–H bonds, which enables a broad array of downstream transformations to afford diverse structures. Advances in both undirected and directed methods for the transition-metal-catalyzed silylation and borylation of C–H bonds have led to their rapid adoption in early-, mid-, and late-stage of the synthesis of complex molecules. In this Review, we review the application of the transition-metal-catalyzed silylation and borylation of C–H bonds to the synthesis of bioactive molecules, organic materials, and ligands. Overall, we aim to provide a picture of the state of art of the silylation and borylation of C–H bonds as applied to the synthesis and modification of diverse architectures that will spur further application and development of these reactions.



### CONTENTS

1. Introduction	B		
2. Transition-Metal-Catalyzed Silylation of C–H Bonds in Complex Molecules	D		
2.1. Silylation of Aryl C–H Bonds in Complex Molecules	D		
2.1.1. Intramolecular Silylation of Aromatic C–H Bonds	D		
2.1.2. Directed Intermolecular Silylation of Aromatic C–H Bonds	D		
2.1.3. Undirected Intermolecular Silylation of Aromatic C–H Bonds	E		
2.2. Silylation of Alkyl C–H Bonds in Complex Molecules	F		
2.2.1. Intramolecular Silylation of Alkyl C–H Bonds: $\gamma$ -Functionalization	F		
2.2.2. Intramolecular Silylation of Alkyl C–H Bonds: $\delta$ -Functionalization	H		
2.2.3. Intramolecular Silylation of Alkyl C–H Bonds: $\beta$ -Functionalization	I		
2.2.4. Intermolecular Silylation of Alkyl C–H Bonds	J		
3. Transition-Metal-Catalyzed Borylation of C–H Bonds in Complex Molecules	K		
3.1. Transition-Metal-Catalyzed Borylation of C–H Bonds in Precursors to Bioactive Molecules	L		
3.1.1. Formation of C–C Bonds in Precursors to Bioactive Molecules Enabled by the Borylation of C–H Bonds	L		
3.1.2. Transition-Metal-Catalyzed Borylation of C–H Bonds in the Synthesis of Precursors to Bioactive Molecules through Oxidation of the Boronic Ester to the Corresponding Alcohol	P		
3.1.3. Transition-Metal-Catalyzed Borylation of C–H Bonds in the Synthesis of Precursors to Bioactive Molecules through the Corresponding Halide or Pseudohalide	P		
3.1.4. Transition-Metal-Catalyzed Borylation of C–H Bonds in the Synthesis of Precursors to Bioactive Molecules through the Formation of C–N Bonds	R		
3.2. Transition-Metal-Catalyzed, Late-Stage Borylation of C–H Bonds in Complex Molecules	R		
3.2.1. Late-Stage Modification of Complex Molecules by the Undirected Borylation of Aryl C–H Bonds	R		
3.2.2. Late-Stage Modification of Complex Molecules by the Directed Borylation of Aryl C–H Bonds	V		

Received: May 19, 2023

3.2.3. Late-Stage Modification of Complex Molecules by the Undirected Borylation of Alkyl C–H Bonds	W
3.2.4. Late-Stage Modification of Complex Molecules by the Directed Borylation of Alkyl C–H Bonds	W
3.3. Transition-Metal-Catalyzed Borylation of C–H Bonds in the Synthesis of Organic Materials	Y
3.3.1. Transition-Metal-Catalyzed Borylation of Aryl C–H Bonds for the Synthesis and Modification of Polyaromatic Hydrocarbons	Z
3.3.2. Transition-Metal-Catalyzed Borylation in the Synthesis and Modification of Dendrimers	AC
3.3.3. Transition-Metal-Catalyzed Borylation for the Postpolymerization Modification of Polymers	AD
3.3.4. Transition-Metal-Catalyzed Borylation for the Synthesis of Oligopyrroles, Corroles, Porphyrins, and Porphyrin Analogues	AE
3.3.5. Transition-Metal-Catalyzed Borylation of Arene C–H Bonds in the Synthesis of Chalcophene Materials	AG
3.4. Transition-Metal-Catalyzed Borylation of C–H Bonds in Synthesis of Ligands	AH
4. Conclusion and Outlook	AI
Author Information	AJ
Corresponding Author	AJ
Authors	AJ
Author Contributions	AK
Notes	AK
Biographies	AK
Acknowledgments	AK
Abbreviations	AK
References	AK

## 1. INTRODUCTION

The direct functionalization of C–H bonds, particularly the site-selective functionalization of C–H bonds, has been a long-standing goal of organic chemists.<sup>1</sup> Beyond the fundamental challenge facing the activation of C–H bonds that are nonpolar and have high bond dissociation energies lies the challenge of functionalizing C–H bonds with high site selectivity and high chemoselectivity in molecules ranging from alkanes to complex molecules containing an array of functional groups interspersed with C–H bonds that sit in varying steric environments and possess varying electronic properties. Systems that lead to the functionalization of one C–H bond in alkanes ranging from methane to linear, low-density polyethylene or one C–H bond in a molecule as complex as natural products, medicinally active compounds, or even sophisticated electronic materials would lead to widely applicable, new approaches to the synthesis of organic molecules valuable for a variety of applications.

Because of this challenge and potential application, chemists have developed over the past few decades a series of strategies for the functionalization of C–H bonds, some of which have been applicable to the functionalization of C–H bonds in such complex molecules.<sup>2</sup> The synthetic utility of a particular

method for the functionalization of C–H bonds can be demonstrated by the types of complex molecules that can be prepared. The C–H bond functionalization can be applied in the “late-stage” of a synthetic sequence or it can be used earlier in the sequence to create building blocks or to install groups that can be diversified later in a synthesis.

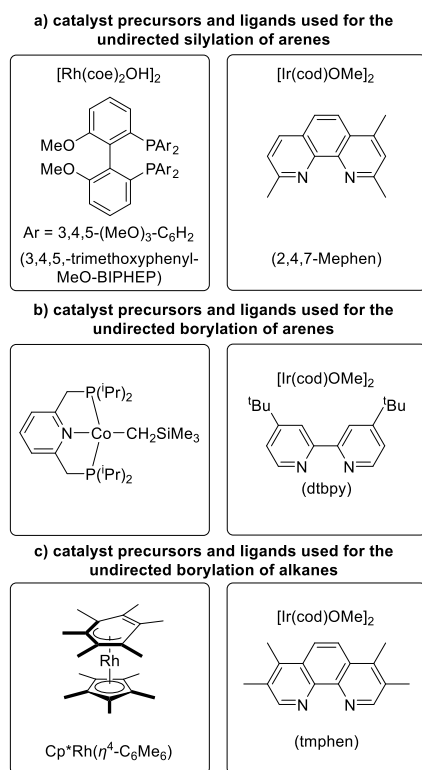
Methods for efficient, catalytic functionalization of unactivated C–H bonds with boron and silicon reagents are particularly attractive for synthetic chemists because of the versatile reactivity of the boryl and silyl functional groups in the products. Both the boryl and silyl groups can serve as transient functional groups to form products containing a variety of functional groups at the position of the C–B or C–Si bond. For example, both arylboron and arylsilicon reagents undergo cross-coupling with carbon-electrophiles in the presence of an appropriate catalyst to form C–C bonds, undergo oxidation by H<sub>2</sub>O<sub>2</sub> to form alcohols, undergo halogenations to form aryl halides, and undergo aminations to form a variety of products containing carbon–nitrogen bonds. The mechanism, scope, and applications of these reactions have been presented in several reviews.<sup>3–5</sup> The wide scope, mild conditions, high-turnover numbers, and predictable site selectivity of these reactions, in combination with their value as synthetic intermediates, have caused the widespread adoption of these methods.

Examples of the borylation and silylation of C–H bonds can be subdivided into three classes: (1) undirected, intermolecular; (2) directed, intermolecular; and (3) intramolecular. Reactions that occur intramolecularly or that occur after binding of the catalyst to a directing group require tethering of the reagent to the substrate, the presence of a suitable directing group on the substrate, or installation of the directing group. Reactions that occur intermolecularly without a directing group typically occur with lower reaction rates, but they do not require the substrate to contain a functional group that can serve as or attach to a directing group.

The most commonly employed catalysts for undirected intermolecular silylation and borylation of C–H bonds contain Group 9 metals (Co, Rh, and Ir),<sup>3,4</sup> although several examples that comprise Group 10 metals,<sup>6–17</sup> Group 8 metals,<sup>18–24</sup> and Group 7 metals<sup>25</sup> are known. The silylation of aryl C–H bonds is typically conducted with a hydrosilane, and common catalysts are rhodium complexes containing bisphosphine ligands, such as 3,4,5-trimethoxyphenyl-MeO-BIPHEP,<sup>26</sup> and iridium complexes containing dipyriddy-type ligands, such as 2,4,7-trimethyl-1,10-phenanthroline.<sup>27</sup> The borylation of aryl C–H bonds is typically conducted with B<sub>2</sub>pin<sub>2</sub> or HBpin as the boron source, and common catalysts are PNP pincer complexes containing cobalt,<sup>28</sup> and iridium complexes containing bipyridine-type ligands, such as 4,4′-ditert-butyl-2,2′-bipyridine (dtbpy)<sup>29</sup> and 3,4,7,8-tetramethyl-1,10-phenanthroline (tmphen).<sup>30,31</sup> The borylation of alkyl C–H bonds occurs with rhodium piano stool complexes, such as Cp\*Rh(η<sup>4</sup>-C<sub>6</sub>Me<sub>6</sub>),<sup>32</sup> and iridium complexes containing bipyridine-type ligands (Scheme 1).

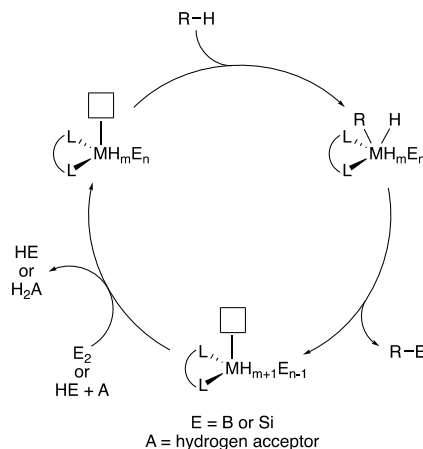
The undirected silylation of aryl C–H bonds are run with hydrosilanes and often require the addition of a hydrogen acceptor. The borylation of alkyl and aryl C–H bonds are typically run with diboron reagents and generate hydroborane as the byproduct, although there are also many examples in which the reaction is conducted with hydroborane without a hydrogen acceptor.

### Scheme 1. Common Group 9 Catalyst Precursors and Ligands for the Silylation and Borylation of C–H Bonds

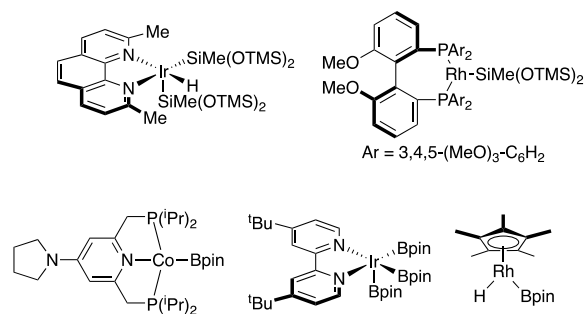


### Scheme 2. (a) Generalized Mechanism of Transition-Metal-Catalyzed Silylation and Borylation of C–H bonds and (b) Complexes Implicated in the Reactions

#### a) generalized mechanism of the silylation and borylation of C–H bonds



#### b) intermediates implicated in the silylation and borylation of C–H bonds



Mechanistic studies suggest that the borylation of aryl C–H bonds with cobalt pincer complexes occurs by a mechanism comprising a combination of Co(I) and Co(III) intermediates.<sup>28,33</sup> Mechanistic studies on both the borylation of alkyl C–H bonds and silylation of aryl C–H bonds with rhodium complexes indicate that the reactions occur by mechanisms comprising Rh(I) and Rh(III) intermediates. In stark contrast, the silylation and borylation of aryl and alkyl C–H bonds with iridium complexes is accepted to occur by a cycle comprising Ir(III) and Ir(V) intermediates.<sup>29,31,34–37</sup> Broadly speaking, however, these reactions occur under the same mechanistic manifold: the C–H bond of the substrate undergoes oxidative addition to the active catalyst  $L_2M^{ox}H_mE_n$  (E = B or Si; L = nitrogen-donor or phosphorus-donor ligand) to generate  $L_2M^{ox+2}H_{m+1}E_nR$ . The metal–alkyl or metal–aryl intermediate then undergoes reductive elimination to form the C–E (E = B or Si) bond. Catalyst turnover is achieved by reaction with the main group reagent and hydrogen acceptor (if present) (Scheme 2).

With these mechanisms in mind, the site selectivity and strategies for the silylation and borylation of C–H bonds can be rationalized. Because these transition-metal-catalyzed functionalizations of C–H bonds occur through the formation of an aryl–metal or alkyl–metal intermediate, reactivity trends in the absence of steric factors tend to parallel measures of metal–carbon bond strength or C–H acidity, as have been studied for other metal-catalyzed C–H arylation processes.<sup>38,39</sup> Undirected borylations and silylations tend to favor functionalization of the most acidic heteroaryl C–H bond over aryl C–H bonds, aryl C–H bonds over alkyl C–H bonds, and primary alkyl C–H bonds over secondary or tertiary C–H bonds. Moreover, the pronounced steric bulk around the metal complexes have led to exquisite, sterically driven selectivities

for appropriately substituted arenes and heteroarenes with good *meta*-selectivity. This sterically driven selectivity often overrides electronic factors. Several reviews and models to predict site selectivity have been published.<sup>40–42</sup> Intramolecular silylations occur by replacement of one of the boryl or silyl substituents bound to the metal center with the silyl group of the substrate containing an Si–H bond. For intermolecular, directed borylations or silylations, two coordination sites are needed. The lack of two open coordination sites in the iridium catalysts ligated by chelating dative ligands and the steric bulk of the ancillary ligands in other cases lead to the requirement of alternative types of ligands, including hemilabile ligands, LX ligands, and ligands with charges for ionic interactions (see below for examples).

This Review focuses on the application of the silylation and borylation of C–H bonds catalyzed by transition metal catalysts for the synthesis of complex molecules. The Review has been organized into two main sections: the transition-metal-catalyzed silylation of C–H bonds for the synthesis of complex molecules and the transition-metal-catalyzed borylation of C–H bonds for the synthesis of complex molecules.

Several alternative strategies for the borylation and silylation of C–H bonds are emerging, such as those occurring by Friedel–Crafts mechanisms,<sup>43,44</sup> borylation of alkanes by HAT processes,<sup>45–47</sup> silylation of heteroarenes by radical chain processes,<sup>48</sup> and borylation and silylation of heteroarenes by Minisci-type reactions.<sup>49–52</sup> Although some of these reactions contain transition-metal photocatalysts, the bond cleavage and bond formation do not involve a transition-metal catalyst and, therefore, are not covered in this Review. Also excluded from

this Review are processes occurring by the combination of lithiation and borylation of the resulting organolithium species.<sup>53</sup>

## 2. TRANSITION-METAL-CATALYZED SILYLATION OF C–H BONDS IN COMPLEX MOLECULES

Motivated by the potential for the broad impact of methods that transform C–H bonds to C–Si bonds discussed in the introduction, significant research has been devoted to discovering transition metal catalysts that lead to the mild and highly selective silylation of aryl and alkyl C–H bonds. Reviews have been published that outline the history and recent progress of such systems.<sup>4,54–56</sup> This section of this Review provides information on the application of these catalytic systems to the silylation of C–H bonds in complex molecules and fragments thereof.

### 2.1. Silylation of Aryl C–H Bonds in Complex Molecules

Arylsilanes are traditionally prepared by the reaction between chlorosilanes or cyclosiloxanes and Grignard or organolithium reagents. One main limitation of this method is the functional-group incompatibility of Grignard and organolithium reagents. Also, large-scale synthesis using this method creates a large amount of metal salt byproducts. Alternatively, arylsilanes can be prepared by cross-coupling of aryl halides with hydrosilanes or disilanes catalyzed by transition metal complexes. While this approach overcomes the functional group incompatibility of Grignard and organolithium reagents, this approach requires prefunctionalization of the arene, and the regioselectivity of silylation is limited by the halogenation step.

Methods to prepare aryl organosilanes by the silylation of C–H bonds are attractive because they eliminate the requirement for prefunctionalization of the arene. Also, they could form products with regioselectivity that is distinct from that of halogenation and silylation of the derived organomagnesium intermediate.

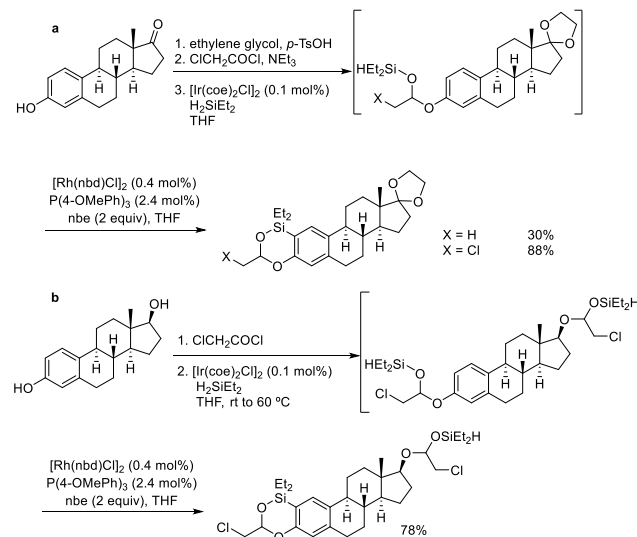
Examples of the silylation of aryl C–H bonds can be divided into three classes: (1) intramolecular, (2) directed intermolecular, and (3) undirected intermolecular silylations of C–H bonds. Intramolecular silylation produces the products of the silylation of C–H bonds in good yields, but this strategy requires tethering a suitable silane to the arene. Intermolecular silylation of C–H bonds directed by a coordinating group on the arene occurs with good selectivity from the directing group but is limited to substrates that have suitable groups that will coordinate the catalyst. Until recently, undirected intermolecular silylation of aryl C–H bonds had required high temperatures and a large excess of arene. These characteristics limited the synthetic utility of the silylation of C–H bonds. Systems discovered by our laboratory have overcome this restriction.<sup>26,63</sup>

**2.1.1. Intramolecular Silylation of Aromatic C–H Bonds.** The intramolecular silylation of aryl C–H bonds catalyzed by transition metals leverages a silane on the reactant as an X-type ligand to direct the activation of a C–H bond. Upon Si–C reductive elimination, silacycles are formed. The connection between the silane and the aryl C–H bond in the reactants undergoing intramolecular silylation have been silyl acetals or a siloxane from a phenol in complex molecules.

For example, in 2016, Jeon et al. reported a Rh-catalyzed intramolecular silylation of an aryl C–H bond on estrone and estradiol to furnish six-membered aryl silanes.<sup>57</sup> The silyl acetal acting as the intramolecular silylation reagent was formed by

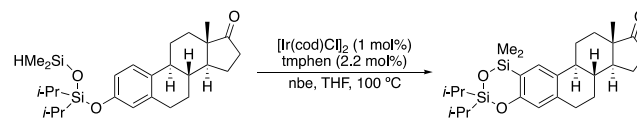
acylation of the phenol, followed by Ir-catalyzed hydro-silylation of the resulting ester (Scheme 3).

### Scheme 3. Rh-Catalyzed Silylation of Aromatic C–H Bonds of Estrone (a) and Estradiol (b)



Cui and Xu et al. also reported the intramolecular silylation of an aryl C–H bond on estrone, in this case with an Ir catalyst and a disiloxane tether to form a six-membered aryl silane.<sup>58</sup> The tethered disiloxane was formed by reaction of the silanol derived from the starting phenol with a chlorodisiloxane (Scheme 4).

### Scheme 4. Ir-Catalyzed Silylation of Siloxane-Tethered Estrone

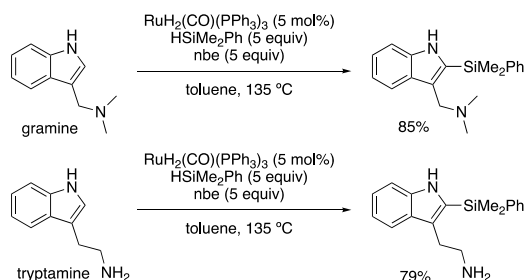


**2.1.2. Directed Intermolecular Silylation of Aromatic C–H Bonds.** The intermolecular silylation of aryl C–H bonds can occur with or without a directing group on the arene. The directed methodologies have been limited mostly to silylation *ortho* and *meta* to the directing group, and when the directing group is not present in the desired product, the directing group must be installed and removed. Despite these challenges, directed silylation has received considerable attention because it is faster and it provides greater control of regioselectivity than the undirected reactions.

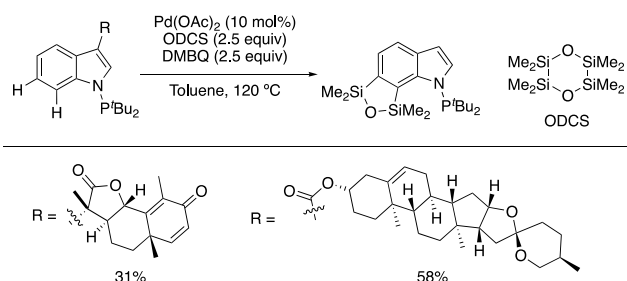
The directed silylation of aryl C–H bonds was applied to the functionalization of gramine and tryptamine by Gates and Pilarski et al.<sup>59</sup> They reported a C2-selective, amine-directed silylation catalyzed by ruthenium. This reaction occurs with perfect regioselectivity (Scheme 5).

Shi, Wang, and Houk et al. reported a Pd-catalyzed, double silylation of indoles tethered to complex molecule scaffolds using octamethyl-1,4-dioxacyclohexasilane (ODCS) as the silylating reagent.<sup>60</sup> The first C–H silylation was directed to C7 by a P<sup>III</sup>-group appended to the indole nitrogen. The second C–H silylation was an intramolecular silylation of the C–H bond on C6 to afford the cyclized product (Scheme 6).

### Scheme 5. Ru-Catalyzed Silylation of Gramine and Tryptamine Directed by Amines

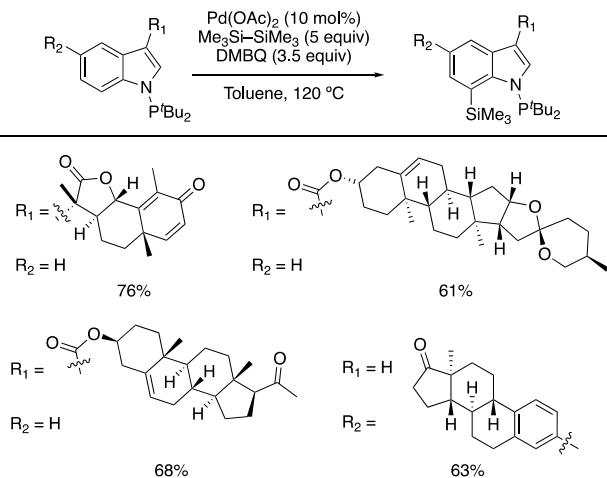


### Scheme 6. Pd-Catalyzed Disilylation of Indoles Directed by Phosphorus



The same P<sup>III</sup> directing group bound to the indole nitrogen was used again by Shi and Houk et al. in 2021 to achieve the C7-selective, monosilylation of indoles catalyzed by palladium.<sup>61</sup> Hexamethyldisilane was used to install a TMS group on several indole substrates with tethered complex molecules (Scheme 7).

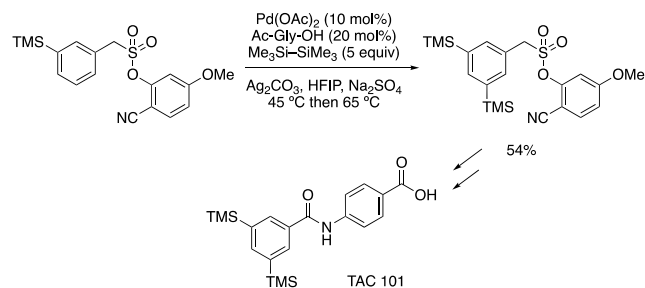
### Scheme 7. Pd-Catalyzed Monosilylation of Indoles Directed by Phosphorus



While these examples of intra- and intermolecular silylations of aryl C–H bonds have occurred on complex molecules or substrates with such scaffolds appended, the directed, intermolecular silylation of aryl C–H bonds has also been reported for the synthesis of pharmaceutical precursors. TAC-101, a retinoid that has shown promising antitumor activity, contains a disilylated arene in the final structure. In 2017, Maiti et al. reported a Pd-catalyzed method for the *meta*-selective silylation of 1,3-disubstituted arenes directed by a nitrile-based template for the disilyl arene.<sup>62</sup> Removal of the directing group

reveals a functional handle that can be leveraged to complete the formal synthesis of TAC 101 (Scheme 8).

### Scheme 8. Pd-Catalyzed, *meta*-Selective Silylation Directed by a Nitrile toward the Synthesis of TAC 101



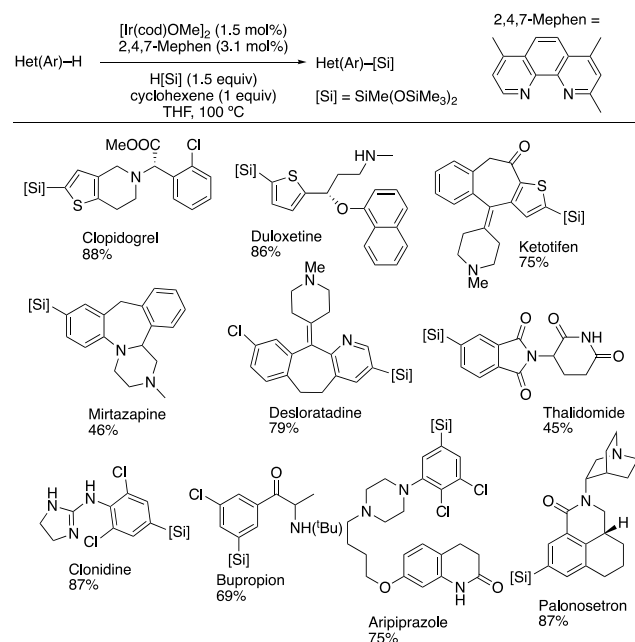
### 2.1.3. Undirected Intermolecular Silylation of Aromatic C–H Bonds.

Methods for the intermolecular silylation of aryl C–H bonds without a directing group are valuable because they do not require specific functionalities to be present in the substrate. The regioselectivity of such reactions is more difficult to control than that of intramolecular and directed reactions, and reactions can be sensitive to the identity of the silane. Nevertheless, selective and functional-group-tolerant methods for the undirected silylation of aryl C–H bonds have been developed and applied to the functionalization of a range of complex molecule scaffolds.

In 2015, our laboratory published an Ir-catalyzed method for the undirected silylation of aryl C–H bonds with 2,4,7-trimethylphenanthroline as ligand and 1,1,1,3,5,5,5-heptamethyltrisiloxane as silyl source.<sup>63</sup> The reaction occurs with regioselectivity derived from both steric and electronic factors. The silylation occurs on arenes, thiophenes, and pyridines in a range of pharmaceutical compounds (Scheme 9).

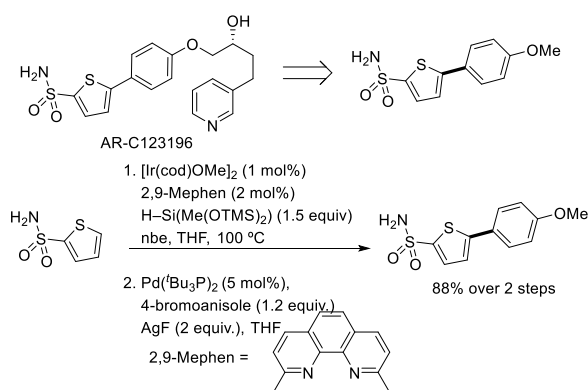
In 2019, our laboratory reported more active catalysts containing a sterically encumbered 2,9-dimethylphenanthroline

### Scheme 9. Undirected Silylation of C–H Bonds Catalyzed by Iridium

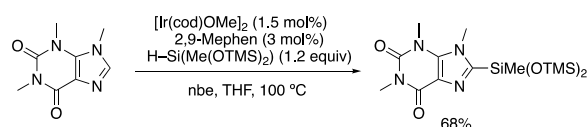


ligand, in combination with  $[\text{Ir}(\text{cod})\text{OMe}]_2$ .<sup>27</sup> This system catalyzes the silylation of aryl C–H bonds at lower temperatures and with faster rates than previously reported ones. Computational studies indicated that the resting state of the iridium catalyst containing the more sterically encumbered 2,9-dimethylphenanthroline is a disilyl hydride complex, which is less sterically hindered and more reactive than the iridium trisilyl resting state generated from less hindered phenanthroline ligands.<sup>36</sup> This catalytic system was used in a two-step, silylation/cross-coupling sequence on 2-thiophenesulfonamide to access a key intermediate in the synthesis of AR-C123196, an anti-inflammatory for asthma (Scheme 10). In a 2020 report, this same system catalyzed the silylation of caffeine in good yield (Scheme 11).<sup>64</sup>

**Scheme 10. Ir-Catalyzed Silylation and Cross-Coupling of 2-Thiophenesulfonamide toward the Synthesis of AR-C123196**



**Scheme 11. Ir-Catalyzed Silylation of Caffeine**



## 2.2. Silylation of Alkyl C–H Bonds in Complex Molecules

Like the silylation of aryl C–H bonds, the silylation of alkyl C–H bonds can be divided into two main classes: (1) intramolecular and (2) directed intermolecular silylations of C–H bonds. The class of intramolecular silylations can be further subdivided into three classes by the site of C–H functionalization, defined by the position relative to the atom to which the silane is attached: (1)  $\gamma$ -C–H functionalization, which has been developed most extensively; (2)  $\delta$ -C–H functionalization, which has been observed with a rhodium catalyst; and (3)  $\beta$ -C–H functionalization, which was achieved by designing an alternative mode of attaching the silane to an alcohol.

Most commonly, intramolecular silylations of alkyl C–H bonds occur by initial reaction of the silane with an alcohol, carbonyl, or alkene to install the silane, followed by the intramolecular C–H silylation and oxidation of the silacycle to reveal a hydroxylated or *O*-acylated product. This sequence has been implemented to achieve site-selective oxidations for the synthesis of complex molecules and to modulate the properties of complex molecules by oxidation.

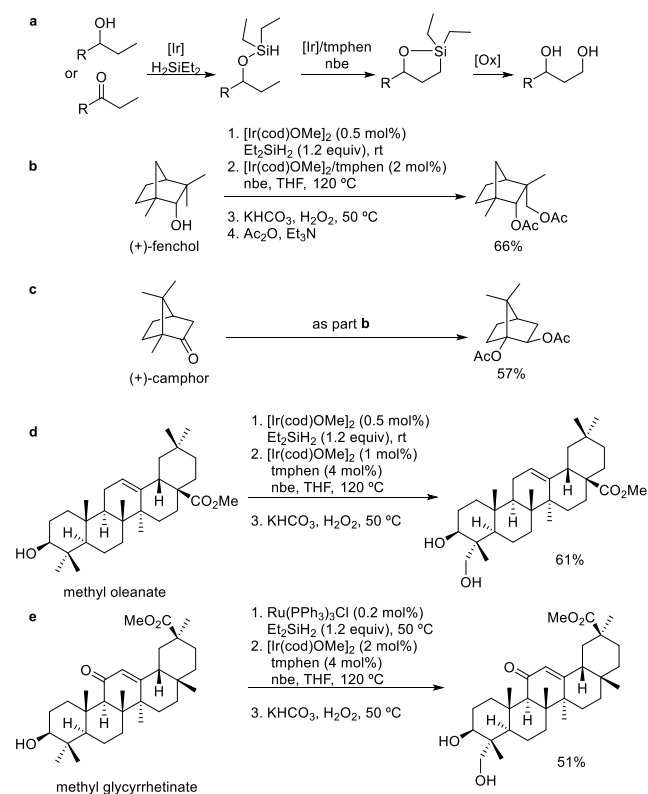
Directed, intermolecular silylation of alkyl C–H bonds is more limited than the intramolecular silylation and has rarely

been applied to the synthesis of complex molecules. However, such reactions have been used to form silylated amino acids and derivatives thereof, for proteomics and genetic technologies.

**2.2.1. Intramolecular Silylation of Alkyl C–H Bonds:  $\gamma$ -Functionalization.** The intramolecular silylation of an alkyl C–H bond  $\gamma$  to a directing group most commonly results from the formation of a five-membered oxasilolane intermediate. This intermediate can be oxidized under Tamao–Fleming conditions to reveal a 1,3-dioxygenated product. The sequence of silylation and oxidation has been employed on a wide range of complex molecules to install hydroxyl or *O*-acyl groups site-selectively.

In 2012, our laboratory published an intramolecular silylation of primary C–H bonds  $\gamma$  to a ketone or alcohol.<sup>65</sup> The innate ketone or alcohol is first transformed to a silyl ether by an Ir-catalyzed hydrosilylation or dehydrogenative silylation reaction, respectively. The silyl ether undergoes an Ir-catalyzed intramolecular C–H functionalization reaction with tetramethylphenanthroline as ligand and norbornene as the hydrogen acceptor to form a five-membered oxasilolane. Upon oxidation of the oxasilolane, a 1,3-diol is formed (Scheme 12a). Further functionalization to form a diacetate product has been performed to facilitate purification and isolation.

**Scheme 12. Ir-Catalyzed Silylation of Primary C–H Bonds to Afford 1,3-Diols after Tamao–Fleming Oxidation**

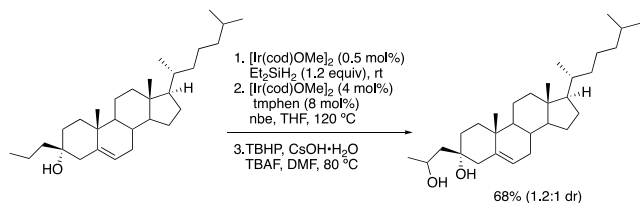


In this 2012 paper, such a sequence was performed to oxidize (+)-fenchol and (+)-camphor to their corresponding 1,3-diacetate products (Scheme 12b,c).<sup>65</sup> In addition, the site-selective C–H silylation and oxidation was performed on methyl oleanate and methyl glycyrrhetinate to form the corresponding 1,3-diols (Scheme 12d,e). The importance of the synthesis of the 1,3-diol from methyl oleanate using this

method was highlighted in work by Nishikawa and Qi et al. reported in 2018 during which they synthesized a library of neurotogenic derivatives by esterification of the secondary alcohol of the 1,3-diol formed from methyl oleanate.<sup>66</sup>

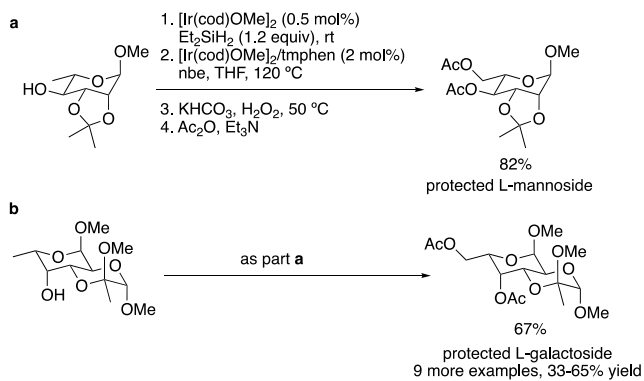
In 2014, our laboratory reported the intramolecular C–H silylation of secondary C–H bonds  $\gamma$  to a tertiary alcohol catalyzed by the same iridium system reported in 2012.<sup>67</sup> This expansion in scope allowed this process to occur on a tertiary alcohol derived from cholesterol to form a 1,3-diol product (Scheme 13).

### Scheme 13. Ir-Catalyzed Silylation of Secondary C–H Bonds to Form 1,3-Diol after Tamao–Fleming Oxidation



The method reported by our laboratory in 2012 was employed for the functionalization of carbohydrates. In 2012, Pedersen and Bols et al. adopted the combination of deoxygenative silylation and C–H silylation to transform L-rhamnoside and L-fucoside, two accessible L-sugars, to L-mannoside and L-galactoside, which are two rare L-sugars (Scheme 14a).<sup>68</sup> In a 2014 paper, they report the same

### Scheme 14. Ir-Catalyzed Silylation of Primary C–H Bonds to Form Glycosides after Oxidation

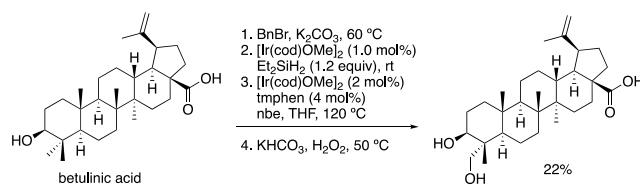


sequence to transform eight 6-deoxy thioglycosides to their corresponding L-glycopyranosyl donors.<sup>69</sup> This work represented the first general method for the preparation of all eight L-hexoses masked as their thioglycosyl donors primed for glycosylation (Scheme 14b).

Our group's method was used in 2014 by Houk and Baran et al. during their systemic study of the ability of aliphatic C–H oxidation to modulate the physical properties of betulin and betulinic acid, a poorly water-soluble, but bioactive, natural product.<sup>70</sup> Upon benzylation of betulinic acid, the sequence to form the 1,3-diol was employed and was followed by debenylation to form C23-hydroxybetulinic acid. The diol was modestly more soluble than betulinic acid in assays performed in simulated intestinal fluids (Scheme 15).

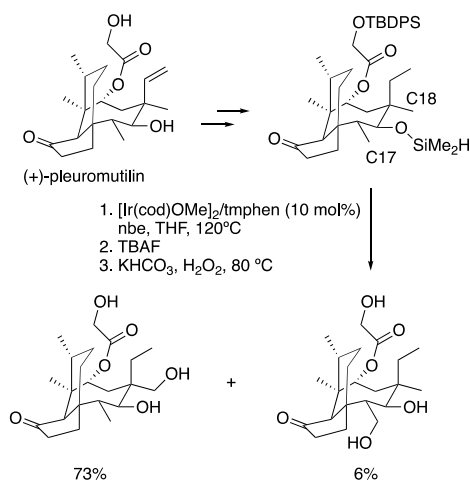
Herzon et al. published an application of our laboratory's method in 2018 for the C–H oxidation of (+)-pleuromutilin.<sup>71</sup> From (+)-pleuromutilin, the protection of the C22 primary

### Scheme 15. Ir-Catalyzed Silylation of Primary C–H Bonds for the Late-Stage Oxidation of Betulinic Acid



alcohol, hydrogenation of the C19–C20 alkene, and treatment with chlorodimethylsilane afforded the silyl ether substrate for the directed C–H silylation reaction. The subsequent intramolecular C–H silylation afforded a 4:1 mixture of the C11–C18 and C11–C17 silacycles that afforded, upon oxidation and deprotection, the C18 oxidation product in 73% yield and the C17 oxidation product in 6% yield (Scheme 16).

### Scheme 16. Ir-Catalyzed Silylation of a Primary $\gamma$ -C–H Bond of (+)-Pleuromutilin

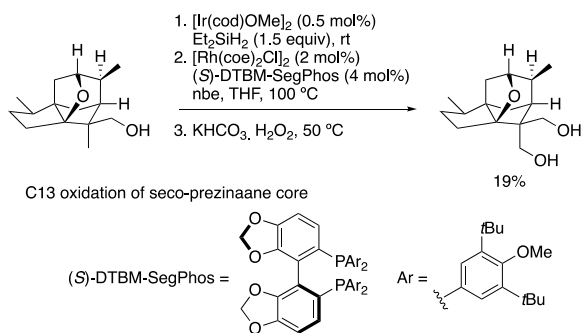


In 2019, Maimone and co-workers conducted the combination of dehydrogenative silylation, C–H silylation, and C–Si oxidation to oxidize C13 of a cedrane skeleton site selectively during the synthesis of the anisatinoid family of natural products.<sup>72</sup> A rhodium catalyst ligated by (*S*)-DTBM-SegPhos was used instead of the iridium catalyst reported by Hartwig et al. The rhodium system catalyzed the intramolecular silylation of a primary C–H bond directed by a secondary alcohol to afford the 1,3-diol upon oxidation (Scheme 17).

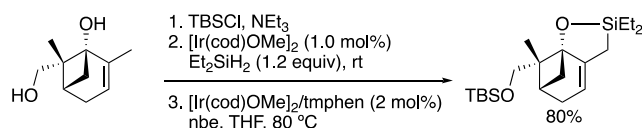
During their work on the total synthesis of the phomactins, Sarpong and co-workers applied our laboratory's silylation conditions to transform the core cyclohexene ring into a bicyclic structure containing an oxasilolane.<sup>73</sup> They proposed the oxasilolane intermediate could act as a coupling partner in a Hiyama-type reaction to install an alkene that could be used for further functionalization (Scheme 18). While the Ir-catalyzed C–H silylation to form the oxasilolane was successful, the subsequent Hiyama-coupling did not give the desired product.

In 2021, Sun et al. reported a 24-step total synthesis of quillaic acid that employed our laboratory's silylation sequence to accomplish the final oxygenation.<sup>74</sup> The secondary alcohol on the A ring was used to direct an intramolecular C–H

### Scheme 17. Rh-Catalyzed Silylation of a Primary $\gamma$ -C–H Bond of a Precursor to the Anisatinoid Family

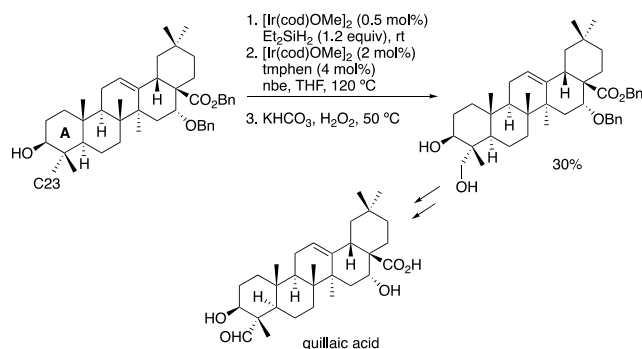


### Scheme 18. Ir-Catalyzed Silylation of Primary C–H Bonds Used toward the Synthesis of the Phomactins



silylation on C23, which was then oxidized to reveal the diol in a fashion akin to the C–H silylation and oxidation performed on methyl oleanate in the 2012 report.<sup>65</sup> From the diol product, the newly installed hydroxyl group was oxidized to the aldehyde, and the compound was debenzylated to reveal quillaic acid (Scheme 19).

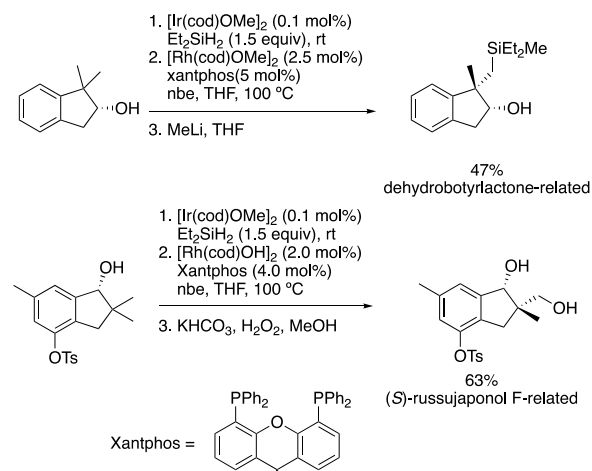
### Scheme 19. Ir-Catalyzed Silylation of Primary C–H Bonds Used toward the Synthesis of the Quillaic Acid



In 2021, Lu et al. published the combination of diastereoselective reduction of 1-indanone and 2-indanone-derived molecules and silylation of the resulting alcohol.<sup>75</sup> This method maintained the Ir-catalyzed dehydrogenative silylation to form the silyl ether from the alcohol directing group but employed a catalyst formed from a rhodium precursor and Xantphos to achieve a C–H silylation to form a five-membered oxasilolane. The oxasilolane was opened by treatment with methyl lithium to reveal a silane or with oxidizing conditions to reveal a 1,3-diol. The resulting silanes are related to (S)-russujaponol and dehydrobotrylactone, which are two sesquiterpenoids (Scheme 20).

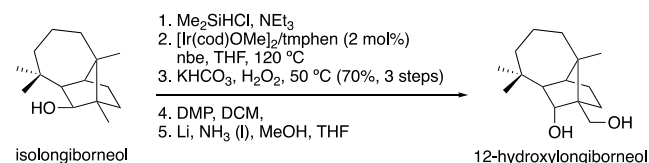
Sarpong et al. applied our laboratory's silylation conditions in the late stage to synthesize 12-hydroxylongiborneol.<sup>76</sup> Isolongiborneol was treated with chlorodimethyl silane to afford the silyl ether. The intramolecular C–H silylation and oxidation then yielded iso-12-hydroxylongiborneol, which was epimerized to the desired stereoisomer by oxidation and

### Scheme 20. Rh-Catalyzed Silylation of a Primary $\gamma$ -C–H Bond for the Synthesis of Indanes



dissolving metal reduction (Scheme 21). The reaction does not occur at one of the geminal dimethyl groups likely because the

### Scheme 21. Ir-Catalyzed Silylation of Isolongiborneol to Form 12-Hydroxylongiborneol



iridacycle intermediate formed by C–H cleavage at the geminal methyl group is more strained than that formed by C–H cleavage at the bridgehead methyl group. The iridacycle formed at the geminal methyl group includes both the bridged ring and the borneol ring system, while that formed at the bridgehead methyl includes only the borneol ring system.

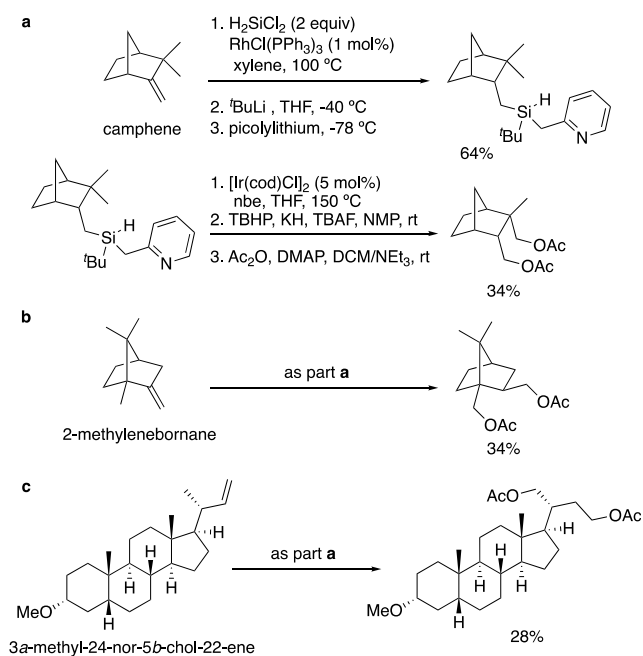
**2.2.2. Intramolecular Silylation of Alkyl C–H Bonds:  $\delta$ -Functionalization.** The installation of a silane on an innate functional group, followed by intramolecular C–H silylation, also can lead to the silylation of alkyl C–H bonds  $\delta$  to the carbon or oxygen to which the silane is attached. The formation of silacycles by this method has been used to form stereochemically defined polycyclic structures that contain silicon. The oxidation of such silacycles affords 1,4-dioxygenated products.

In one case reported by Gevorgyan et al., the silane was installed by hydrosilylation of an alkene.<sup>77</sup> Rh-catalyzed hydrosilylation with chlorosilane followed by a series of substitution reactions generated the corresponding *t*-butylpicolyl(hydrido)silane. The authors propose that Si,N-chelation with the picolyl moiety enables the C–H activation step of the catalytic cycle and that the *t*-butyl group stabilizes the silane. The *t*-butylpicolyl(hydrido)silane then underwent intramolecular silylation of the primary C–H bond  $\delta$  to the silane to form a silolane that yielded a 1,4-dioxygenated product upon Tamao–Fleming oxidation. The synthetic utility of this method was exemplified by reactions on camphene, 2-methylenebornane, and a cholene derivative (Scheme 22).

Silyl ethers derived from alcohols in the substrate have also been shown to undergo intramolecular silylation to modify complex molecules. Akin to the method for the formation of

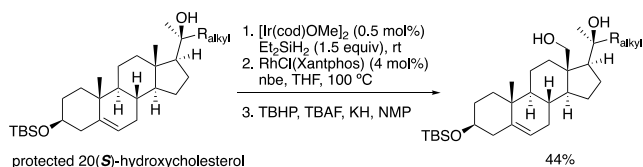


### Scheme 22. Hydrosilylation of Alkenes Affords Precursors for Ir-Catalyzed $\delta$ -C–H Bond Silylation to Yield Acetyl-Protected 1,4-Diols after Oxidation



1,3-diols, a method to form 1,4-diols was reported by our laboratory in 2018 to occur by dehydrogenative silylation of an alcohol, followed by intramolecular C–H silylation and oxidation.<sup>78</sup> In this method, functionalization of the C–H bond  $\delta$  to the alcohol would occur by the formation of a seven-membered metallacycle that would undergo reductive elimination to form a six-membered oxasilolane. This reaction occurred with a catalyst generated from  $\text{Rh}(\text{Xantphos})\text{Cl}$ . Oxidation of the oxasilolane revealed the 1,4-diol product. This method was applied to the C–H silylation of a protected oxysterol (Scheme 23).

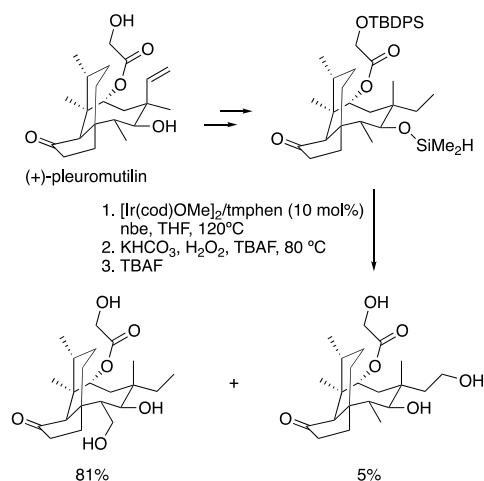
### Scheme 23. Ir-Catalyzed Silylation of a Primary $\delta$ -C–H Bond of a Cholesterol Derivative



Herzon et al. also observed the silylation of C–H bonds  $\delta$  to an alcohol during studies on the late-stage functionalization of 12-*epi*-pleuromutilin. The reaction occurs in high yield to give a mixture of products from functionalization of the C–H bonds  $\delta$  and  $\gamma$  to the hydroxyl group. These studies were conducted with the combination of iridium and tmphen and formed the product from silylation at the C–H methyl group  $\delta$  to the hydroxyl group but also formed the product from functionalization  $\gamma$  to the hydroxyl group as the major product. (Scheme 24).<sup>71</sup> The product from silylation at the C–H bond  $\gamma$  to the hydroxyl group is favored because of the formation of a six-membered iridacycle from C–H activation.

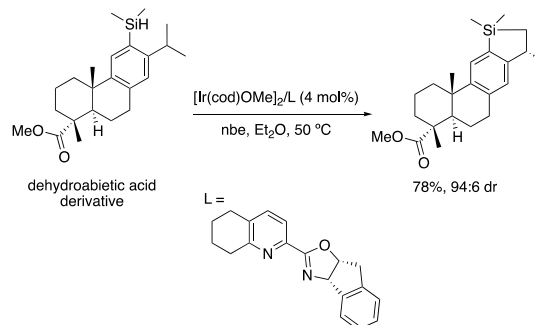
Aryl silanes also undergo intramolecular silylation of alkyl C–H bonds. In 2017, our laboratory reported the enantioselective, Ir-catalyzed silylation of methyl C–H bonds

### Scheme 24. Ir-Catalyzed Silylation of a Primary $\delta$ -C–H Bond of (+)-Pleuromutilin



$\delta$  to an aryl silane with a tetrahydroquinoline-fused oxazoline ligand.<sup>79</sup> The intramolecular C–H activation step to form a six-membered iridacycle was shown to be rate-limiting. Reductive elimination from such an iridacycle would be expected to form the silolane product. This enantioselective silylation was applied to the functionalization of dehydroabietic acid, which demonstrates the potential of late-stage C–H silylation to control stereoselectivity during the diversification of complex molecules (Scheme 25).

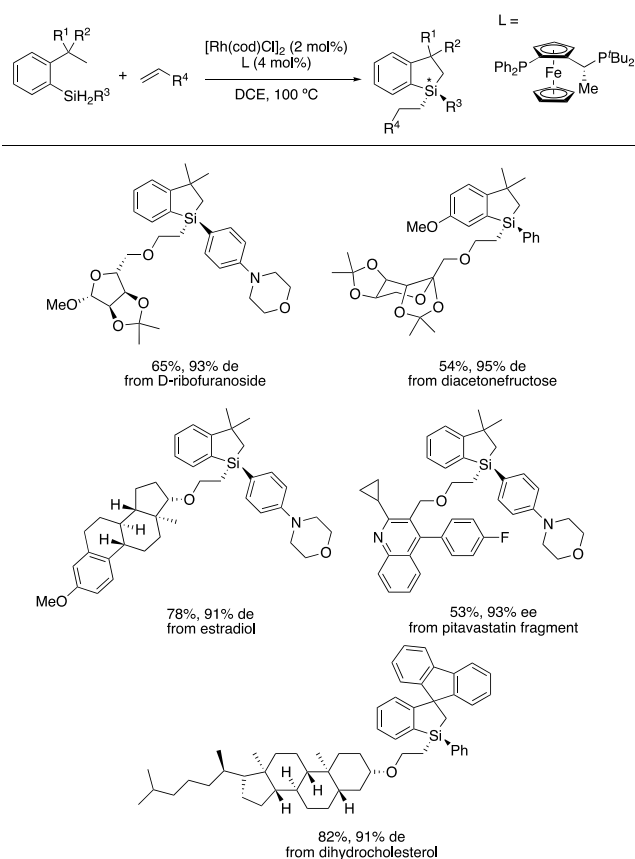
### Scheme 25. Ir-Catalyzed Silylation of a Primary C–H Bond $\delta$ to an Aryl Hydrosilane



Silylations of alkyl C–H bonds also can generate a stereogenic center at silicon. Such methods are valuable because of the broad application of organosilanes in synthetic and materials chemistry. In 2020, the combination of hydrosilylation of an alkene and enantioselective C–H silylation was reported by He et al. to generate molecules with a stereogenic center at silicon.<sup>80</sup> The authors showed that the combination of  $[\text{Rh}(\text{cod})\text{Cl}]_2$  and a JosiPhos-type ligand catalyzed enantioselective, intramolecular silylations of methyl C–H bonds in dimethylsilanes. The resulting monohydrosilane was trapped in one pot by an alkene in a stereospecific fashion to generate chiral, enantioenriched, tetrasubstituted dihydrobenzosiloles. To demonstrate the use of this method on complex scaffolds, the reactions were conducted on substrates containing an array of alkenes tethered to multifunctional compounds (Scheme 26).

### 2.2.3. Intramolecular Silylation of Alkyl C–H Bonds: $\beta$ -Functionalization. The synthesis of 1,3- and 1,4-diols by a

### Scheme 26. Rh-Catalyzed Silylation of a Primary C–H Bond $\delta$ to an Aryl Hydrosilane and Hydrosilylation to Form Silicon-Stereogenic Dihydrobenzosiloles

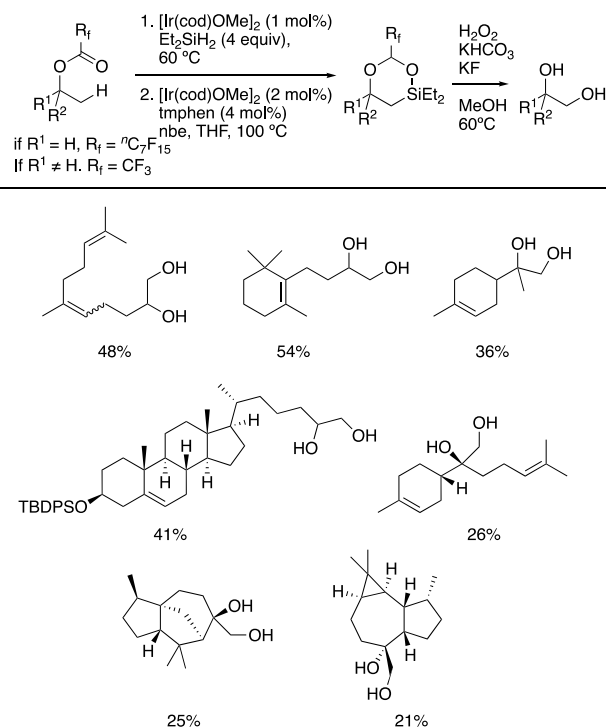


sequence of silylation of an alcohol or ketone, intramolecular C–H silylation, and oxidation is accomplished by the formation of a five-membered or six-membered oxasilolane. The site-selective formation of 1,2-diols by a similar sequence would be equally valuable, but formation of the requisite four-membered oxasilolane is disfavored because of ring strain. Nevertheless, methods have been developed to form 1,2-diols by intramolecular silylation of a C–H bond  $\beta$  to a directing group. Such methods occur with an alcohol or amine on the substrate and a linker of appropriate length to form the requisite cyclic oxasilolane without high ring strain.

Our laboratory published a method of this type in 2018 that leveraged an inherent alcohol as the directing group.<sup>81</sup> To avoid the four-membered oxasilolane intermediate, the alcohol was transformed to a perfluoroalkyl ester, which subsequently underwent hydrosilylation. The resulting silyl ether was transformed to a six-membered oxasilolane by an iridium-catalyzed, intramolecular silylation of the  $\beta$ -C–H bond. Subsequent oxidation revealed the desired 1,2-diol product. This method was applied to the selective oxidation of an array of complex molecules (Scheme 27).

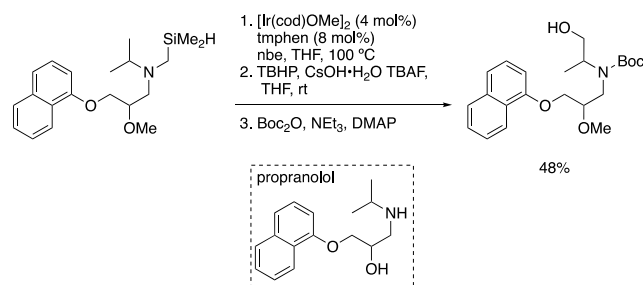
Our laboratory also reported an intramolecular silylation of alkyl C–H bonds  $\beta$  to aliphatic amines to form 1,2-amino alcohols.<sup>82</sup> In this method, the four-membered silolane was circumvented by linking a hydrosilyl group to the nitrogen of the amine by a methylene group. Such a linker was installed by alkylation of the amine with a chloromethylsilane. From the hydrosilane, an iridium-catalyzed,  $\beta$ -selective silylation of a C–H bond formed the five-membered silapyrrolidine, which was

### Scheme 27. Ir-Catalyzed Silylation of Primary C–H Bonds to Afford 1,2-Diols after Tamao–Fleming Oxidation



oxidized to give a 1,2-amino alcohol. This method was applied to the late-stage oxidation of methoxy-protected propranolol, a commonly prescribed beta-blocker (Scheme 28).

### Scheme 28. Ir-Catalyzed Silylation of C–H Bonds $\beta$ to an Amine



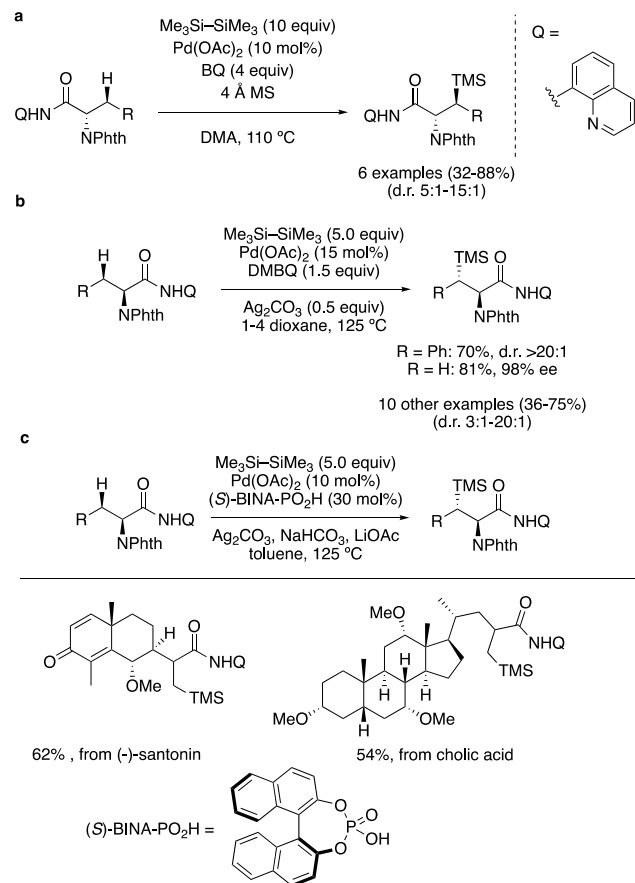
#### 2.2.4. Intermolecular Silylation of Alkyl C–H Bonds.

Intermolecular silylations of alkyl C–H bonds on complex molecules are less developed than intramolecular silylations. The published examples of intermolecular silylations of alkyl C–H bonds on complex molecules are catalyzed by palladium complexes and are assisted by a functional group appended to the substrate that enables two-point binding of the substrate to the catalyst. This reaction type has been used primarily for the formation of silicon-containing amino acids because the incorporation of silicon has the potential to modify the properties of amino acids.

For example, two methods employing this general strategy were published concurrently in 2016 by the Zhang and Shi groups with  $\text{Pd}(\text{OAc})_2$  as catalyst, HMDS as the silyl source, and 8-aminoquinoline as the auxiliary directing group.<sup>83,84</sup> Both authors propose the auxiliary-bound substrate binds to the palladium center as an LX-type ligand. The two-point

binding facilitates the C–H activation step of the catalytic cycle. Zhang et al. applied this method to synthesize six  $\beta$ -silyl- $\alpha$ -amino acids (Scheme 29a). Shi et al. reported the silylation

### Scheme 29. Pd-Catalyzed Silylation of Primary and Secondary C–H Bonds of Phthalimide (NPhth)-Protected $\alpha$ -Amino Acids Using a Quinoline Auxillary

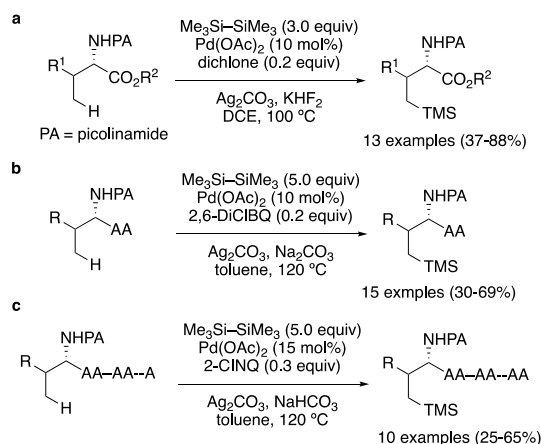


of alanine, phenylalanine, and 10 other derivatized amino acids (Scheme 29b). In addition, Shi synthesized silylated derivatives of (–)-santonin and cholic acid by a closely related method with BINA-PO<sub>2</sub>H as ligand (Scheme 29c).

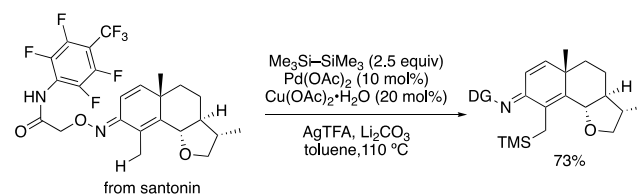
In 2019, Shi et al. used the same general strategy to access  $\gamma$ -silyl- $\alpha$ -amino acids and silylated peptides with picolinoamide as the auxiliary instead of 8-aminoquinoline.<sup>85</sup> Only slight modifications to the oxidant were needed to achieve the silylation of varied substrate types. The authors reported 13 examples of the silylation of  $\alpha$ -amino acids and  $\alpha$ -amino alcohols (Scheme 30a), 15 examples of the silylation of dipeptides (Scheme 30b), and 10 examples of the silylation of tri- and tetrapeptides (Scheme 30c). That work contains the first applications of the silylation of C–H bonds to the late-stage modification of peptides.

The functional group that binds to the catalyst and allows the installation of the auxiliary is not limited to amines and amides. In 2021, Jiang and Li reported a directed, intramolecular C–H silylation of a substrate containing an aminoxyamide auxiliary.<sup>86</sup> From the ketone, an oxime linked by a methylene to a *N*-fluoroaryl amide is installed. The auxiliary is proposed to engage in two-point binding with the catalyst to enable the C–H activation. This method was applied to the late-stage silylation of santonin (Scheme 31).

### Scheme 30. Pd-Catalyzed Silylation of Primary and Secondary C–H Bonds of $\alpha$ -Amino-Acids Using a Quinoline Auxillary



### Scheme 31. Pd-Catalyzed Silylation of Santonin Using an Aminoxyamide Auxiliary



## 3. TRANSITION-METAL-CATALYZED BORYLATION OF C–H BONDS IN COMPLEX MOLECULES

While many aryl and alkyl silanes are produced on large scales, making silane reagents inexpensive, analogous boranes undergo a wider range of reactions or undergo these reactions under milder conditions. The use of common reagents, such as HBpin and B<sub>2</sub>pin<sub>2</sub>, for the borylation of C–H bonds and the capability of borylated products to undergo some of the reactions most used by synthetic chemists, such as Suzuki couplings, oxidations, and halogenations, has made the borylation of C–H bonds one of the most valuable C–H functionalization reactions.

Among methods for the borylation of C–H bonds, methods for the borylation of aryl C–H bonds are well established. Those for the borylation of alkyl C–H bonds are evolving. Catalytic systems for the borylation of aryl C–H bonds are highly selective and form aryl and heteroaryl boronates under mild conditions with limiting substrate.

The undirected borylation of the C–H bonds in arenes occurs with regioselectivity controlled by steric factors. For example, 1,3-disubstituted and 1,2,3-trisubstituted arenes undergo selective borylation at the 5-position. For heteroaryl substrates, steric factors are important, but the electronic properties of the heteroarenes can sometimes override the steric preference for the activation of one C–H bond over another or distinguish between reactivity at sterically similar C–H bonds. Guidelines for predicting the selectivity of undirected C–H borylation reactions on heteroarenes are presented in a 2014 paper from our laboratory.<sup>31</sup> Methods for the undirected borylation of aryl C–H bonds have been developed that occur with selectivities that are different from those mentioned above. Such methods achieve complementary selectivity with ligands that can interact with functional groups

on the substrate. Additionally, directed methods for the borylation of aryl C–H bonds have been developed to control regioselectivity. All such methods that have been applied to borylation of complex molecules will be reviewed in this section.

It was not until recently that new catalysts were developed with the potential to achieve the borylation of alkyl C–H bonds with the selectivities and mild reaction conditions developed for aryl C–H bonds. The selectivity of such methods was explained in the [Introduction](#) of this Review.

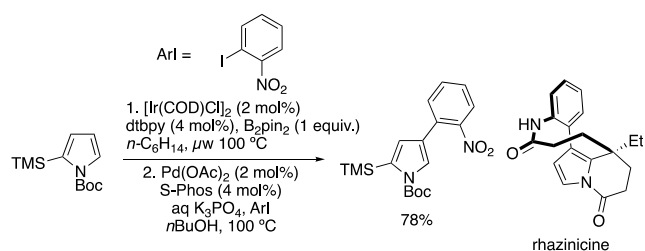
Because of the characteristics of this C–H functionalization strategy, the selective introduction of a C–B bond into a highly functionalized molecule constitutes a powerful strategy to access products that circumvents *de novo* syntheses often required to access derivatives of complex molecules with minor modifications. Therefore, C–H borylation methods are valuable for the functionalization of complex molecules in drug discovery and natural product synthesis in the early, mid, and late stage, as well as for the functionalization of organic materials and ligand scaffolds. The application of C–H borylation in all these contexts is reviewed in this section.

### 3.1. Transition-Metal-Catalyzed Borylation of C–H Bonds in Precursors to Bioactive Molecules

As noted in the introduction, the borylation of C–H bonds catalyzed by transition metal catalysts occur with high functional group tolerance and with selectivities that can be determined by steric effects or by specific functional groups that direct the transition metal to the site of borylation. Access to these borylated products under mild conditions has spurred the development of synthetic methodologies for the transformation of boronic ester products in a telescoped manner to those containing many functional groups. Taken together, these methods provide a powerful approach to the synthesis of highly decorated building blocks. This section reviews the application of this approach in synthetic campaigns toward biologically active molecules. The examples in this section are subdivided by the reaction that derivatizes the organoboron product of C–H bond functionalization.

**3.1.1. Formation of C–C Bonds in Precursors to Bioactive Molecules Enabled by the Borylation of C–H Bonds.** The capability of boronic esters and boronic acids to participate in C–C bond-forming reactions, such as Suzuki–Miyaura couplings,<sup>87,88</sup> makes the borylation of C–H bonds a particularly powerful way to disconnect complex molecules. In one of the earliest examples, Gaunt et al. synthesized rhazinicine by a borylation cross-coupling sequence of the appropriate pyrrole ([Scheme 32](#)).<sup>89</sup> Under microwave irradiation, the combination of  $[\text{Ir}(\text{cod})\text{Cl}]_2$  and dtbpy catalyzed the borylation of the 3-position of *N*-Boc-2-trimethylsilylpyrrole. The 3-borylpyrrole product was immedi-

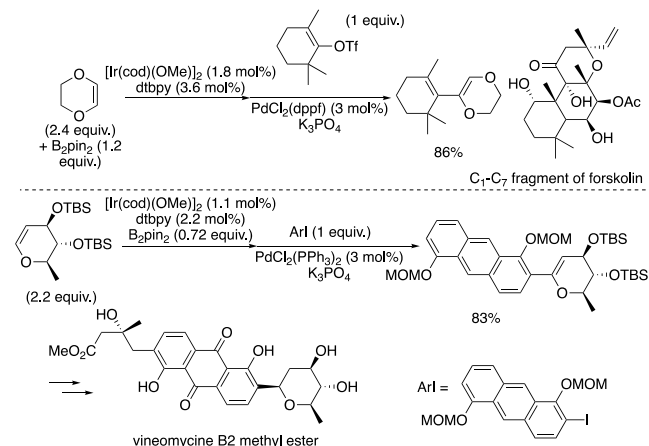
#### Scheme 32. Borylation and Subsequent Cross-Coupling of *N*-Boc-2-trimethylsilylpyrrole en route to Rhazinicine



ately engaged in a Suzuki–Miyaura cross-coupling reaction. Neier et al. later used a similar strategy for the synthesis of rhazininam analogues.<sup>90</sup>

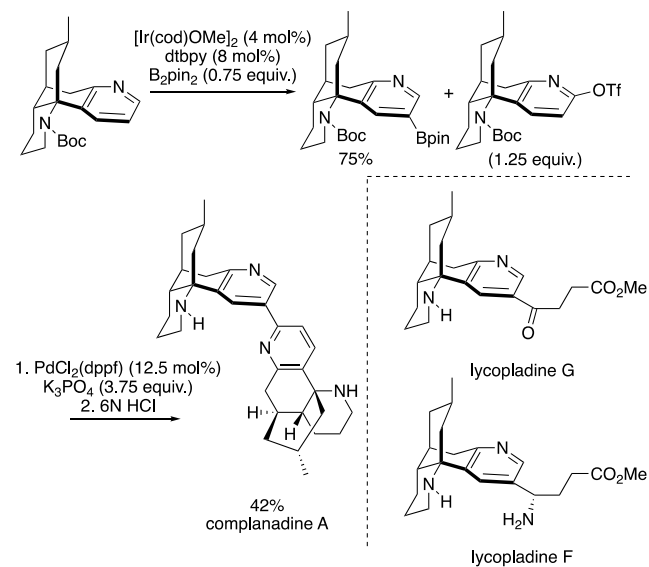
In 2008, Miyaura et al. disclosed that the combination of dtbpy and iridium catalyzes the borylation of vinyl C–H bonds without deleterious hydroboration of the olefin. The telescoped borylation cross-coupling sequence of enol ethers was applied to the synthesis of key fragments of forskolin and vineomycine B2 methyl ester ([Scheme 33](#)).<sup>91</sup>

#### Scheme 33. Synthesis of Forskolin and Vineomycine B2 Methyl Ester Enabled by the Borylation of Vinyl C–H Bonds



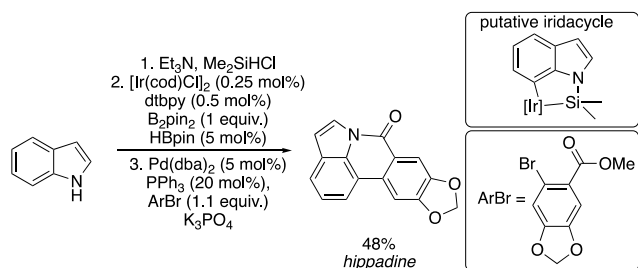
Sarpong et al. reported a synthesis of complanadine A that exploited the innate symmetry of the molecule. Complanadine A was recognized to be an unsymmetrical dimer of lycodine. Borylation of the pyridine ring of *N*-Boc lycodine, subsequent dimerization with the lycodine triflate, and global deprotection afforded the desired natural product. Lycopladiene F and lycopladiene G were also synthesized from the same 3-borylpyridine intermediate ([Scheme 34](#)).<sup>92</sup>

#### Scheme 34. *meta*-Selective Borylation of Lycodine for the Preparation of the Key Intermediate in the Synthesis of Complanadine A, Lycopladiene F, and Lycopladiene G



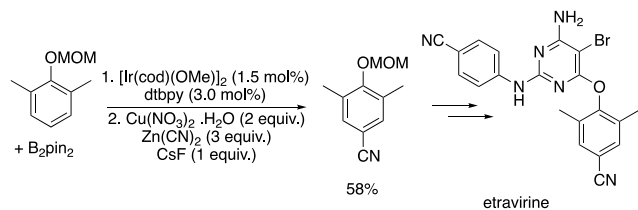
Unprotected indoles lacking a 2-substituent typically react to form 2-boryl indoles. In 2010, our laboratory reported a procedure for the silyl-directed borylation of indoles leading to 7-borylated indoles. Indole was allowed to react with dimethylchlorosilane to install a silylamine directing group. Under iridium catalysis, the silane Si–H oxidatively adds to the iridium center and the 7-C–H bond is cleaved to form a five-membered metallacycle, which leads to the observed site selectivity. This method was used to create a one-pot silylation–borylation cross-coupling sequence to synthesize hippadine in good yield (Scheme 35).<sup>93</sup>

**Scheme 35. Silyl-Directed 7-Borylation of Indoles in the Synthesis of Hippadine**



In 2010, our laboratory developed copper-mediated conditions for a telescoped borylation–cyanation sequence that enabled the formal C–H cyanation of arenes with zinc cyanide. This method was applied to the synthesis of a key benzonitrile intermediate en route to etravirine (Scheme 36).<sup>94</sup>

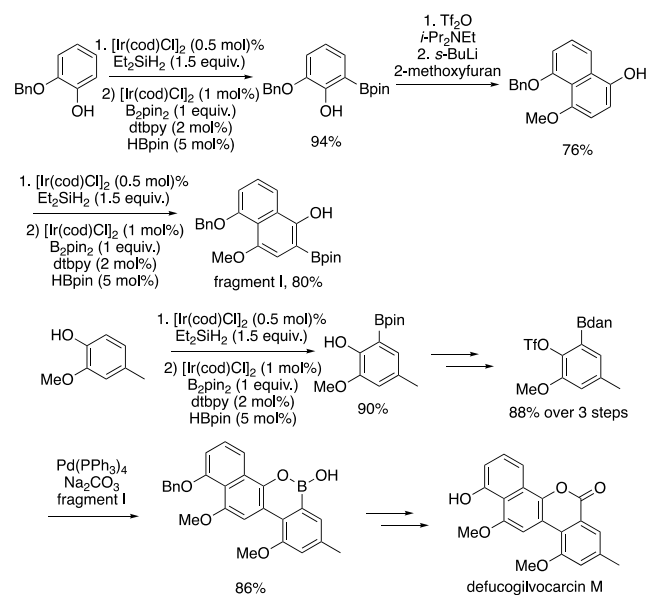
**Scheme 36. Formal Cyanation of Aryl C–H Bonds Applied to the Synthesis of Etravirine**



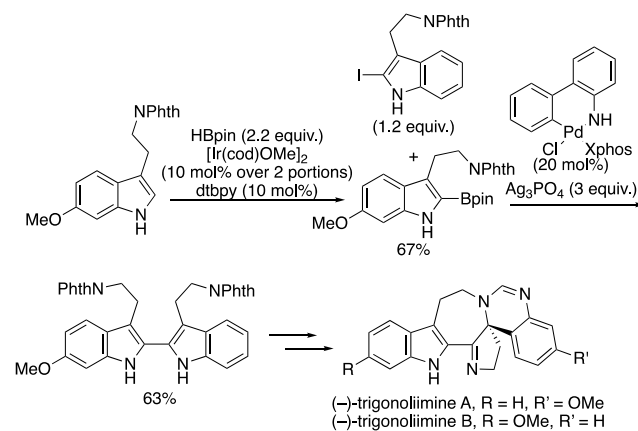
In 2014, Hosoya et al. developed a route to defucogilvocarcin M that utilizes silyl-directed *ortho*-borylation of phenols extensively (Scheme 37). Monobenzy catechol was silylated and *ortho*-borylated to afford an *ortho*-boryl phenol. The phenol was converted to the corresponding triflate. Addition of *s*-BuLi induced benzyne formation, which in turn was trapped in a [4 + 2] cycloaddition with 2-methoxyfuran, to afford fragment I. The other half of the molecule was also constructed via silyl-directed *ortho*-borylation of creosol. The creosol boronic ester was converted to the corresponding Bdan triflate. Suzuki coupling of the two fragments followed by carbonylation of the boronic acid and finally global deprotection afforded the desired natural product.<sup>95</sup>

Movassaghi et al. reported that the combination of [Ir(cod)OMe]<sub>2</sub> and dtbpy catalyzes the 2-selective borylation of tryptamine with HBpin. The coupling of the 2-borylindole product and a 2-iodoindole in the presence of Xphos–Pd–G3 and silver phosphate afforded 2,2′-bisindole precursors en route to the synthesis of trigonoliimine A and B (Scheme 38).<sup>96</sup>

**Scheme 37. Silyl-Directed *ortho*-Borylation of Phenols in the Synthesis of Defucogilvocarcin M**



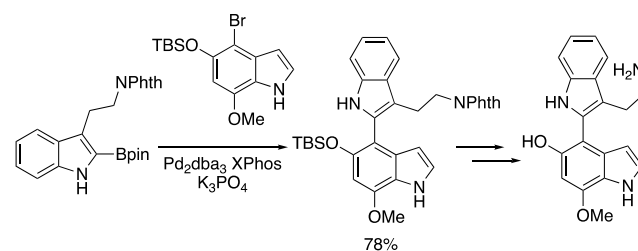
**Scheme 38. Synthesis of Trigonoliimine A and B via the 2-Selective Borylation of Tryptamine Derivatives**



Movassaghi et al. again utilized the selective 2-borylation of tryptamine to synthesize 2,5′-bisindole precursors that enabled cyclizations to form bisindole alkaloids (Scheme 39).<sup>97</sup>

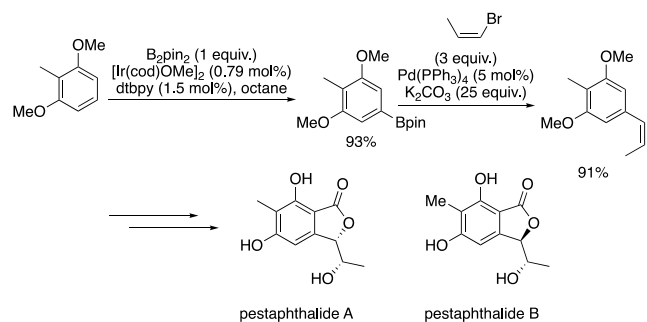
Koert et al. reported the synthesis of pestaphthalide A and B by the borylation of a dimethoxyarene to provide the precursor to cross-coupling with a vinyl bromide. A short sequence comprising a Jacobsen epoxidation of the olefin and stereo-

**Scheme 39. Synthesis of 2,5′-Bisindoles from the Cross-Coupling of 5-Bromoindoles and 2-Borylindole**



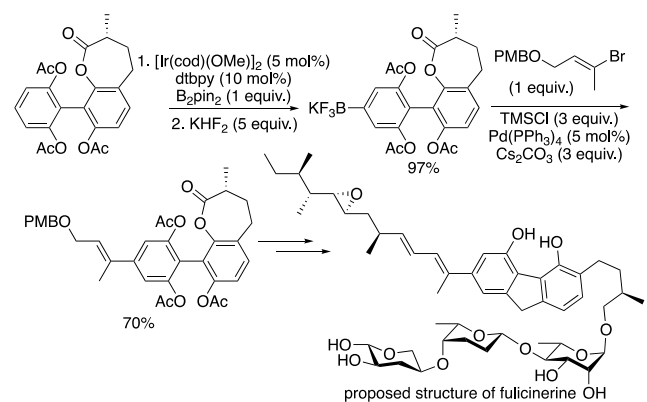
divergent epoxide opening afforded the two natural products (Scheme 40).<sup>98</sup>

#### Scheme 40. Synthesis of Pestaphthalide A and B via the *meta*-Selective Borylation of a Dimethoxyarene



Koert et al. applied a borylation cross-coupling sequence to the synthesis of the proposed structure of fucinerine and fucineroside (Scheme 41). Comparison of the spectral data

#### Scheme 41. Borylation Cross-Coupling Enabled the Structural Reassignment of Fucinerine

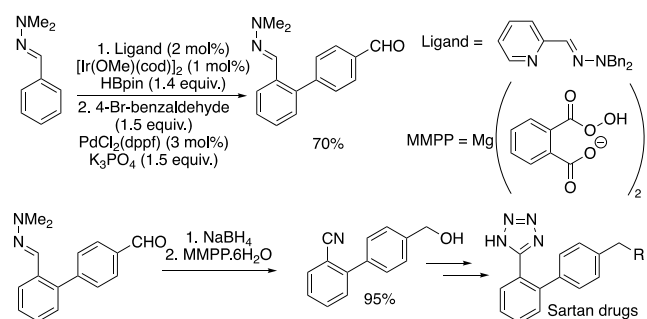


obtained from the synthetic material to that of the isolated natural product suggested a structural misassignment in the original isolation report.<sup>99</sup>

In 2012, Lassaletta et al. developed a hemilabile hydrazonepyridine ligand for the *ortho*-selective borylation of aryl hydrazones. The boronic ester products underwent cross-coupling to afford precursors to sartan drugs (Scheme 42).<sup>100</sup>

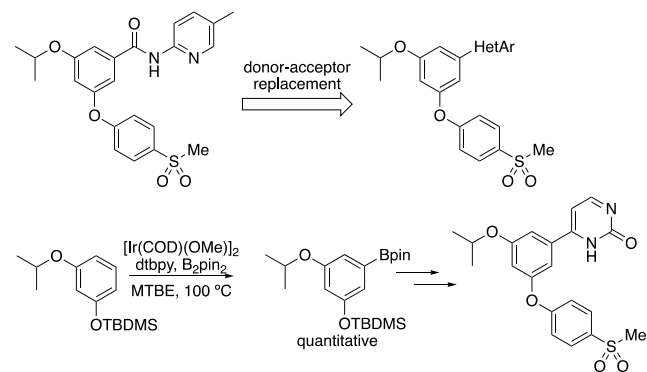
Filipski and co-workers at Pfizer endeavored to conduct donor–acceptor replacement of a heteroaryl amide with a series

#### Scheme 42. Synthesis of Sartan Drugs via the *ortho*-Selective Borylation of Aryl Hydrazones



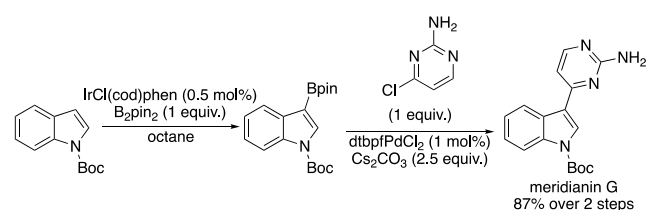
of heteroaryl groups as part of a glucokinase-activator discovery campaign. The pyrimidone derivative was synthesized by the elaboration of a dialkoxyarene using a borylation cross-coupling sequence (Scheme 43).<sup>101</sup>

#### Scheme 43. Borylation Cross-Coupling Enables the Synthesis of Glucokinase Activators



In 2014, Colacot et al. reported a phenanthroline-ligated precatalyst for the borylation of arenes. With this precatalyst, they conducted the borylation of *N*-Boc indole selectively at the 3-position and cross-coupled the product to an aminopyrazine in a concise synthesis of meridianin G (Scheme 44).<sup>102</sup> The 3-selectivity arises from steric factors and is preceded by the borylation of *N*-Boc indoles with more typical catalyst precursors.<sup>103</sup>

#### Scheme 44. Borylation Cross-Coupling in the Synthesis of Meridianin G



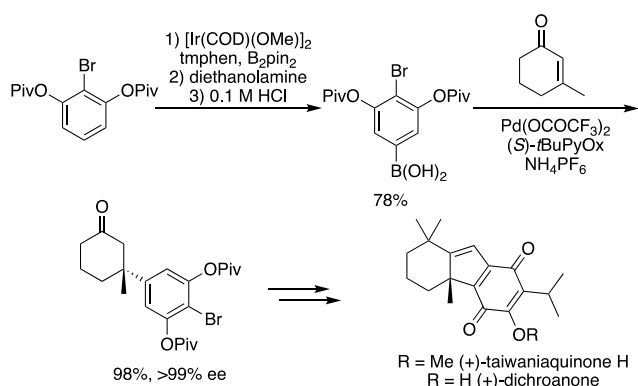
In 2014, Stoltz et al. reported the total synthesis of dichroanone and taiwaniaquinone, during which a bromoarene was borylated at a C–H bond to afford a key boronic acid. Engagement of this boronic acid with a palladium catalyst containing a chiral PyOx ligand resulted in enantioselective conjugate addition to a cyclohexenone (Scheme 45).<sup>104</sup>

Gaunt et al. reported a synthesis of dictyodendrin B that included six direct functionalizations of the initial 4-bromo indole. Of the six functionalizations, five were functionalizations of C–H bonds. Notably, formal C–H arylation of the C-7 position was achieved via a borylation cross-coupling sequence (Scheme 46).<sup>105</sup>

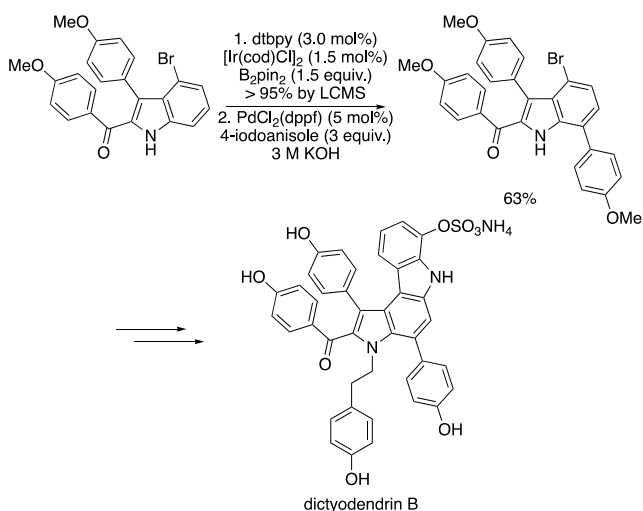
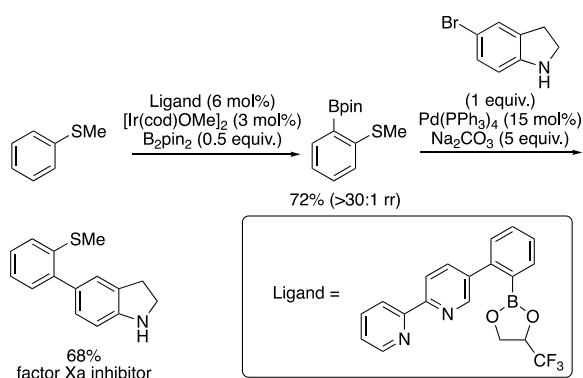
In 2017, Kanai et al. reported that catalysts formed from bipyridine ligands containing a boryl substituent catalyze the borylation of thioanisoles with high *ortho*-selectivity. The selectivity was presumed to arise from attractive interactions between the Lewis basic sulfide and the Lewis acidic boryl substituent on the ligand. This borylation was applied to the synthesis of an intermediate in the preparation of a factor Xa inhibitor (Scheme 47).<sup>106</sup>

In 2017, Kuninobu et al. reported that catalysts formed from bipyridine ligands containing a trifluorotolyl substituent

Scheme 45. Borylation Conjugate Addition in the Synthesis of Taiwaniaquinone H and Dichroanone

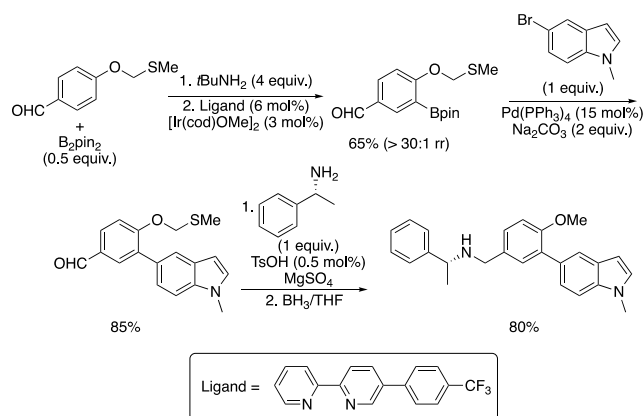
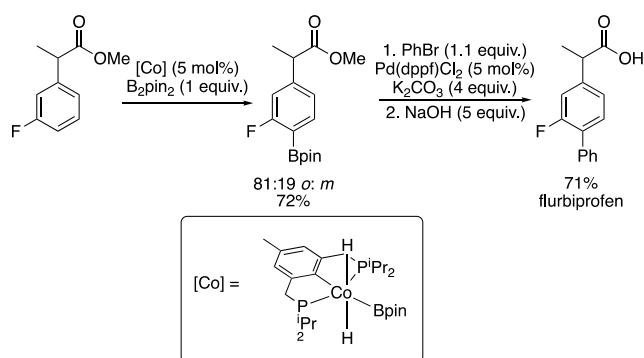


Scheme 46. Borylation Cross-Coupling in the Synthesis of Dictyodendrin B

Scheme 47. *ortho*-Selective Borylation of Thioanisoles Enable the Synthesis of a Factor Xa Inhibitor

catalyze the borylation of methylthiomethyl ethers with *ortho*-selectivity. The protecting group was then cleaved under reductive conditions to reveal a methyl ether. This borylation process was used as part of the synthesis of a calcium receptor modulator (Scheme 48).<sup>107</sup>

Chirik et al. has developed a variety of cobalt complexes that catalyze the borylation of aryl C–H bonds. In 2017, this group reported the PCP-ligated cobalt catalyst shown in Scheme 49 for the selective *ortho*-borylation of fluoroarenes. The observed

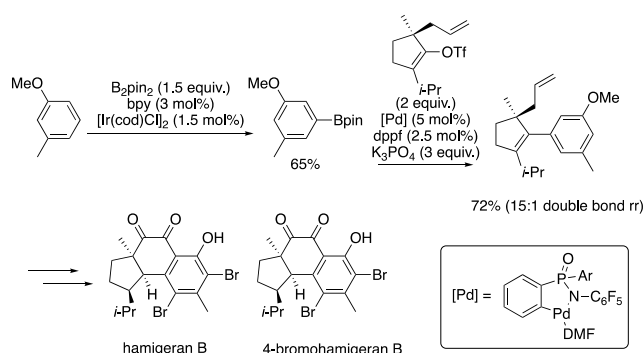
Scheme 48. *ortho*-Selective Borylation of Methylthiomethyl Ethers in the Synthesis of a Calcium Receptor ModeratorScheme 49. Cobalt-Catalyzed *ortho*-Borylation of Fluoroarenes Applied to the Synthesis of Flurbiprofen

*ortho*-selectivity was attributed to the enhanced sensitivity of a first-row metal to electronic factors overriding the greater steric sensitivity typical of the precious metal catalysts. Cross-coupling of the boronic ester product was conducted as part of the synthesis of flurbiprofen.<sup>108</sup>

Han et al. reported the synthesis of (–)-hamigeran B and (–)-4-bromohamigeran B, during which a 3-methylanisole was borylated selectively and cross-coupled to a vinyl triflate to afford the key intermediate. Subsequent oxidation and Friedel–Crafts cyclization afforded the core of the molecule (Scheme 50).<sup>109</sup>

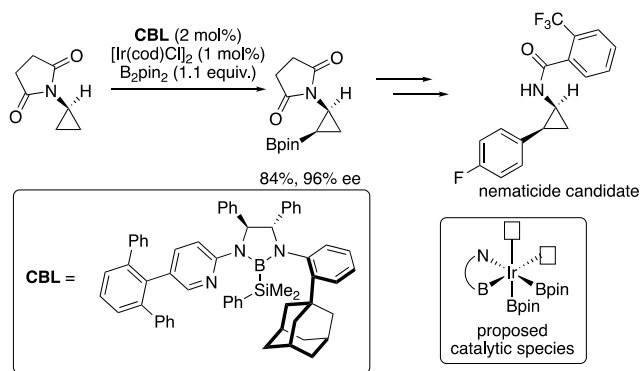
In 2022, Xu et al. reported a chiral boryl ligand that binds to iridium and generates a catalyst for the enantioselective

Scheme 50. Borylation Cross-Coupling en route to Hamigeran B and 4-Bromohamigeran B



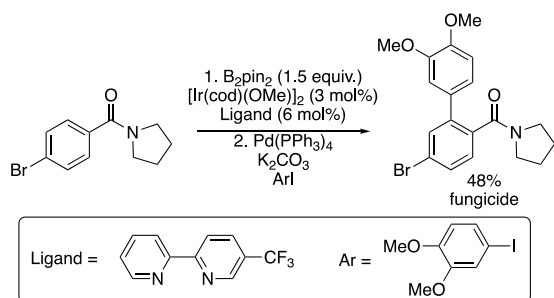
borylation of aminocyclopropanes. The chiral borylpyridine ligand is presumed to bind to iridium in an LX fashion, thereby imparting a chiral environment, while maintaining an open coordination site available to interact with directing groups. This reaction was applied to the synthesis of a nematocide candidate (Scheme 51).<sup>110</sup>

### Scheme 51. Enantioselective Borylation of Aminocyclopropanes Enables the Synthesis of a Nematocide Candidate



Mascareñas et al. reported that the combination of iridium with a 3-trifluoromethylbipyridine ligand forms a catalyst for the borylation of aryl amides with exclusive *ortho*-selectivity. The selectivity is understood to arise from noncovalent interactions between the amide functionality and the trifluoromethyl-substituted ring of the bipyridine. This reaction was applied to a concise synthesis of a fungicide by a borylation and cross-coupling sequence (Scheme 52).<sup>111</sup>

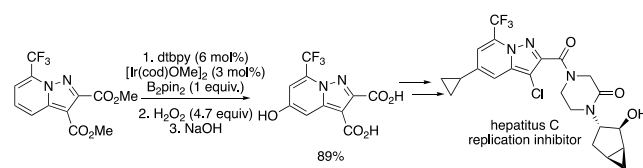
### Scheme 52. *ortho*-Selective Borylation of Amides in the Synthesis of a Fungicide



**3.1.2. Transition-Metal-Catalyzed Borylation of C–H Bonds in the Synthesis of Precursors to Bioactive Molecules through Oxidation of the Boronic Ester to the Corresponding Alcohol.** The oxidation of boronic esters is one of the oldest transformations of boronic esters. The combination of a *meta*-selective borylation followed by oxidation to the alcohol can be considered a formal *meta*-selective oxidation of arenes.

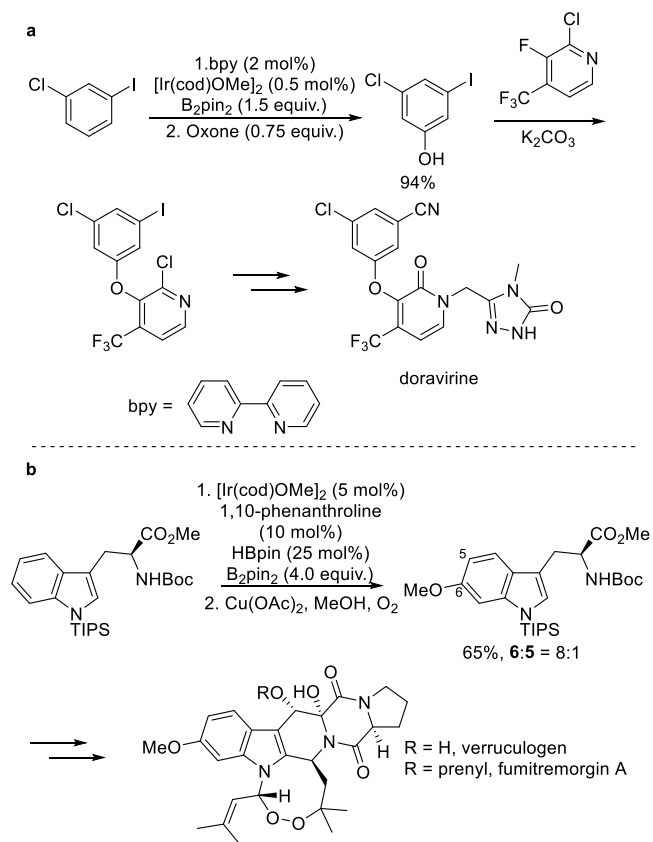
In 2014, Peat and co-workers from GlaxoSmithKline applied a borylation–oxidation sequence to the synthesis of hepatitis C replication inhibitors (Scheme 53).<sup>112</sup> The resulting phenol was converted to the triflate and coupled to a cyclopropyl boronic acid to form the pyrazolo[1,5-a]pyridine substituted at the 5-position.

### Scheme 53. Formal Oxidation of Aryl C–H Bonds via Borylation–Oxidation Applied to the Synthesis of Hepatitis C Replication Inhibitors



Campeau and co-workers at Merck reported the synthesis of doravirine by the combination of borylation and oxidation. To deliver the necessary chloriodophenol intermediate on a 75 kg scale, a borylation–oxidation sequence was developed. 2,2'-Bipyridine was chosen as an economical replacement for the more expensive dtbpy ligand for the borylation. The 3-chloro-5-iodophenol intermediate was then further coupled with cyanide, and the resulting benzonitrile was used in an  $S_NAr$  reaction to afford doravirine (Scheme 54a).<sup>113</sup> In Baran et al.'s

### Scheme 54. Formal Oxidation of Aryl C–H Bonds through Borylation–Oxidation Enabled a Synthesis of Doravirine on 100 kg Scale and the Total Synthesis of Verruculogen and Fumitremorgin A



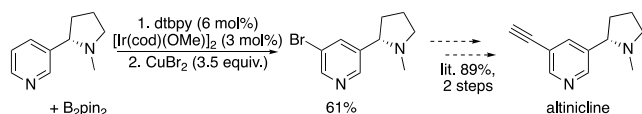
synthesis of verruculogen and fumitremorgin A, a key 6-methoxyindole intermediate was synthesized by the 6-selective borylation of an *N*-triisopropylsilyl (TIPS)tryptophan, with the *N*-TIPS protecting group shielding the 2- and 7- positions from undergoing borylation (Scheme 54b).<sup>289</sup>

**3.1.3. Transition-Metal-Catalyzed Borylation of C–H Bonds in the Synthesis of Precursors to Bioactive Molecules through the Corresponding Halide or**



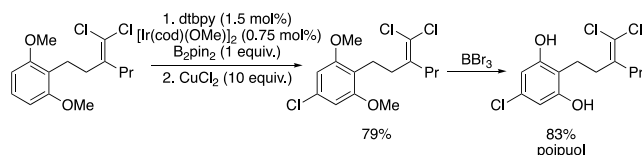
**Pseudohalide.** In 2007, our laboratory developed copper-mediated conditions that transformed aryl boronic esters into the corresponding halide. The reaction sequence has been telescoped into a one-pot, two-step sequence that provides a method for the halogenation of arenes with selectivities distinct from those of electrophilic aromatic substitution, often leading to selective halogenation at the meta-position of an arene or heteroarene. For example, the *meta*-selective borylation of nicotine, followed by oxidative bromination, afforded 5-bromonicotine, which is an intermediate en route to the synthesis of altinicline (Scheme 55).<sup>114</sup>

**Scheme 55. Borylation–Bromination of the Pyridine Intermediate en route to Altinicline**



Koert et al. used the *meta*-selective borylation followed by chlorination to synthesize the key chloride intermediate in a synthesis of poipool. Notably, a tetrasubstituted olefin was tolerated in this sequence (Scheme 56).<sup>115</sup>

**Scheme 56. Formal Chlorination of Aryl C–H Bonds by the Combination of Borylation and Chlorination in the Synthesis of Poipool**

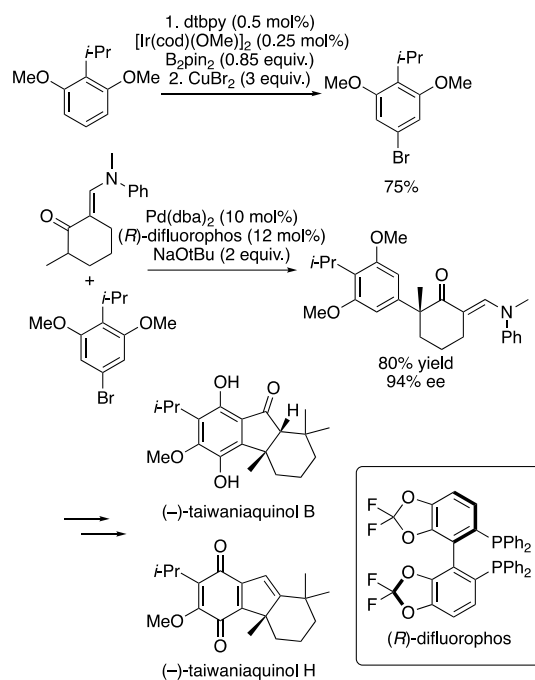


In 2011, our laboratory reported a synthesis of taiwaniaquinone H and taiwaniaquinone B that included this sequence. Ir-Catalyzed, *meta*-selective borylation of a 1,2,3-trisubstituted arene followed by conversion of the boronic ester to the bromide afforded a densely functionalized bromoarene. The bromo-arene was a suitable substrate for the Pd-catalyzed, enantio-selective  $\alpha$ -arylation of a 2-methylcyclohexenone derivative to set a quaternary stereocenter (Scheme 57).<sup>290</sup>

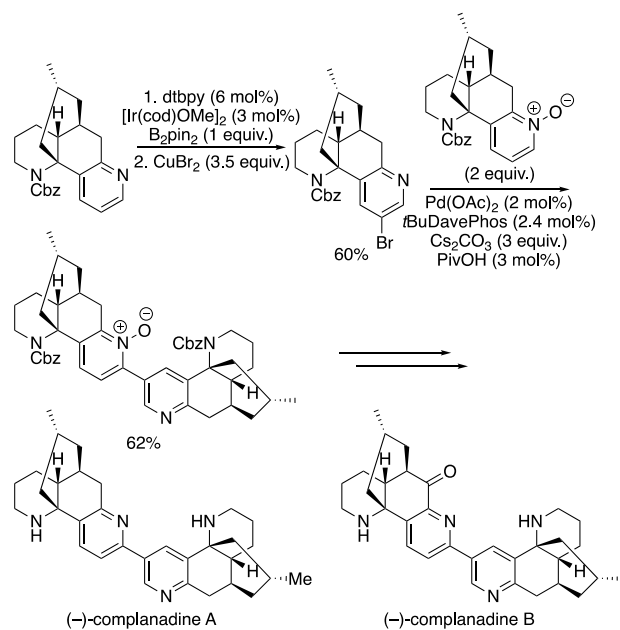
Hirama et al. used this sequence for the synthesis of complanadine A and B. Similar to the approach of Sarpong et al., Hirama's group included disconnection of the molecules into two lycodine fragments. Selective borylation of the 3-position of the pyridine was achieved in the presence of dtbpy and [Ir(cod)OMe]<sub>2</sub> to generate the desired 3-borylpyridine intermediate. In contrast to Sarpong et al.'s approach, the 3-borylpyridine was transformed to the corresponding bromide and engaged in a palladium-catalyzed arylation of a pyridine oxide (Scheme 58).<sup>116,117</sup>

Singer and co-workers at Pfizer reported the synthesis of a nicotine hapten on a 10 kg scale by the combination of borylation and bromination. They found that the reaction of nicotine with B<sub>2</sub>pin<sub>2</sub>, with [Ir(cod)Cl]<sub>2</sub> and tmphen as ligand, resulted in higher yields of 5-borylnicotine than those containing [Ir(cod)OMe]<sub>2</sub> and dtbpy. Subsequent bromination with CuBr<sub>2</sub> provided the bromide in good yield. Workup with aqueous ammonia and recrystallization with L-DBTA (L-dibenzoyltartaric acid) resulted in nearly complete removal of metal contaminants and avoided the need for chromatographic

**Scheme 57. Key Bromoarene Required for the Enantioselective Synthesis of Taiwaniaquinol B and Taiwaniaquinol H Synthesized by a Borylation–Bromination Sequence**



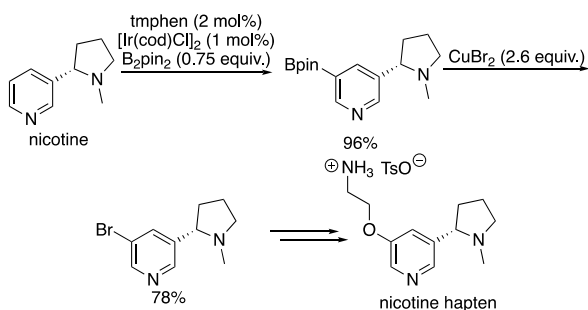
**Scheme 58. Borylation–Bromination of Lycodine in the Synthesis of Complanadine A and B**



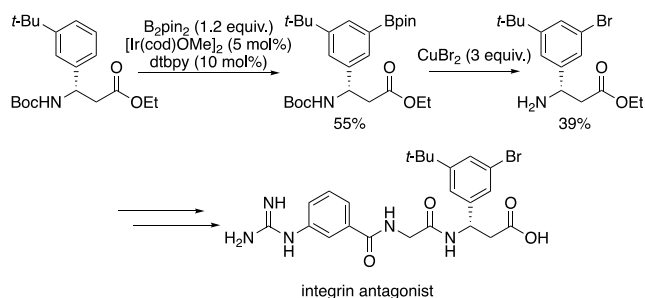
purification. Further elaboration of the bromide resulted in the desired nicotine hapten (Scheme 59).<sup>118</sup>

Nortcliffe et al. reported the borylation of a beta-aryl beta-amino acid derivative catalyzed by the combination of [Ir(cod)OMe]<sub>2</sub> and dtbpy. The boryl products underwent subsequent halogenation to the corresponding bromide smoothly. The borylation–bromination sequence did not erode the enantiomeric excess of the material and was applied to the synthesis of an integrin antagonist (Scheme 60).<sup>119</sup>

### Scheme 59. Borylation–Bromination in the Synthesis of Nicotine Hapten



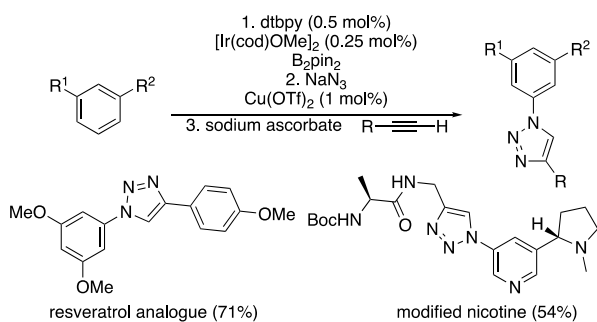
### Scheme 60. Borylation–Bromination of Beta-Aryl Propionic Acids en route to an Integrin Antagonist



**3.1.4. Transition-Metal-Catalyzed Borylation of C–H Bonds in the Synthesis of Precursors to Bioactive Molecules through the Formation of C–N Bonds.** The amination, azidation, or nitration of boronic esters further extends this strategy. The one-pot, two-step sequence of meta-selective borylation, followed by reactions that form a C–N bond, has led to selective azidation or nitration at the meta-position of an arene or heteroarene for the synthesis of medicinally active compounds. In 2014, Abell et al. developed conditions for the copper-mediated azidation of aryl boronic esters. The resulting azides were immediately engaged in a Huisgen cycloaddition to form triazoles. The telescoped borylation–azidation sequence was applied to the synthesis of triazole-substituted arenes, including a resveratrol analogue and a nicotine derivative (Scheme 61).<sup>120</sup>

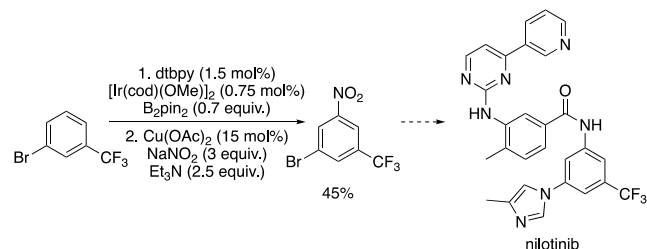
In 2019, Srinivasan et al. developed copper-mediated conditions for the nitration of aryl boronic esters. This reaction, in combination with C–H borylation, enables the rapid synthesis of nitroarenes and the corresponding anilines.

### Scheme 61. Formal Azidation of Aryl C–H Bonds by the Combination of Borylation and Azidation Applied to the Synthesis of Triazole-Decorated Natural Products



The telescoped borylation–nitration protocol was applied to the synthesis of the core of nilotinib (Scheme 62).<sup>121</sup>

### Scheme 62. Formal Amination of Aryl C–H Bonds by the Combination of Borylation and Nitration Applied to the Synthesis of Nilotinib



## 3.2. Transition-Metal-Catalyzed, Late-Stage Borylation of C–H Bonds in Complex Molecules

This section of the review provides information on the application of the borylation of C–H bonds to the late-stage functionalization of complex molecules. Examples of the borylation of C–H bonds will be divided into methods that functionalize aryl C–H bonds and methods that functionalize alkyl C–H bonds. Within those categories, the methods will be further divided into undirected examples and directed examples.

### 3.2.1. Late-Stage Modification of Complex Molecules by the Undirected Borylation of Aryl C–H Bonds.

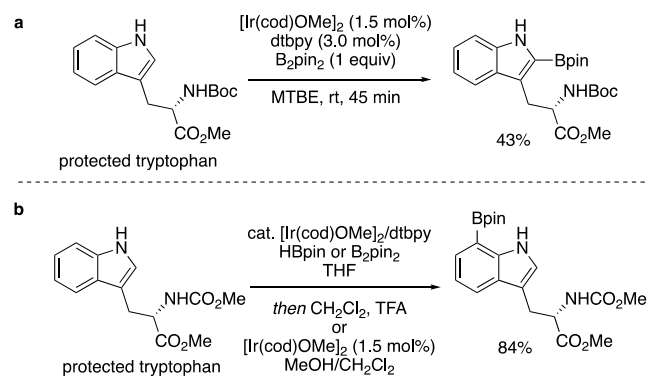
Many applications of the undirected, metal-catalyzed borylations of aryl C–H bonds in complex molecules have been reported. For late-stage functionalization of such compounds, material is often limited and valuable. Thus, it is especially advantageous to achieve high regioselectivity without the requirement of additional synthetic steps to install and remove directing groups.

The general set of conditions for the undirected borylation of aryl C–H bonds that is most used for the late-stage functionalization of complex molecules is a catalyst formed from [Ir(cod)OMe]<sub>2</sub> and either 3,4,7,8-tetramethyl-1,10-phenanthroline (tmphen) or 4,4'-di-*tert*-butyl-2,2'-bipyridine (dtbpy) and HBpin or B<sub>2</sub>pin<sub>2</sub> as the boron source. Other ligand systems form catalytic complexes from iridium precatalysts for the directed borylation of aryl C–H bonds on complex molecules, and such systems will be reviewed second in this section.

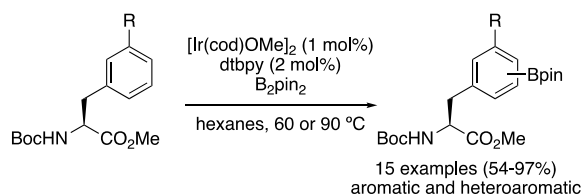
The catalyst generated from the combination of [Ir(cod)OMe]<sub>2</sub> and dtbpy was reported for the C2 borylation of protected tryptophan by Smith and Maleczka et al. in 2009 (Scheme 63A).<sup>103</sup> In this study, the authors reported that C2 monoborylation occurred alongside competing diborylation at the C2 and C7 positions. The C2/C7 diborylated product of this reaction has been shown to undergo C2-selective protodeboronation to furnish the C7-monoborylated product when subjected to TFA, as reported by Movassaghi et al. in 2014,<sup>122</sup> or when subjected to catalytic [Ir(cod)OMe]<sub>2</sub> in MeOH/CH<sub>2</sub>Cl<sub>2</sub>, as reported by Smith and Maleczka et al. in 2015 (Scheme 63B).<sup>123</sup>

In 2010, James et al. published the C–H borylation of 15  $\alpha$ -amino acid derivatives containing aromatic and heteroaromatic side chains with a catalyst generated from [Ir(cod)OMe]<sub>2</sub> and dtbpy (Scheme 64).<sup>124</sup> Substrates with arene side chains in this study were *meta*-substituted and formed 3,5-disubstituted

**Scheme 63. C–H Borylation of Protected Tryptophan: (a) C2 Monoborylation of Protected Tryptophan and (b) C7 Monoborylation of Protected Tryptophan by Diborylation/C2-Selective Protodeborylation**



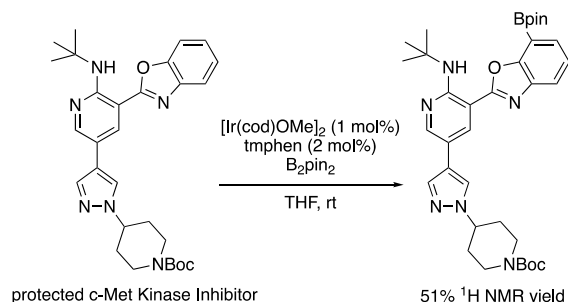
**Scheme 64. Borylation of Aryl C–H Bonds in  $\alpha$ -Amino Acid Derivatives**



aryl–Bpin products. Heteroaryl substrates included thiophene, pyridine, and indole side chains. Late-stage borylation of  $\alpha$ -amino acid derivatives is an important strategy for the synthesis of novel therapeutic agents. Methods that modify existing  $\alpha$ -amino acid derivatives are attractive because the key  $\alpha$ -stereocenter is already present, and the configuration is retained.

A benzoxazole-containing c-Met kinase inhibitor that was identified as a potential cancer therapeutic underwent borylation with a catalyst generated from  $[\text{Ir}(\text{cod})\text{OMe}]_2$  and tmphen, as reported by our laboratory in 2014 (Scheme 65).<sup>31</sup> The selectivity of borylation *ortho* to oxygen in

**Scheme 65. Late-Stage Borylation of a c-Met Kinase Inhibitor**

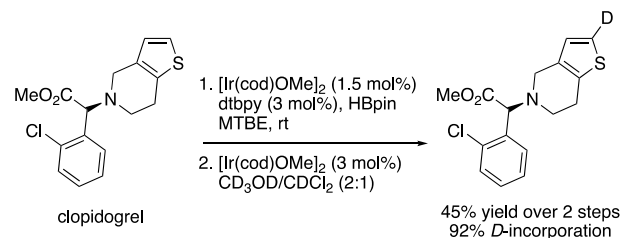


benzoxazoles is proposed to result from electronic effects.<sup>32</sup> Modification of the substitution pattern on the benzoxazole led to species with high c-Met kinase inhibition, which underscored the importance of methods that can rapidly generate diverse structures in the late stage.

The general conditions for the undirected borylation of aryl C–H bonds can be applied to two-step borylation/functionalization sequences on complex molecules, as well as

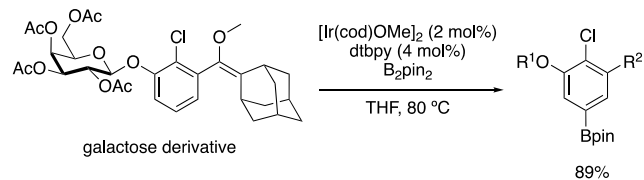
the combination of borylation and protonation of the resulting boronate to enable isotopic labeling at specific positions. Maleczka and Smith et al. used this approach to achieve a net C–H deuteration of clopidogrel, an active ingredient of Plavix. The first step consisted of C–H borylation at the 2-position of a thiophene moiety catalyzed by  $[\text{Ir}(\text{cod})\text{OMe}]_2$  and dtbpy, followed by a deuterioborylation catalyzed by  $[\text{Ir}(\text{cod})\text{OMe}]_2$  in  $\text{CD}_3\text{OD}/\text{CDCl}_3$  to afford 2-deuterioclopidogrel.<sup>123</sup> Deuterium-labeled compounds are widely used for pharmacokinetics and enzyme kinetic studies (Scheme 66).

**Scheme 66. Borylation/Deuteroborylation of Clopidogrel**



The combination of  $[\text{Ir}(\text{cod})\text{OMe}]_2$  and dtbpy catalyzed the borylation at the 5-position of a 1,2,3-trisubstituted benzene ring in a galactose derivative in a synthesis reported by Shabat et al. in 2016 (Scheme 67).<sup>125</sup> The resultant boronic ester was used to append a fluorophore to the core structure to generate chemiluminescent probes for sensing and imaging.

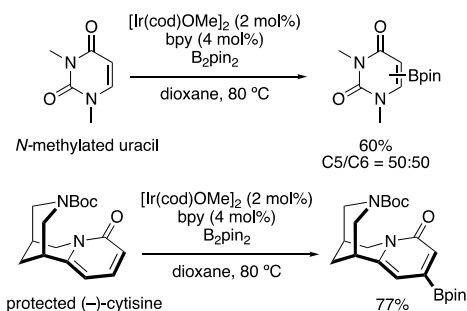
**Scheme 67. C–H Borylation of a 1,2,3-Trisubstituted Benzene on a Galactose Derivative**



In 2017, Hirano and Miura et al. published C–H borylation of 2-pyridones with a catalyst generated from  $[\text{Ir}(\text{cod})\text{OMe}]_2$  and 2,2'-bipyridine.<sup>126</sup> This catalyst system was applied to the borylation of uracil to produce the C4- and C5-borylated products in a 50:50 ratio and to the borylation of Boc-protected (–)-cytosine, which occurred with perfect site selectivity (Scheme 68).

2-Pyridones are frequently occurring substructures in complex molecules, such as ciclopirox, milrinone, camptothecin, fredericamycin, and perampanel. The importance of their

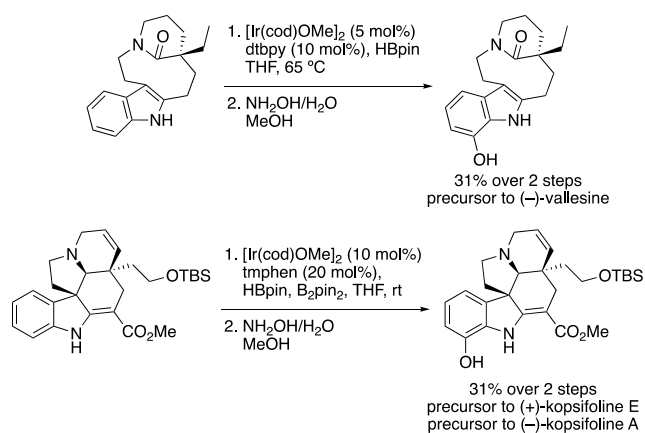
**Scheme 68. C–H Borylation of Bioactive 2-Pyridones**



borylation is exemplified in Sarpong et al.'s total synthesis of complanadine A discussed above (Scheme 68).<sup>127</sup>

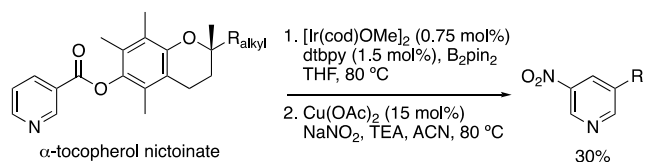
Movassaghi et al. published the C7 borylation of indole fragments in the core of the aspidosperma family of natural products to produce late-stage intermediates in the synthesis of three different natural products. In a 2018 paper, an iridium complex ligated by dtbpy catalyzed the C7-indole borylation of a polycyclic lactam.<sup>128</sup> After oxidation, the hydroxyindole intermediate generated was converted in three steps to the natural product (–)-vallesine. In a paper they published in 2021, an iridium complex ligated by tmphen catalyzed the borylation of an indole at the C7 position of a polycyclic intermediate related to the polycyclic lactam used in the synthesis of (–)-vallesine.<sup>129</sup> After oxidation, the hydroxyindole intermediate generated was converted in three steps to (+)-kopsifoline E and in four steps to (–)-kopsifoline A (Scheme 69).

### Scheme 69. C–H Borylation on the Indole Fragment of the Aspidosperma Family of Natural Products



The one-pot, two-step C–H borylation and nitration presented in Section 3.1.4 of this Review was applied to the nitration of  $\alpha$ -tocopherol nicotinate.<sup>121</sup> First, Ir-catalyzed C–H borylation with dtbpy as ligand installed a boronic ester at the C3 position of the pyridine moiety of  $\alpha$ -tocopherol nicotinate. In the same pot, the copper-catalyzed nitration furnished the 3-nitro derivative of  $\alpha$ -tocopherol nicotinate (Scheme 70).

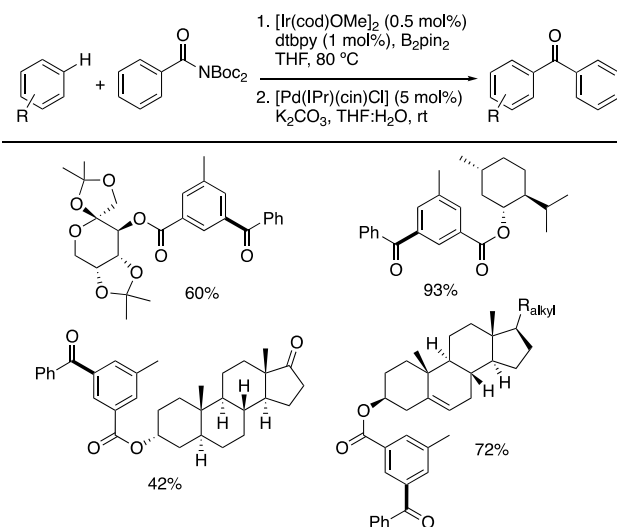
### Scheme 70. One-Pot, Two-Step Borylation/Nitration of $\alpha$ -Tocopherol Nicotinate



A two-step sequence comprising C–H borylation and acylation was published by Szostak et al. in 2020 that was performed without the isolation of the boronic ester intermediate.<sup>130</sup> Various 1,3-disubstituted arenes were borylated at the 5-position with a catalyst generated from  $[\text{Ir}(\text{cod})\text{OMe}]_2$  and dtbpy. The resulting boronic ester was subjected to Pd-catalyzed cross-coupling conditions with a bis(Boc-protected), twisted benzamide as the coupling partner to form a biaryl ketone product. This general method was

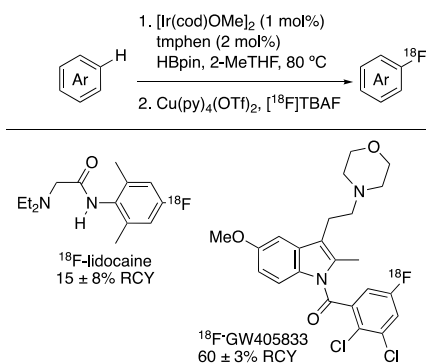
applied to the acylation of four complex molecules with the boronic ester generated by C–H borylation as the coupling partner (Scheme 71).

### Scheme 71. Two-Step Borylation/Acylation Sequence with Complex Molecules as the Boronic Ester Coupling Partner



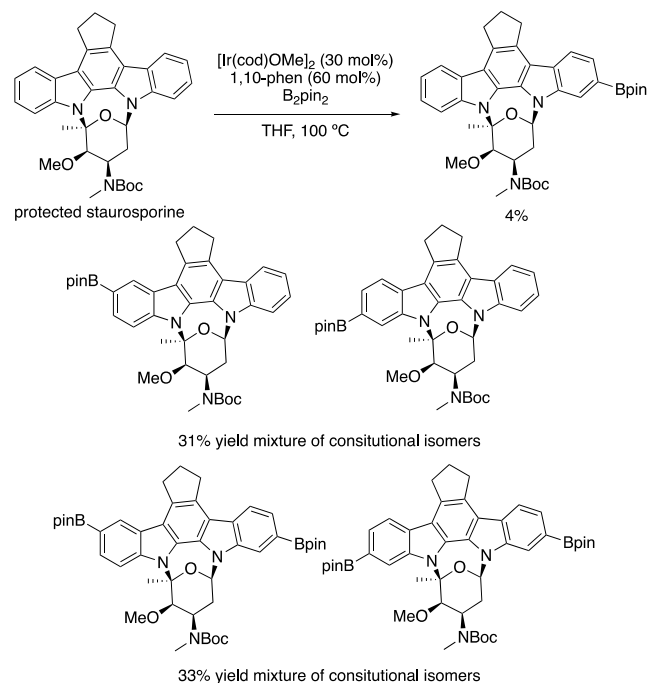
Sanford and Scott et al. published a sequence comprising C–H borylation and radiofluorination in 2021 that did not require the isolation of the borylated intermediate.<sup>131</sup> C–H borylation catalyzed by a complex generated from  $[\text{Ir}(\text{cod})\text{OMe}]_2$  and tmphen yielded the crude boronic ester intermediate, which was directly subjected to Cu-mediated radiofluorination conditions to forge the C–<sup>18</sup>F bond. This method was applied to the radiofluorination of lidocaine and a cannabinoid receptor 2 partial agonist, GW405833. The favorable properties of <sup>18</sup>F for PET highlights the importance of such methods to access bioactive <sup>18</sup>F-labeled compounds (Scheme 72).<sup>132</sup>

### Scheme 72. C–H Borylation/Radiofluorination Sequence to Access Radiolabeled, Complex Molecules



In a 2020 publication, Taube and Wood et al. applied undirected C–H borylation to generate analogues of staurosporine, a natural product with potent inhibitory properties against a majority of the human kinome.<sup>133</sup> The combination of  $[\text{Ir}(\text{cod})\text{OMe}]_2$  and 1,10-phenanthroline catalyzed the borylation of staurosporine to form five different borylated products: three from monoborylation and two from diborylation of the indoline moieties (Scheme 73). Two

## Scheme 73. C–H Borylation of Staurosporine

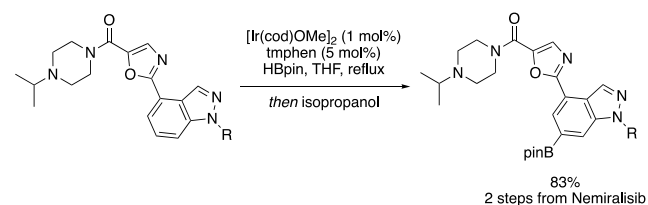


monoborylated products and the two diborylated products were not separable as boronic esters. However, upon oxidation to the corresponding phenols, the constitutional isomers could be separated.

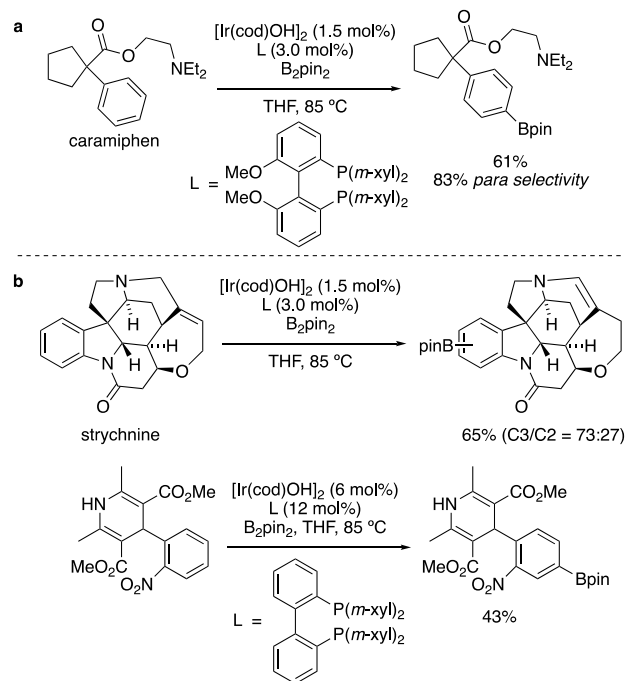
The cytotoxic activity of the monophenol constitutional isomers was evaluated against two tumor-derived cell lines. The study did not reveal increased potency over that of staurosporine. Although the reaction was unselective, the formation of five products from a single reaction, all of which could be further diversified, shows how the borylation of C–H bonds is a valuable tool for the rapid generation of complex molecule analogues.

The late-stage borylation of aryl C–H bonds in complex molecules has been applied to the large-scale synthesis of pharmaceutical compounds. In 2021, Wheelhouse and Ironmonger et al. from GSK published the borylation of an indazole C–H bond on an advanced intermediate in a route to nemiralisib, a kinase inhibitor in development as a treatment for chronic obstructive pulmonary disease.<sup>134</sup> Diborylation of the complex intermediate on the benzopyrazole ring and the oxazole ring was catalyzed by the combination of  $[\text{Ir}(\text{cod})\text{OMe}]_2$  and tmphen. The addition of isopropanol led to selective monoborylation at the oxazole to reveal a monoborylated intermediate that was transformed to nemiralisib in two steps (Scheme 74). The synthetic route was used to deliver >100 kg of nemiralisib.

## Scheme 74. C–H Borylation of an Advanced Intermediate in the Synthesis of Nemiralisib



The undirected borylation of C–H bonds on complex molecules can be achieved with iridium catalysts generated from ligands other than tmphen and dtbpy. In 2015, Itami et al. published the *para*-selective borylation of caramiphen by a catalyst generated from  $[\text{Ir}(\text{cod})\text{OH}]_2$  and OMe-xyl-BIPHEP (Scheme 75A).<sup>135</sup> Catalysts generated from the OMe-xyl-

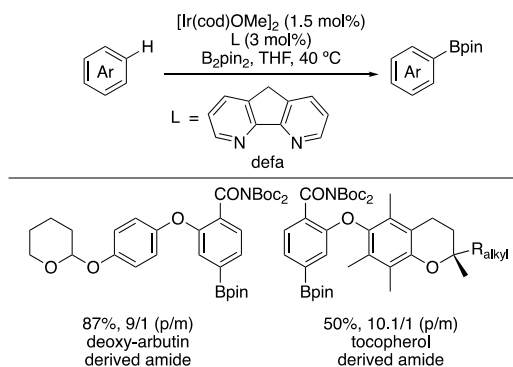
Scheme 75. *para*-Selective C–H Borylation Enabled by xyl-BIPHEP Ligands

BIPHEP ligand react with higher *para* selectivity than the iridium catalysts generated from tmphen and dtbpy. The authors suggest that the origin of the higher regioselectivity is a steric interaction between the bulky phosphine ligand and the *para* substituent on the substrate. In 2020, Itami et al. published the borylation of strychnine, a natural product, and nifedipine, a calcium channel agonist, with a catalyst generated from  $[\text{Ir}(\text{cod})\text{OH}]_2$  and a related xyl-BIPHEP ligand (Scheme 75B).<sup>136</sup> In the case of strychnine, olefin isomerization was also observed.

In 2022, Sunoj and Chattopadhyay et al. published *para*-selective, iridium-catalyzed borylations of aryl C–H bonds on twisted amides catalyzed by iridium and a 4,5-diazafluorene (defa) (Scheme 76).<sup>137</sup> Computational evidence suggests the intervening methylene on the ligand causes an in-plane distortion, which leads to a steric interaction between the ligand and the twisted amide on the substrate. The interaction is minimized by the approach of the substrate at its *para* position. This method was applied to achieve the *para*-selective borylation of two bioactive compounds.

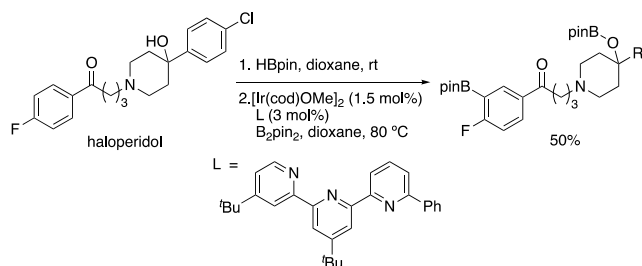
A catalytic system formed by the combination of  $[\text{Ir}(\text{cod})\text{OMe}]_2$  and a terpyridine ligand published by Ilies et al. in 2021 enabled C–H borylation *ortho* to fluorine in fluoroarenes.<sup>138</sup> Mechanistic studies suggest that the terpyridine ligand undergoes cyclometalation to generate an  $N,N,C$ -ligated iridium complex that may undergo reductive elimination to produce a borylated ligand. Computational studies suggested that both the cyclometalated iridium complex and the iridium complex containing the borylated ligand increase the energy

### Scheme 76. *para*-Selective C–H Borylation of Bioactive Compounds Enabled by a *de*fa Ligand



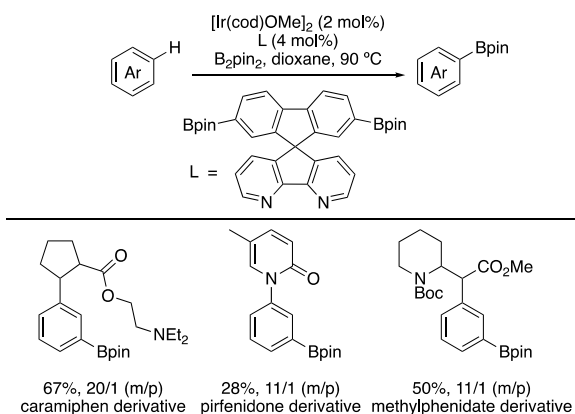
difference between the transition states for cleavage of the *meta*- and *ortho*-C–H bonds over the difference with an iridium complex ligated by dtbpy. This method was applied to achieve the *ortho* borylation of haloperidol (Scheme 77).

### Scheme 77. *ortho*-Selective Borylation of Haloperidol



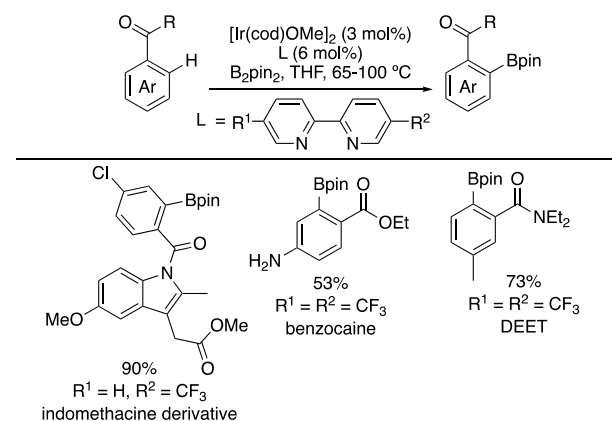
Ilies and Asaka et al. also published a *meta*-selective borylation of C–H bonds with a catalyst generated from  $[\text{Ir}(\text{cod})\text{OMe}]_2$  and a diborylated, spriopyridine ligand.<sup>139</sup> Computational evidence suggests the rooflike structure of the ligand imposes a steric interaction between the *para* substituent on the substrate and the ligand that leads to a more favorable approach of the *meta*-C–H bond than of the *para*-C–H bond. This method was applied to achieve the *meta*-selective borylation of C–H bonds in three active pharmaceutical ingredients (Scheme 78).

### Scheme 78. *meta*-Selective Borylation of Bioactive Compounds Enabled by a Functionalized Spiropyridine Ligand



In 2023, Jiménez-Osés and Mascareñas et al. published a catalytic system generated from  $[\text{Ir}(\text{cod})\text{OMe}]_2$  and either 5-trifluoromethyl-2,2'-bipyridine or 5,5'-ditrifluoromethyl-2,2'-bipyridine for the *ortho*-selective borylation of aromatic amides.<sup>140</sup> Calculations suggest that both complexes undergo the C–H activation step with higher *ortho* selectivity than does the dtbpy-derived complex because of enthalpic stabilization from a noncovalent interaction between the benzamide on the substrate and the electron-deficient ring(s) on the ligand. This system catalyzed the borylation of the *ortho* position of three biologically relevant molecules (Scheme 79).

### Scheme 79. *ortho*-Selective Borylation of Biologically Relevant Molecules Enabled by Trifluoromethyl-Bipyridine Ligands



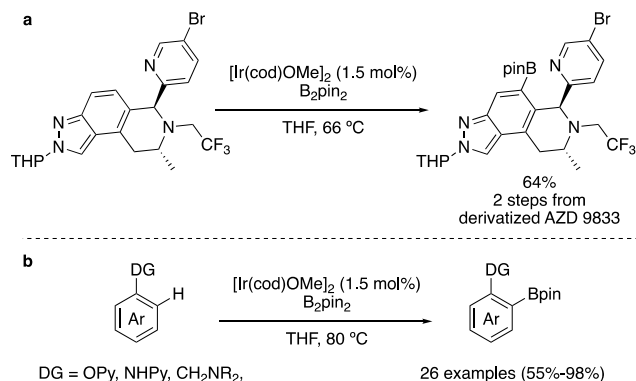
### 3.2.2. Late-Stage Modification of Complex Molecules by the Directed Borylation of Aryl C–H Bonds.

The directed borylation of aryl C–H bonds occurs when a functional group on the substrate serves as a ligand for a transition-metal complex that activates a specific C–H bond of the substrate. Although directed functionalization often requires the installation and removal of such a functional group, these reactions can occur with regioselectivity that is complementary to that of undirected approaches, thereby making them a valuable tool for the functionalization of complex molecules that contain many potential sites for C–H borylation.

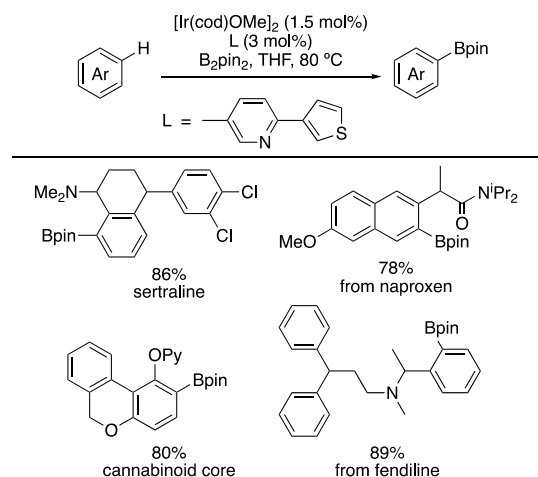
The directed borylation of C–H bonds in complex molecules can occur under ligand-free conditions with  $[\text{Ir}(\text{cod})\text{OMe}]_2$  as the precatalyst. In 2020, Scott and Moss et al. published the pyridine-directed, C–H borylation of a late-stage intermediate in the synthesis of the clinical candidate AZD9833 using  $[\text{Ir}(\text{cod})\text{OMe}]_2$  without added ligand (Scheme 80A).<sup>141</sup> In 2022, Sunoj and Chattopadhyay et al. showed that these ligand-free conditions are compatible with several directing groups and enable the directed borylation of aryl C–H bonds in 26 different complex molecules (Scheme 80B).<sup>142</sup>

Chattopadhyay et al. has also reported that the combination of  $[\text{Ir}(\text{cod})\text{OMe}]_2$  and 5-methyl-2-(thiophen-3-yl) pyridine generates a complex that catalyzes the directed borylation of aryl and heteroaryl C–H bonds.<sup>143</sup> As part of this work, they showed six complex molecules undergo C–H borylation with various directing groups (Scheme 81). The 5-methyl-2-(thiophen-3-yl) pyridine was shown to cyclometalate at the C2 position of the thiophene to form a *N,C*-bound, LX-type

**Scheme 80. Directed C–H Borylation under Ligand-Free Conditions: (a) Pyridine-Directed C–H Borylation of Late-Stage Intermediate in the Synthesis of AZD9833 and (b) Borylation of Complex Molecules Using Various Directing Groups**



**Scheme 81. Aryl C–H Borylation Directed by Various Directing Groups Using an LX-Type Ligand System**



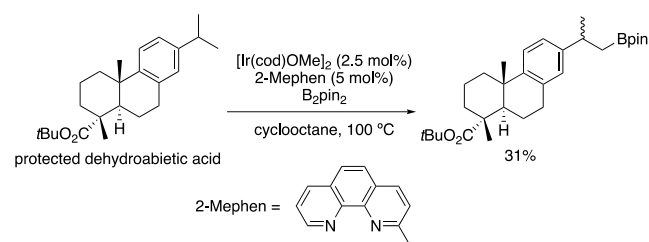
ligand, in contrast to the typical *N,N*-bound, LL-ligands used for C–H borylation.

**3.2.3. Late-Stage Modification of Complex Molecules by the Undirected Borylation of Alkyl C–H Bonds.** The development of methods for the practical, catalytic, and selective functionalization of alkyl C–H bonds without the use of a directing group is a long-standing goal of synthetic chemistry. The undirected borylation of alkyl C–H bonds is particularly valuable because the application of such methods in the late-stage diversification of complex molecules could potentially enable the installment of a wide array of functionalities in previously inaccessible positions.

There is one example of the application of transition-metal-catalyzed, undirected borylation of alkyl C–H bonds that has been applied to a complex molecule. In 2020, our laboratory published the undirected borylation of a primary C–H bond on protected dehydroabiatic acid with a catalyst generated from [Ir(cod)OMe]<sub>2</sub> and 2-methyl-1,10-phenanthroline (Scheme 82).<sup>144</sup>

**3.2.4. Late-Stage Modification of Complex Molecules by the Directed Borylation of Alkyl C–H Bonds.** The directed borylation of alkyl C–H bonds is more developed than the undirected borylation of alkyl C–H bonds. Directed approaches can control the site selectivity of the borylation.

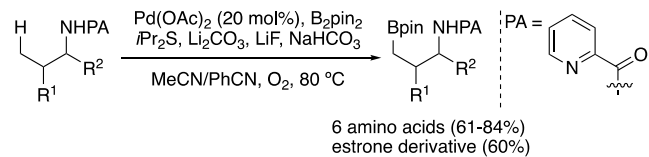
**Scheme 82. Undirected Borylation of a Primary C–H Bond in Protected Dehydroabiatic Acid**



Systems that have been applied to the directed borylation of alkyl C–H bonds in complex molecules are based on both palladium and iridium. In this section, examples with palladium systems will be reviewed first, followed by examples with iridium systems.

In 2014, Shi et al. reported the borylation of primary, alkyl C–H bonds with Pd(OAc)<sub>2</sub> as the precatalyst, diisopropyl sulfide as the ligand, and oxygen as the terminal oxidant.<sup>145</sup> A picolinyl directing group was installed on an amine to direct the C–H functionalization. The method was applied to the borylation of six amino acids and a derivative of estrone (Scheme 83). All complex molecules underwent borylation at a C–H bond  $\gamma$  to the directing group.

**Scheme 83. Pd-Catalyzed Borylation of C–H Bonds  $\gamma$  to a Picolinyl Directing Group on Complex Molecules**



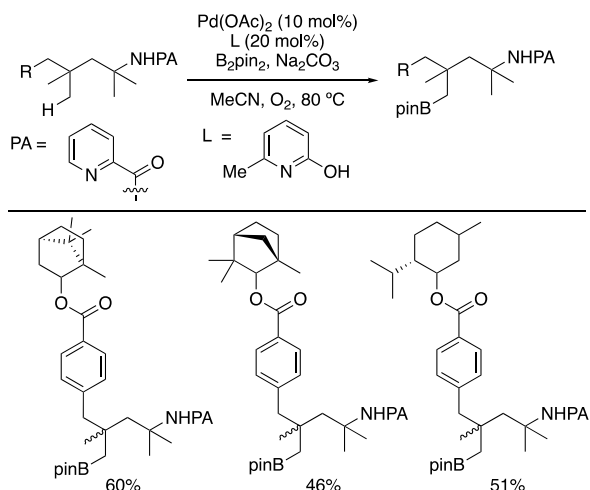
In 2021, Ge and Maiti et al. used a picolinyl directing group to achieve the borylation of primary, alkyl C–H bonds  $\delta$  to the directing group with a catalyst generated from Pd(OAc)<sub>2</sub> and 2-hydroxy-6-methylpyridine.<sup>146</sup> These reactions required the  $\gamma$  position of the substrates to be a quaternary center to avoid C–H functionalization at the  $\gamma$  position. This method was applied to three substrates with small terpenoid natural products appended (Scheme 84).

Yu et al. showed that a fluorinated, *N*-aryl amide could act as a directing group for the borylation of primary C–H bonds  $\beta$  to the directing amide.<sup>147</sup> A complex generated from Pd(OAc)<sub>2</sub> and 2,4-dimethoxyquinoline catalyzed the C–H borylation of a dehydroabiatic acid derivative with the fluorinated, *N*-aryl amide directing group appended (Scheme 85).

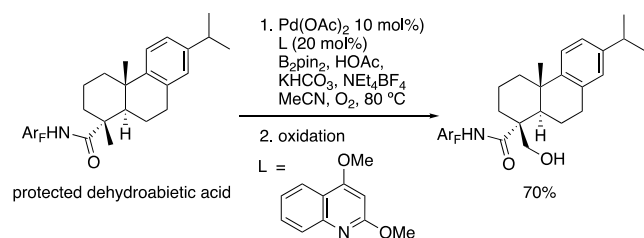
Iridium-catalyzed examples of directed borylation of alkyl C–H bonds on complex molecules have been reported by Xu et al. with a series of chiral, diamino-silylborane ligands that exhibit bidentate, *B,N*-binding. These ligands will be reviewed below. Directed reactions with such ligands are successful because of the generation of a chiral, trisboryl iridium complex with two open coordination sites that can bind the directing group and differentiate two prochiral C–H bonds.

Their publication in 2019 disclosed a system generated from [Ir(cod)Cl]<sub>2</sub> and a diamino-boryl ligand with pyridine substitution on one amino group and biaryl substitution on the other that catalyzed an amide-directed borylation of alkyl C–H bonds of cyclopanes.<sup>148</sup> The catalytic system was

### Scheme 84. Pd-Catalyzed Borylation of C–H Bonds $\delta$ to a Picolinyl Directing Group on Complex Molecules



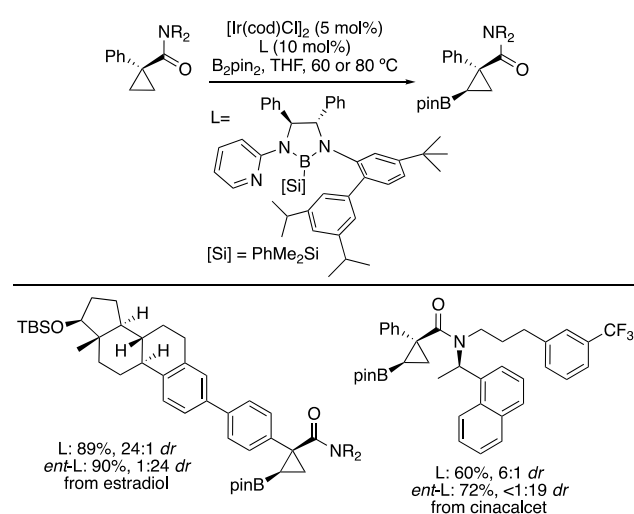
### Scheme 85. Pd-Catalyzed Borylation of C–H Bonds $\beta$ to an Amide Directing Group on a Dehydroabietic Acid Derivative



applied to the catalyst-controlled, diastereoselective borylation of C–H bonds on cyclopropane rings appended to estradiol and cinacalcet (Scheme 86).

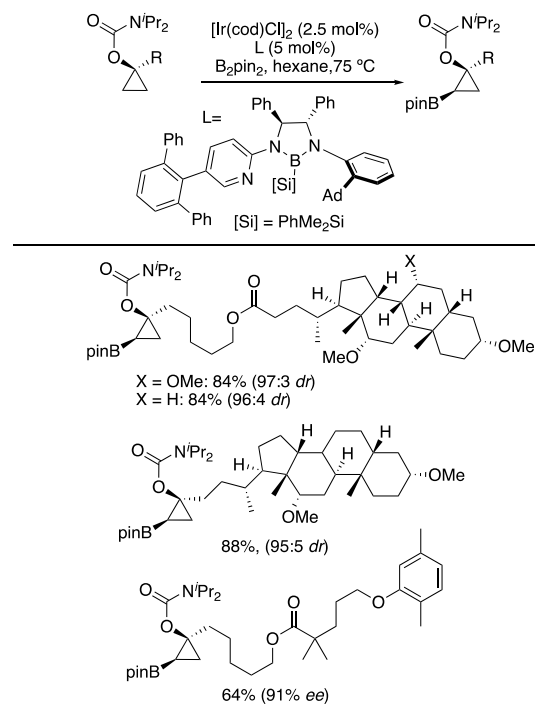
With the same iridium precatalyst and a ligand with a triaryl-substituted pyridine moiety on one amino group and a 2-adamantyl-phenyl substituent on the other, the amide-directed borylation of C–H bonds on cyclopropanols was achieved.<sup>149</sup> Xu and co-workers appended three bioactive molecules to

### Scheme 86. Diastereoselective, Amide-Directed Borylation of Cyclopropanes with a Chiral Boryl Ligand



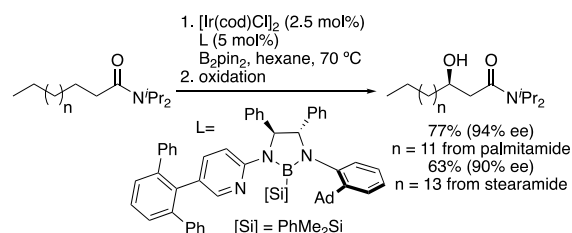
cyclopropanols to exemplify the application of this method in late-stage borylation (Scheme 87).

### Scheme 87. Stereoselective, Carbamate-Directed Borylation of Cyclopropanols with a Chiral Boryl Ligand



Xu et al. reported the same catalytic system for the enantioselective borylation of acyclic amides at C–H bonds  $\beta$  to the directing amide.<sup>150</sup> The method was applied to the enantioselective borylation of  $\beta$ -C–H bonds in three fatty-acid-derived acyclic amides (Scheme 88). Such an application exemplifies a valuable method for the conversion of cheap and abundant carboxylic acids to value-added products.

### Scheme 88. Enantioselective, Amide-Directed Borylation of Fatty Acids with a Chiral Boryl Ligand



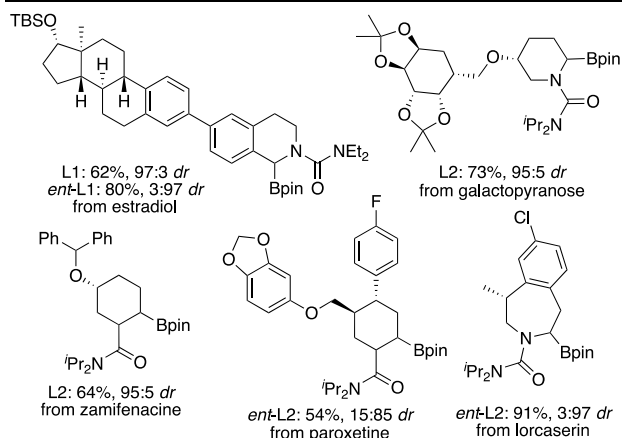
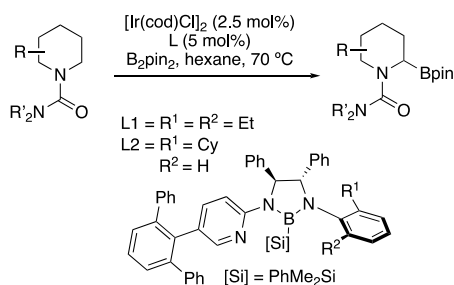
The stereoselective borylation of C–H bonds on carbocycles and azacycles beta to the carbonyl carbon center of amides was reported by Xu et al. in 2020 with a catalyst generated from  $[\text{Ir(cod)OMe}]_2$  and a ligand with a triaryl-substituted pyridine moiety on one amino group and either 2-cyclohexyl-phenyl substitution or 2,6-diethyl-phenyl substitution on the other.<sup>151</sup> This method was applied to the diastereoselective borylation of C–H bonds in saturated rings on six substrates derived from complex molecule (Scheme 89).

The stereoselective borylation of C–H bonds  $\beta$  to a directing nitrogen center also was achieved by a catalyst generated from  $[\text{Ir(cod)OMe}]_2$  and a ligand with pyridine



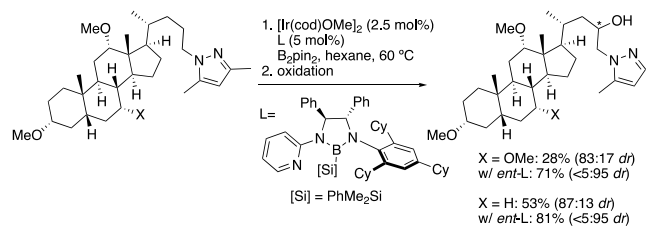
### Scheme 89. Diastereoselective, Amide-Directed Borylation of C–H Bonds on Carbocycles and Azacycles with a Chiral Boryl Ligand

Xu 2020



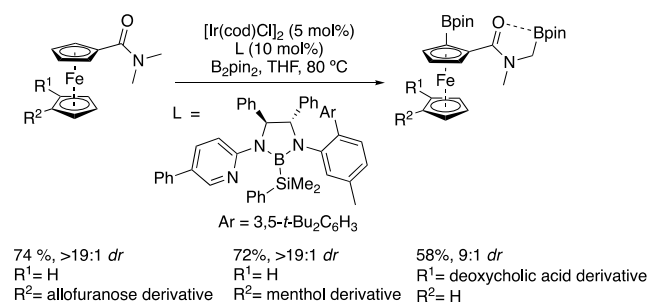
substitution on one amino group and 2,4,6-tricyclohexylphenyl substitution on the other.<sup>152</sup> The method was applied to the borylation of cholic and deoxycholic acid substituted with a pyrazole group (Scheme 90).

### Scheme 90. Diastereoselective, Pyrazole-Directed Borylation of Complex Molecule Derivatives with a Chiral Boryl Ligand



In 2022, Xu and Ke et al. published an amide-directed strategy for the dual borylation of ferrocenes at an alkyl and an aryl C–H bond.<sup>153</sup> This reaction is described here because the ligand framework for these reactions is the same as the others in this section for the directed borylation of alkyl C–H bonds. This transformation was achieved with a catalyst generated from  $[Ir(cod)Cl]_2$  and a ligand containing a 4-phenylpyridine moiety on one amino group and 2-aryl-5-methylphenyl substitution on the other. The authors appended three complex molecules to the ferrocene core and conducted the C–H borylation reaction to exemplify the use of this method on ferrocene-labeled complex molecules (Scheme 91).

### Scheme 91. Amide-Directed, Dual Alkyl–Aryl Borylation of Complex Molecule-Derived Ferrocenes

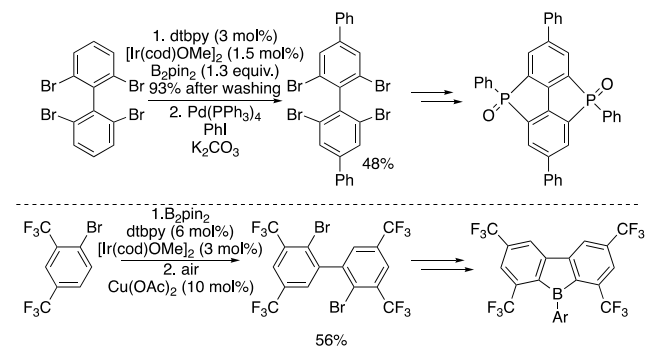


### 3.3. Transition-Metal-Catalyzed Borylation of C–H Bonds in the Synthesis of Organic Materials

The borylation of C–H bonds catalyzed by transition-metal complexes has been applied extensively to the synthesis of molecules or polymers for applications in materials science, often toward molecules with valuable photophysical properties. Molecules with valuable photophysical properties are often rich in aromatic units, thereby making the borylation of C–H bonds particularly valuable for the modification of these structures. Moreover, transition-metal-catalyzed borylations of C–H bonds typically occur at less sterically encumbered positions and with a bias toward electron-poor C–H bonds, and this selectivity is complementary to that of methods occurring through electrophilic aromatic substitution. The resultant boronic esters are versatile chemical handles that can be transformed into the desired functional group or substituent.

The distinction between applications in which the borylation has been used to synthesize valuable building blocks and those in which the borylation is used to introduce modifications at a “late stage” is not always clear. For instance, in 2011 Yamaguchi et al. showed that the borylation of tetrabromobiphenyl occurs cleanly and allows for elaboration of the biphenyl core and, ultimately, the synthesis of  $\pi$ -extended bis(phosphoryl)biphenyls (Scheme 92).<sup>154</sup> Conversely, Mard-

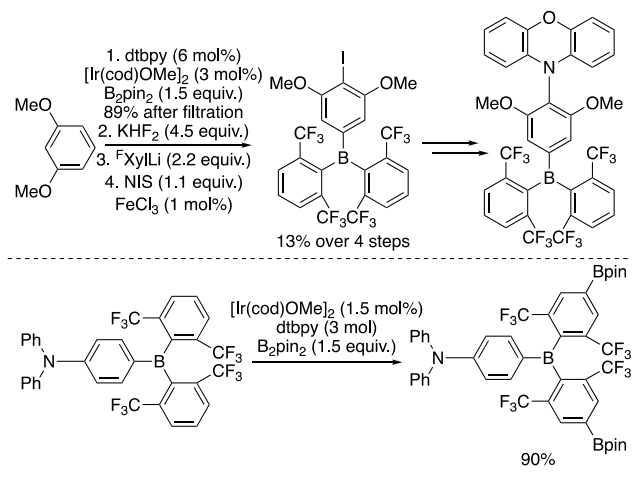
### Scheme 92. Ir-Catalyzed Borylation of Biphenyls and the Preparation of Biphenyls by Homocoupling of Arylboronic Esters Prepared by the Borylation of Arenes



er et al.’s 2020 synthesis of emissive materials containing biphenyl cores was achieved by using the borylation of simple arenes to generate *meta*-substituted boronic esters that were homocoupled to afford biphenyls and subsequently elaborated to the desired borafluorenes (Scheme 92).<sup>155</sup> Likewise, Marder et al. used the borylation of dimethoxybenzene during the synthesis of complex donor–acceptor triarylboranes that

display thermally activated delayed fluorescence (TADF). This borylation of a simple arene was used to install the central boron atom (Scheme 93).<sup>156</sup> They also showed that the

### Scheme 93. Ir-Catalyzed, *meta*-Selective Borylation of and in the Synthesis of Triarylboranes



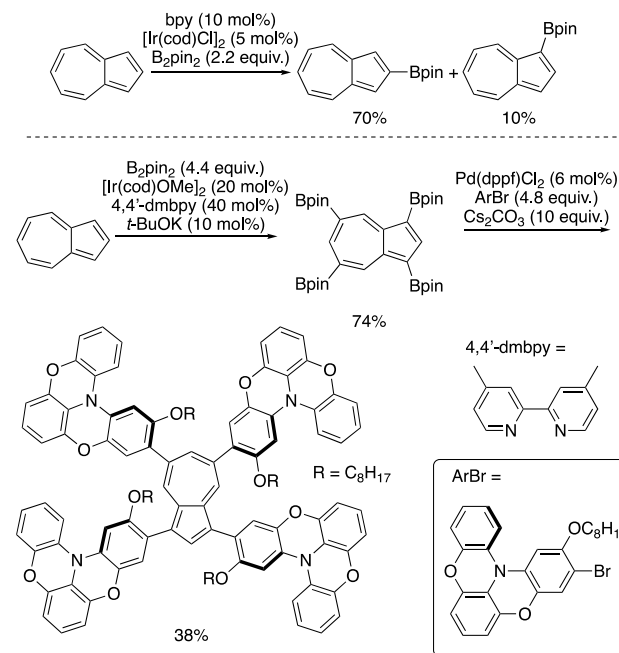
borylation of a triarylborane occurs selectively on the less-hindered, electron-poor acceptor fragment to afford modified triarylboranes that display solvent-dependent emission spectra (Scheme 93).<sup>157</sup> Thus, we have organized the examples of the borylation used to prepare organic materials in this section by structure type and only briefly address whether the borylation reaction was applied to prepare a “building block” or to conduct a “peripheral modification” at the “late stage” of the synthesis of a complex material.

**3.3.1. Transition-Metal-Catalyzed Borylation of Aryl C–H Bonds for the Synthesis and Modification of Polyaromatic Hydrocarbons.** In 2003, Sugihara et al. reported that the borylation of azulene occurs with good selectivity for the five-membered ring, with 2-borylated azulene being the major product and 1-borylated azulene being the minor product (Scheme 94). The authors proposed that the selectivity arises from  $\pi$ -complexation of the substrate to the iridium center prior to borylation.<sup>158</sup> It is also possible that the more acute bond angles in five-membered rings cause the distances between the hydrogen atoms to be longer than those in seven-membered rings and the steric hindrance in five-membered rings to be less, thereby accounting for the observed selectivity. Under more forcing conditions, polyborylation occurred to afford a mixture of products.<sup>159</sup> However, in 2015, Scott et al. showed that polyborylation of azulene converges to 1,3,5,7-tetraborylazulene under conditions that facilitate reversible borylation.<sup>160</sup> This building block was later applied to the synthesis of a hole-transporting material (Scheme 94).<sup>161</sup>

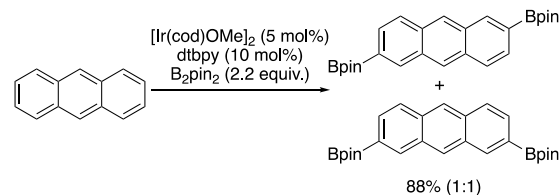
In 2011 and 2017, Kobayashi et al. reported the di-, tri-, and tetra- borylation of anthracenes (Scheme 95).<sup>162,163</sup> The borylation of the 2-position is favored over that of the 1-position. Despite this steric preference, efforts to produce polyboryl compounds resulted in statistical mixtures because the A and C rings reacted independently of one another.

In the same vein, in 2009, Kobayashi et al. reported that the borylation of tetracenes resulted in a 1:1 mixture of 2,8- and 2,9-diborylated products (Scheme 96). These borylated materials served as valuable building blocks for the synthesis

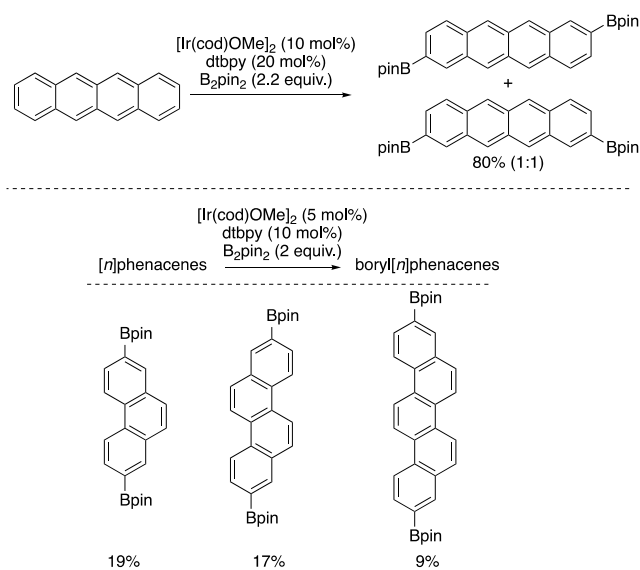
### Scheme 94. Ir-Catalyzed Borylation of Azulenes



### Scheme 95. Ir-Catalyzed Borylation of Anthracene



### Scheme 96. Ir-Catalyzed Borylation of Tetracenes and [*n*]-Phenacenes

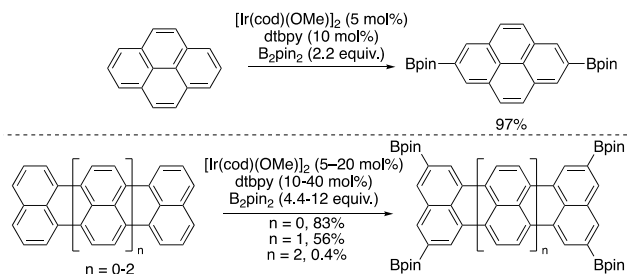


of  $\pi$ -extended tetracenes applied to create organic field-effect transistors (OFETs).<sup>164</sup> Isobe et al. reported the borylation of phenacenes for the modification of single-walled carbon nanotubes (SWNTs). Borylation occurs at the edge positions (2-, 3-, 6-, and 7- for  $n = 3$ ; 2-, 3-, 8-, and 9- for  $n = 4$  or 5) with

essentially statistical preference. Shown in Scheme 96 are the “linear” isomers.<sup>165</sup>

Chemists have had a long-standing interest in pyrenes as chromophores, fluorescent probes, and components of organic semiconductors.<sup>166</sup> Marder et al. has reported the borylation of pyrene and perylene.<sup>167–169</sup> The borylation of pyrenes occurred with good selectivity at the 2- and 7-positions (Scheme 97). Under more forcing conditions, borylation also

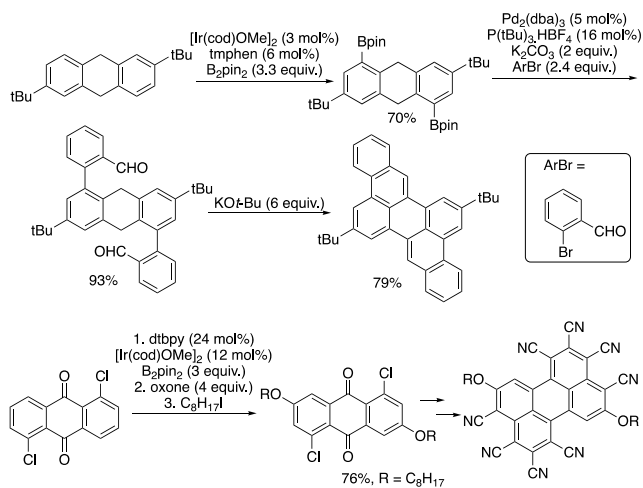
**Scheme 97. Ir-Catalyzed Borylation of Pyrenes, Terylenes, and Terrylenes**



occurred at the 4-position. Yamada and Aratani et al. have reported the borylation of terylene and quaterylenes (Scheme 97).<sup>170</sup> ( $n = 0 =$  perylene,  $n = 1 =$  terylene,  $n = 2 =$  quaterylene)

Mastalerz et al. reported a route to a variety of soluble perylenes that hinges on the regioselective diborylation of a dihydroanthracene. Subsequent Suzuki–Miyaura cross-coupling and cyclization led to the desired perylenes (Scheme 98).<sup>171</sup> Lin et al. used the borylation of anthraquinone and

**Scheme 98. Ir-Catalyzed Borylation of Anthracenes and Anthraquinones in the Synthesis of Perylenes**

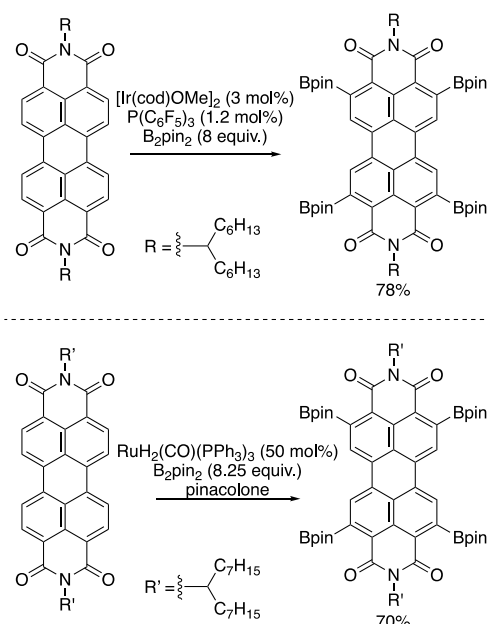


subsequent oxidation to install the desired alkoxy substituents in their synthesis of highly electron-deficient perylene polynitriles (Scheme 98).<sup>172</sup>

Perylenediimides (PDIs) are valuable chromophores for applications in dye chemistry and organic materials. Traditionally, elaboration of the perylenediimide core has been achieved by halogenation and subsequent downstream functionalization of the 1, 6, 7, and 12 “bay positions,” which tend to twist the ring out of planarity.<sup>173</sup> In 2011, the groups of Shinobuko and Müllen disclosed that the iridium- and ruthenium-catalyzed borylations of PDIs occur at the 2, 5,

8, and 11 “ortho positions” and that subsequent functionalization preserves the planarity of the PDI (Scheme 99).<sup>174,175</sup>

**Scheme 99. Ir-Catalyzed and Ru-Catalyzed Borylation of Perylenediimides**



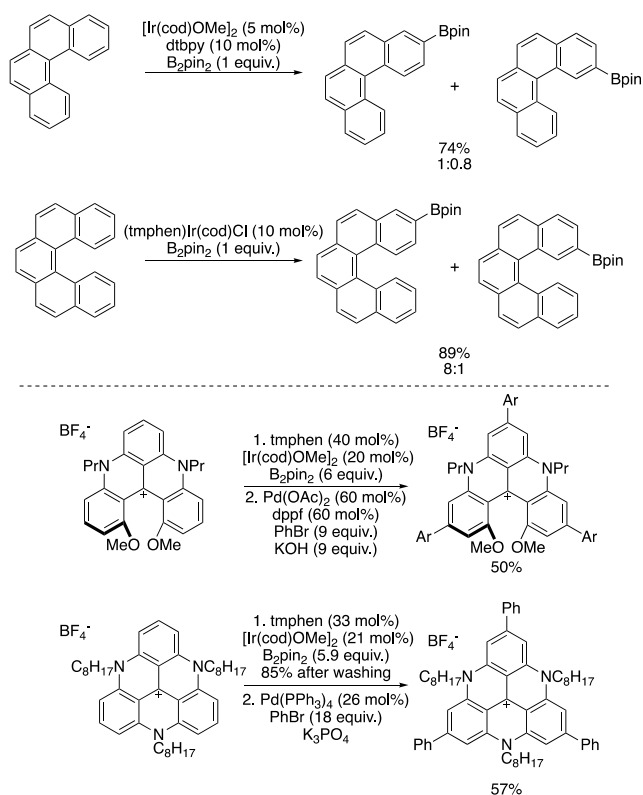
These building blocks have since enabled the synthesis of  $\pi$ -extended PDIs,<sup>176</sup> including corannulene-decorated PDIs capable of serving as sensors of  $C_{60}$ <sup>177</sup> and PDI dimers.<sup>178</sup> The borylation of a nitrogen-bridged naphthalene monoimide dimer also occurred at the position *ortho* to the amide carbonyl.<sup>179</sup>

Nečas et al. reported that [4]helicenes and [5]helicenes undergo borylation with regioselectivities controlled by the steric hindrance imparted by the ring on the other end of the molecule in the helical structures (Scheme 100). The boronic ester products were oxidized to the corresponding alcohols or used in Suzuki–Miyaura cross-coupling reactions.<sup>180,181</sup> In 2016, Matsuda et al. reported the triple borylation and subsequent cross-coupling of triazatriangulene cations for the late-stage tuning of their emissive properties (Scheme 100).<sup>182</sup> Lacour et al. further reported that triple borylation of cationic [4]helicenes occur on the periphery and allow for modular modification of these dyes.<sup>183</sup>

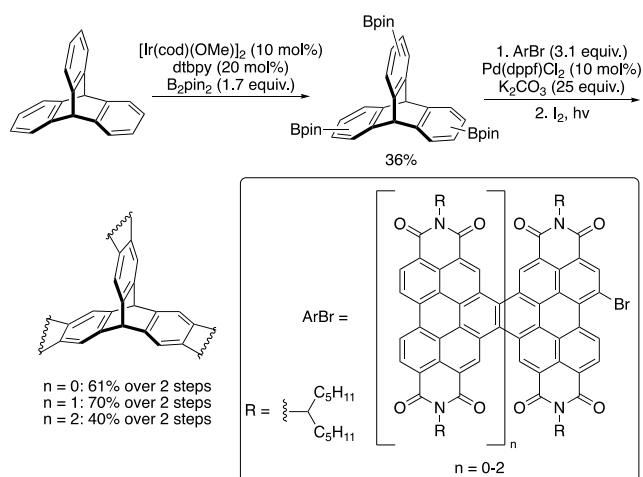
Iridium-catalyzed borylation has been leveraged further as a synthetic method to construct graphene nanostructures. This strategy is especially powerful for the modification of symmetric structures. In 2018, Sisto et al. reported that triptycene undergoes triple borylation to form a mixture of isomers from a single borylation at each of the three aryl rings (Scheme 101). The mixture was used directly for a sequence consisting of cross-coupling and oxidative cyclization to form 3-fold-symmetric graphene nanoribbons, which were used as the electron-extraction layer in perovskite solar cells. The spokelike structure is postulated to facilitate interlayer penetration and to lower the contact resistance.<sup>184</sup>

In 2012 and 2013, the groups of Scott and Itami reported conditions for the clean and efficient synthesis of 5-fold borylated corannulene,<sup>185,186</sup> and in 2018 Nozaki et al. reported the 5-fold borylation of azapentabenzocorannulenes.<sup>187</sup> Subsequent cross-coupling and dehydrocoupling led

### Scheme 100. Ir-Catalyzed Borylation of Helicenes and Triangulene Cations



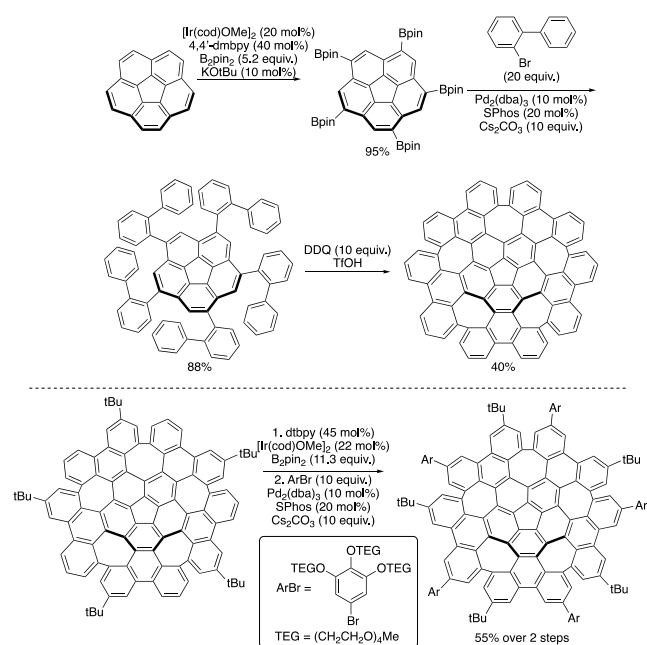
### Scheme 101. Ir-Catalyzed Borylation of Triptycene



to highly warped graphene nanosheets (Scheme 102). These warped nanographenes (WNGs) display solubilities and photophysical properties that differ from those of traditional nanographenes, presumably because of differences in crystal packing. Electronic umpolung to access the corresponding pentabromo or pentaiodo derivatives from the pentaboryl corannulene has also been reported.<sup>188</sup> Further regioselective borylation of these WNGs resulted in modification of the periphery.<sup>189,190</sup>

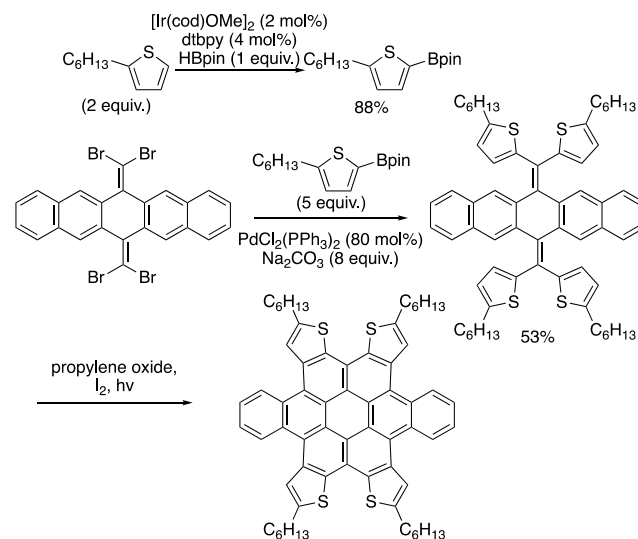
Whereas [5]circulenes possess a bowl-shaped topology, [6]circulenes are planar or nearly planar. Nuckolls et al. reported the synthesis of various thiophene boronic esters and applied them to the synthesis of dibenzotetrathienocoronenes,

### Scheme 102. Ir-Catalyzed 5-Fold Borylation of [5]-Circulene and Subsequent Elaboration to Bowl-Shaped Nanographenes



which display solvent-dependent structural behavior (Scheme 103).<sup>191</sup>

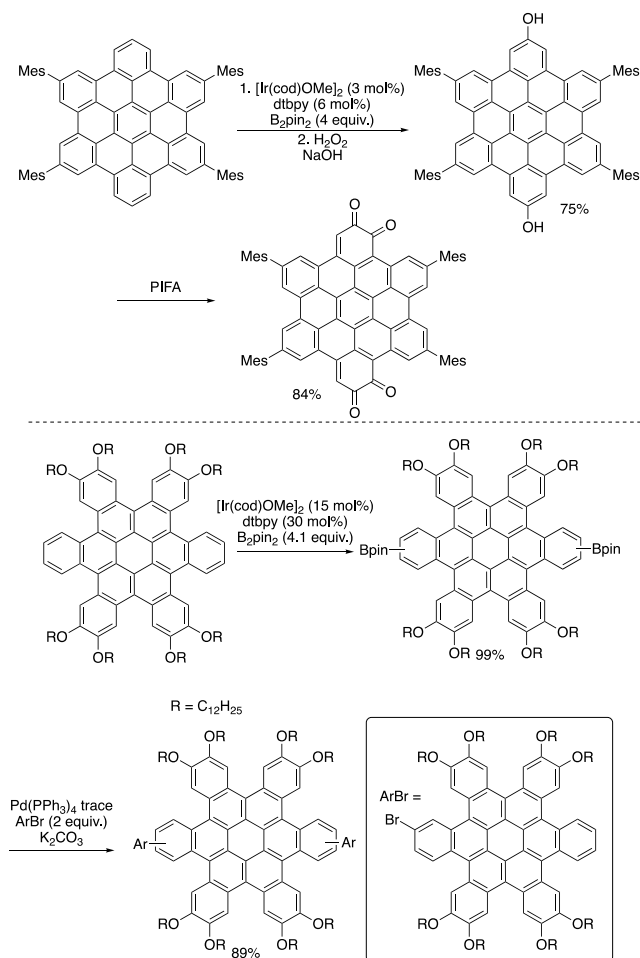
### Scheme 103. Synthesis of [6]-Circulenes Enabled by Ir-Catalyzed Borylation of Thiophene



In 2012 and 2013, the groups of Shinokubo and Itami first demonstrated that the mono-, di-, tri-, and hexaborylation of hexabenzocoronenes (HBCs) occur cleanly and provide access to oxidized and arylated HBCs that are difficult to synthesize by Scholl oxidation.<sup>192–195</sup> The peripheral borylation of HBCs also has been applied to the synthesis of oligo-HBCs by Nuckolls et al. (Scheme 104).<sup>196</sup>

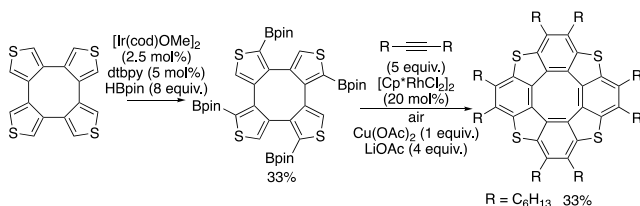
In 2015, Shinokubo et al. reported the synthesis of tetrathia[8]circulenes from cyclic tetrathiophenes by a sequence comprising borylation and annulation (Scheme 105).<sup>197</sup> This modular route enabled the study of the

## Scheme 104. Ir-Catalyzed Borylation of [6]-Circulenes



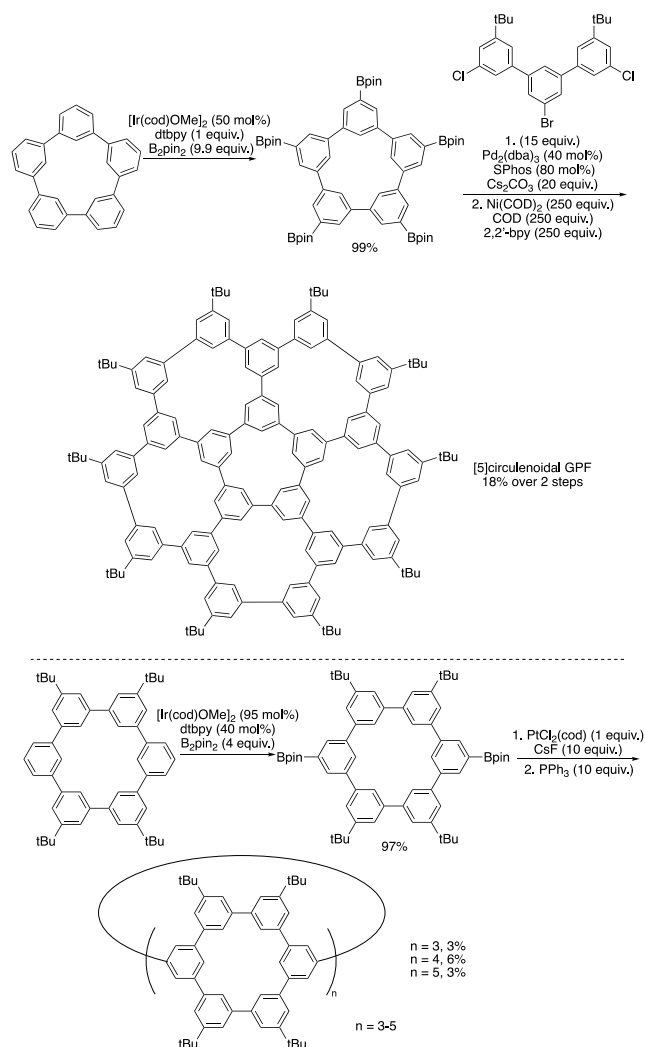
relationship between the substitution patterns of the circulene and the aggregation or emission spectra of the molecules.<sup>198</sup>

## Scheme 105. Ir-Catalyzed Borylation of Tetrathiophenes Enables the Synthesis of Tetrathia-[8]-circulenes



The geodesic structures derived from 1,3,5-substituted benzenes (phenines) are topologically related to the corannulenes. Isobe et al. first demonstrated in 2016 that the borylation of cyclo-*meta*-phenylenes (CMPs) occurs in high yield. The 5-fold borylated [5]CMP has been used as an intermediate for the modular synthesis of various arylated [5]CMPs, which have performed well as components of single-layer OLEDs (Scheme 106).<sup>199</sup> The borylated [5]CMP, [7]CMP and [8]CMP, and [6]CMP were later found to be valuable building blocks for the synthesis of bowl-shaped, saddle-shaped, and cylindrical geodesic phenine frameworks (GPFs), respectively (Scheme 106).<sup>200–203</sup>

Mastalerz et al. reported that the borylation of truxene and tribenzotriquinacene occurs with good selectivity for the  $\text{C}_3$ -

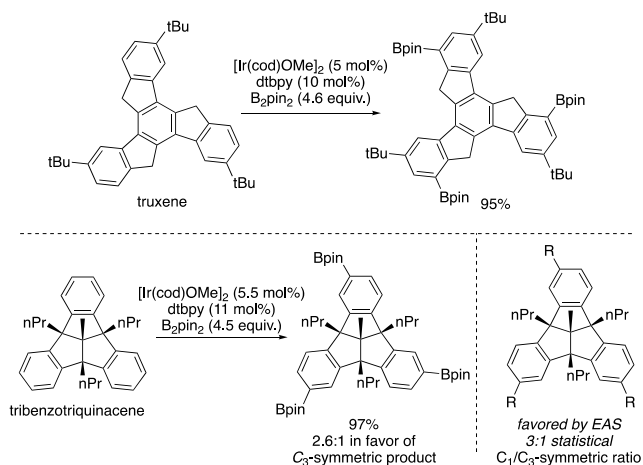
Scheme 106. Ir-Catalyzed Borylation of Cyclo-*meta*-phenylenes

symmetric isomer, which is complementary to selectivities obtained by electrophilic aromatic substitution (Scheme 107).<sup>204,205</sup> These curved molecules are valuable as precursors to curved buckybowl.

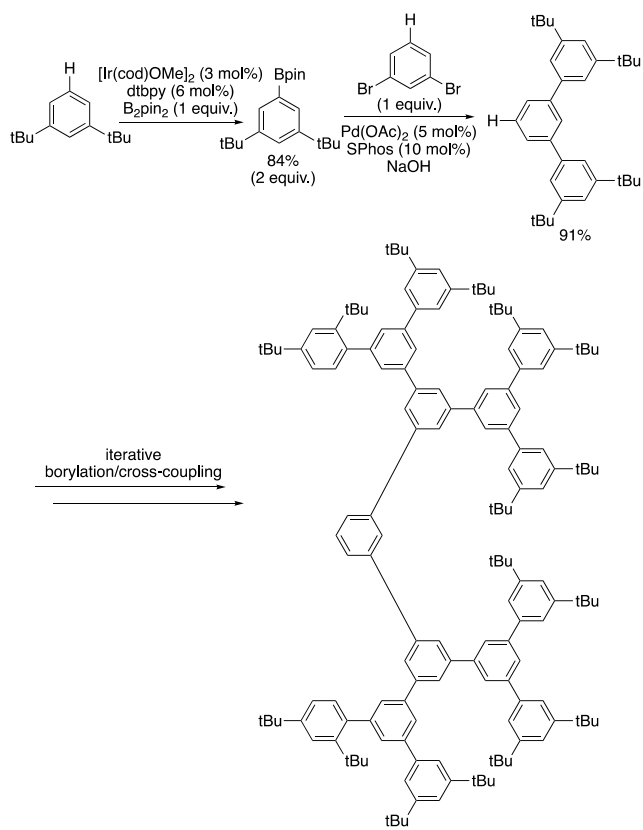
**3.3.2. Transition-Metal-Catalyzed Borylation in the Synthesis and Modification of Dendrimers.** Dendrimers are radially symmetric molecules with well-defined and monodisperse structures,<sup>206</sup> and they have received much attention because of their medicinal, biological, and materials applications.<sup>207</sup> Oligophenylene dendrimers have been investigated for OLED applications.<sup>208</sup> Their synthesis has typically relied on iterative Suzuki–Miyaura couplings of boronic ester building blocks with bifunctional “focal points.” These focal points are haloarenes containing masked boronic acids, which then require demasking between the cross-coupling steps. An alternative strategy is to harness the borylation of C–H bonds to introduce the desired boronic ester functionality directly in the appropriate step in the synthesis.

In 2008 and 2009, the groups of Moore and Suginome reported that the borylation of *meta*-substituted arenes provides a rapid way to synthesize polyphenylene dendrimers by iterative borylation and cross-coupling of the borylated building blocks (Scheme 108).<sup>209,210</sup>

### Scheme 107. Ir-Catalyzed Borylation of Truxenes and Tribenzotriquinacenes



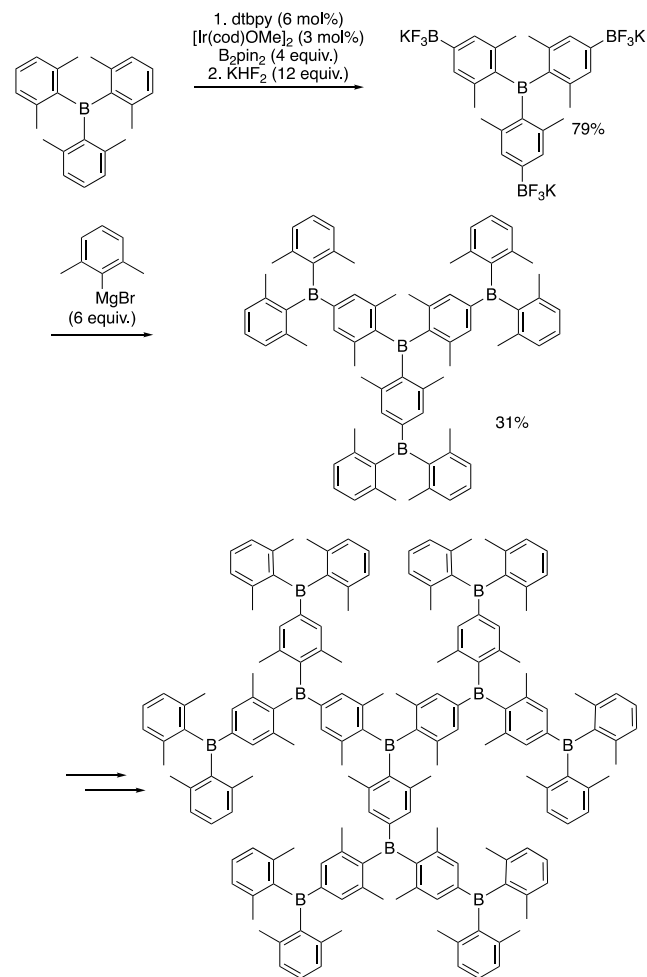
### Scheme 108. Ir-Catalyzed Borylation of Arene Building Blocks in the Synthesis of Dendrimers



In contrast to coupling borylated arenes to a central “focal point” in a building block approach, the groups of Marder and Goto reported that the borylation of the periphery of dendrimers enables the rapid expansion of a dendrimer architecture (Scheme 109).<sup>211,212</sup>

**3.3.3. Transition-Metal-Catalyzed Borylation for the Postpolymerization Modification of Polymers.** The borylation of C–H bonds also has been applied to the postpolymerization functionalization of polymers. Early efforts focused on the functionalization of polyolefins. The borylation of polyolefins provides an avenue to access hydroxylated or arylated polyolefins that contain polar functional groups and

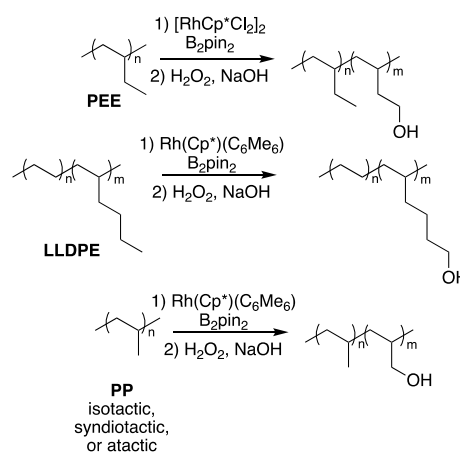
### Scheme 109. Ir-Catalyzed Peripheral Borylation of Dendrimers



with high molecular weights, a class of polymers that have been difficult to synthesize through copolymerization strategies.

In 2002, our laboratory in collaboration with Hillmyer’s showed the feasibility of this approach in the two-step borylation–hydroxylation of polyethylene (PEE).<sup>213</sup> This method was later expanded to achieve the functionalization of linear low-density polyethylene (LLDPE) and polypropylene (PP) (Scheme 110).<sup>214,215</sup> Bae et al. later

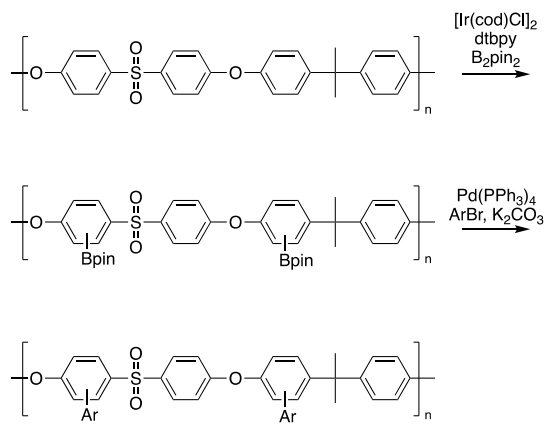
### Scheme 110. Rh-Catalyzed Borylation of Polyolefins



reported that isotactic poly(1-butene) and polystyrene undergo borylation in a similar fashion.<sup>216,217</sup> These functionalized polyolefins were decorated further by functional group manipulations or graft polymerization, and the resulting polymers exhibited changes in crystallinity and the ability to serve as compatibilizers in polymer blends.

In 2009, Bae et al. pioneered the application of the borylation of C–H bonds for the modification of aromatic main-chain polymers, in particular to the postpolymerization functionalization of poly(arylene ether sulfone) (Scheme 111).<sup>218,219</sup> The reactions occurred cleanly with essentially

**Scheme 111.** Ir-Catalyzed Borylation of Poly(arylene ether sulfones)

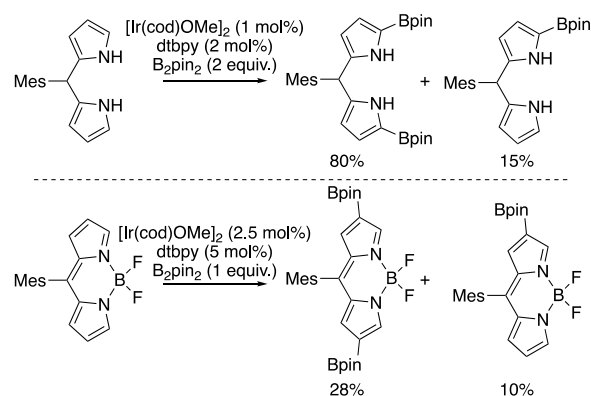


no cross-linking or chain cleavage, as inferred from the polydispersity index of the resultant polymer. Bielawski et al. leveraged this method to synthesize poly(arylene ether sulfone) polymers decorated by Lewis basic heterocycles as proton-exchange membrane materials (Scheme 111).<sup>220</sup> Scott et al. reported that the borylation of 1,3-bis(3-phenoxyphenoxy)benzene occurs on the ends of the polymer chains and can be applied to the synthesis of polyphenylether–epoxy resin–triamine adhesives.<sup>221</sup>

**3.3.4. Transition-Metal-Catalyzed Borylation for the Synthesis of Oligopyrroles, Corroles, Porphyrins, and Porphyrin Analogues.** The borylation of C–H bonds also has been applied to the synthesis or modification of oligopyrroles, corroles, and porphyrins. 4,4-Difluoro-4-bora-3a,4a-diaza-*s*-indacenes (BODIPYs) are small molecules that exhibit strong fluorescence with sharp peaks.<sup>222,223</sup> Osuka et al. reported that the borylation of a *meso*-substituted dipyrromethane occurs in high yield and with high  $\alpha$ -selectivity, whereas the borylation of a dipyrin (BODIPY) occurs with moderate yield and  $\beta$ -selectivity (Scheme 112). This selectivity created complementary approaches to the synthesis of both  $\alpha$ - and  $\beta$ -alkenylated BODIPYs.<sup>224</sup>

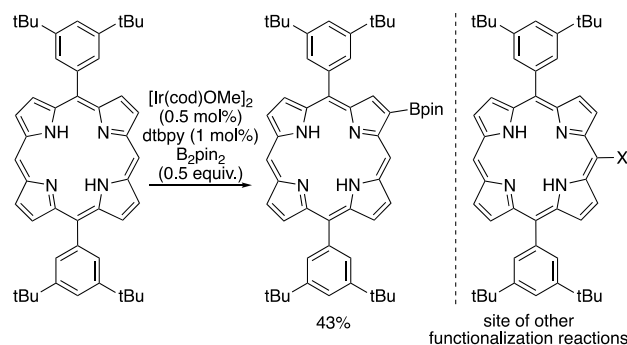
Porphyrins are  $18\pi$  aromatic macrocyclic compounds that are ubiquitous in nature and in organic optoelectronics. Porphyrins have long been studied in fields as varied as photosynthesis, biocatalysis, dyes, information storage, ligand design, and supramolecular chemistry.<sup>225</sup> In 2005, Osuka et al. pioneered the borylation of porphyrins and reported that the direct borylation of porphyrins occurs at the  $\beta$ -position, while other functionalization methods, such as electrophilic aromatic substitution, tend to modify the *meso*-position (Scheme 113).<sup>226</sup> The borylated porphyrins were further functionalized

**Scheme 112.** Ir-Catalyzed Borylation of Pyrroles and BODIPYs



by Suzuki cross-coupling reactions or Heck-type reactions.<sup>227,228</sup>

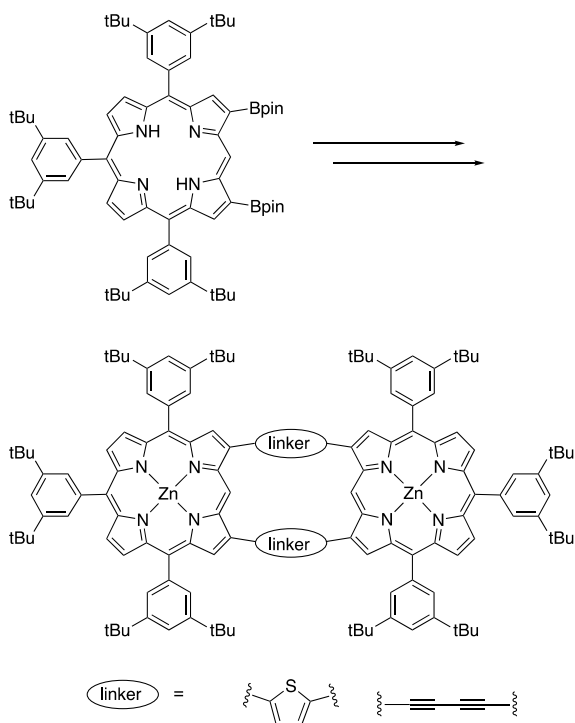
**Scheme 113.** Ir-Catalyzed,  $\beta$ -Selective Borylation of Porphyrins



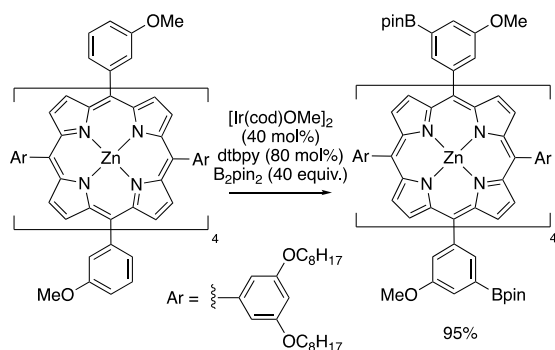
Leveraging the predictable selectivity of C–H borylation, Osuka and others combined appropriate borylated porphyrins with linkers of choice in a “building block” approach to synthesize oligo-porphyrin architectures (Scheme 114). Many novel porphyrins were synthesized by this approach. For example, doubly 1,3-butadiyne-bridged and 2,5-thienylene-bridged diporphyrins were synthesized from doubly borylated porphyrins, and the two-photon absorption cross sections of the bridged diporphyrins were abnormally large.<sup>229,230</sup> Other exotic porphyrin oligomers were synthesized with this strategy, such as porphyrin nanobelts,<sup>231–238</sup> cyclometalated porphyrin complexes,<sup>239–245</sup> or cyclophane-like oligoporphyrins.<sup>246</sup>

If the *meso*- and  $\beta$ -positions on the porphyrin ring are sterically hindered, and aryl C–H bonds on the distal aryl substituents are sterically accessible, then borylation occurs at the distal aryl C–H bonds. This scenario leads to the highly selective terminal borylation of a tetraarylporphyrin (Scheme 115).<sup>247</sup>

Corroles are  $18\pi$  aromatic tetrapyrrolic compounds that contain a direct pyrrole–pyrrole linkage and are studied for their unique coordination chemistry and optical properties.<sup>248,249</sup> In 2005, Osuka et al. reported that the borylation of corrole, like the borylation of porphyrins, occurs with  $\beta$ -selectivity. These borylated corroles have provided a route to the corrole–porphyrin dimers<sup>250</sup> and doubly bridged corrole dimers, which possess singlet biradical character (Scheme 116).<sup>251,252</sup>

Scheme 114.  $\beta$ -Borylated Porphyrins as Building Blocks for the Synthesis of Oligoporphyrins

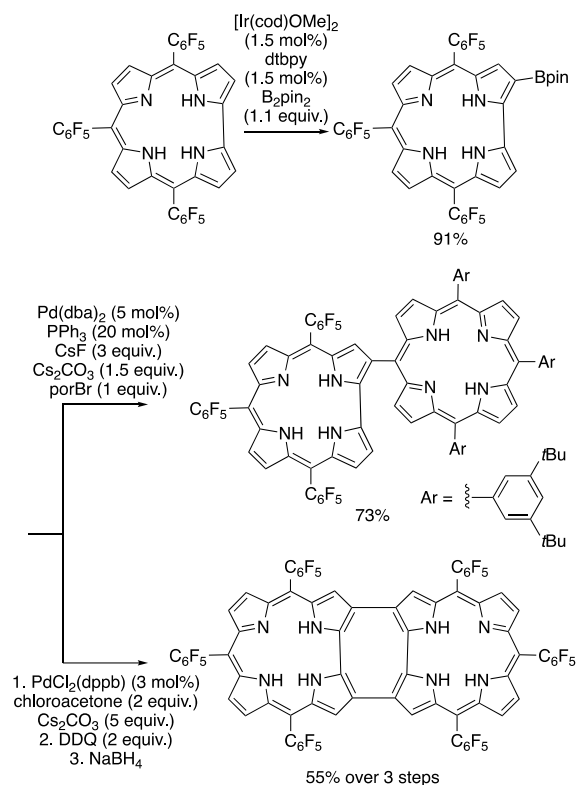
Scheme 115. Ir-Catalyzed Peripheral Borylation of Oligoporphyrins



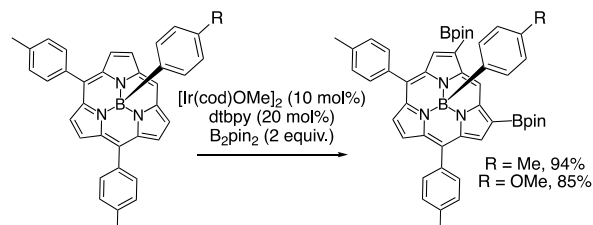
Subporphyrins are ring-contracted analogues of porphyrins with a  $14\pi$  aromatic system, a bowl-shaped structure, and often possess nonlinear optical properties.<sup>253,254</sup> In 2015, Osuka et al. reported that subporphyrins undergo clean double borylation at the *meso* positions (Scheme 117). The boronic ester products were further elaborated into  $\pi$ -extended subporphyrins and subporphyrin dimers.<sup>255</sup>

In 2021, Tanaka and Osuka et al. used the borylation of phenylene-linked dipyrroles and tripyrroles to provide starting materials for the synthesis of cyclic oligopyrroles (Scheme 118).<sup>256</sup> Subsequent oxidation of these oligopyrroles formed the corresponding circulenes.<sup>257,258</sup>

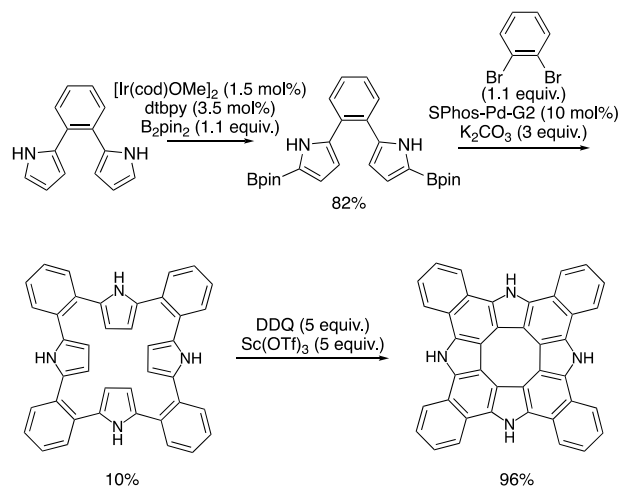
Song et al. reported that the double borylation of tripyrroles occurred cleanly and applied the diboronic ester products to the synthesis of  $\pi$ -extended "earring" porphyrins (Scheme 119). The UV-vis spectra of these materials contained bands that are highly red-shifted, relative to the parent porphyrin.<sup>259,260</sup>

Scheme 116. Ir-Catalyzed,  $\beta$ -Selective Borylation of Corroles

Scheme 117. Ir-Catalyzed Borylation of Subporphyrins

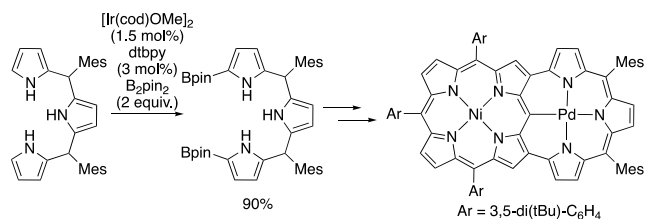


Scheme 118. Ir-Catalyzed Borylation of Dipyrroles in the Synthesis of Cyclic Oligopyrroles



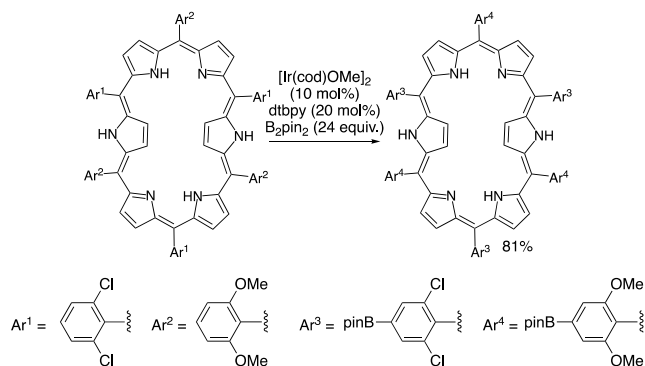


## Scheme 119. Ir-Catalyzed Borylation of Tripyrroles



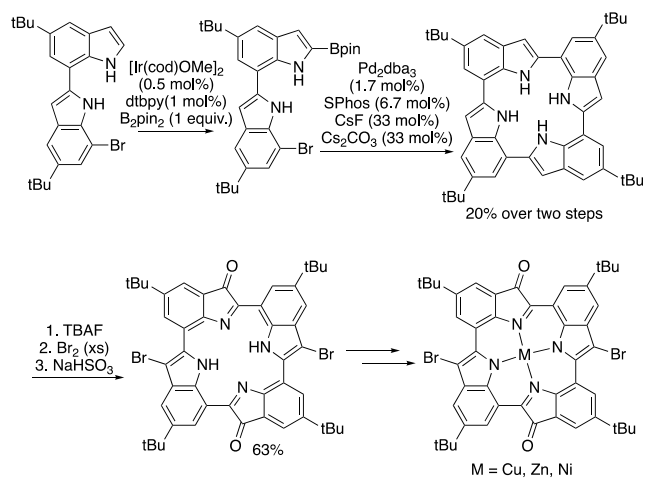
In a similar fashion, clean 6-fold borylation occurred on the distal aryl C–H bonds of a hexaphyrin derivative containing 2,6-substituted aryl groups (Scheme 120).<sup>261</sup>

## Scheme 120. Ir-Catalyzed Borylation of Hexaphyrins



Cyclic tetraindoles are considered  $\pi$ -extended porphyrin analogues, and they can be transformed into a planar porphyrin-like structure by oxidation. Shinokubo et al.'s 2012 route involved the borylation of a bisindole and subsequent dimerization (Scheme 121).<sup>262</sup> Similar analogues containing benzofuran and benzothiophene units also have been prepared by this route.<sup>263</sup>

## Scheme 121. Ir-Catalyzed Borylation of Bisindoles in the Synthesis of Porphyrinogen Analogues



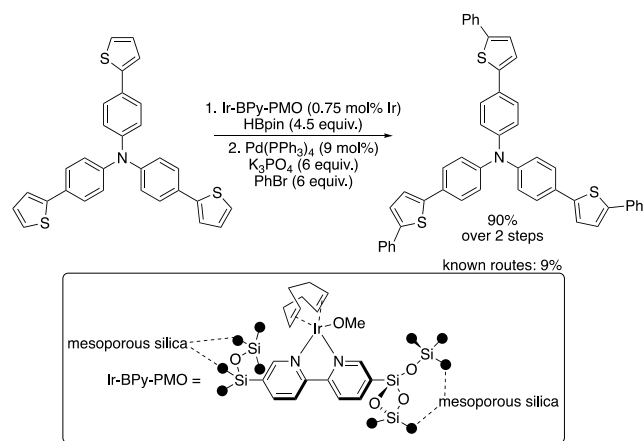
## 3.3.5. Transition-Metal-Catalyzed Borylation of Arene C–H Bonds in the Synthesis of Chalcophene Materials.

Because of their solution processability and ability to form stable films, semiconducting polymers are valuable for organic field-effect transistors (OFETs) and organic photovoltaic devices (OPVs). Within this field of research, much effort

has been devoted to the exploration of heteroaromatic rings incorporated into the building unit to modulate the electronic properties and structural ordering of the polymers. Thiophene-based building blocks have received particular attention in recent years.<sup>264</sup>

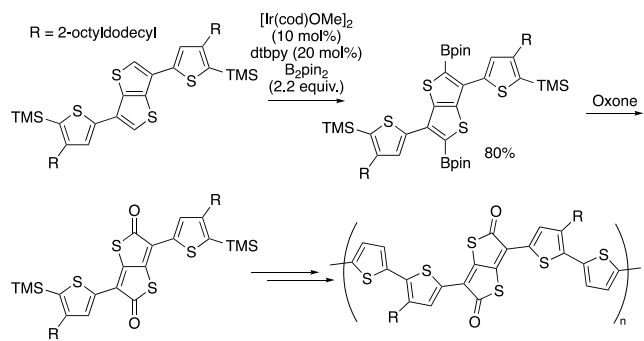
In 2015, Inagaki et al. studied the borylation of various thiophene derivatives with a silica-supported iridium catalyst. In one case, the combination of borylation and cross-coupling resulted in the synthesis of a triarylamine hole transport material in yields that are much higher than those of the prior routes (Scheme 122).<sup>265</sup>

## Scheme 122. Borylation of a Trithiophene Hole-Layer Material



In 2014, Takimiya et al. reported the diborylation of thienothiophene in high yield. Subsequent oxidation formed the corresponding thienothiophenedione—a strong, electron-deficient acceptor unit for use in organic semiconductors (Scheme 123).<sup>266</sup>

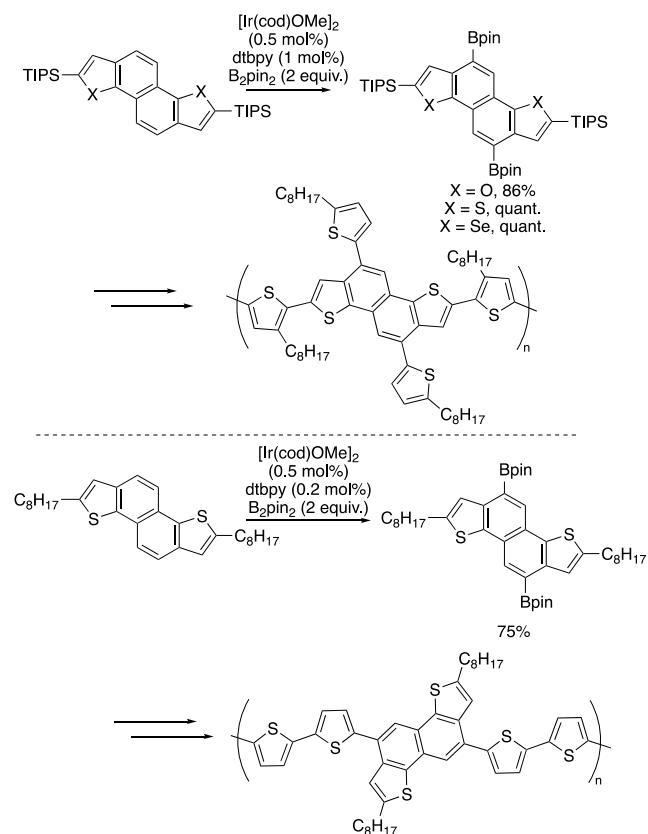
## Scheme 123. Ir-Catalyzed Borylation of Thienothiophene and Application to the Synthesis of Thienothiophenedione



The borylation of naphthodichalcogenophenes and naphthothiadiazoles has been applied to the rapid synthesis of semiconductor materials. For example, in 2012, Takimiya et al. reported the selective 5,10-diborylation of naphthodithiophenes and synthesized organic semiconductors for OFET and OPV applications (Scheme 124). The different charge mobilities of the two polymeric forms shown in Scheme 124 are attributable to the different levels of twist in the backbone.<sup>267–269</sup>

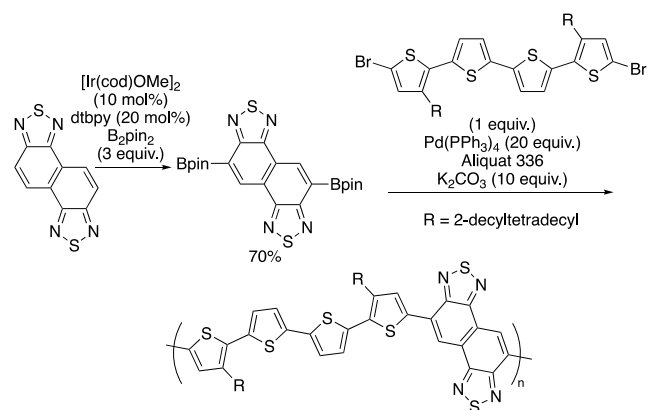
Naphthothiadiazole units are also valuable as electron-deficient units in semiconducting polymers. In 2013, Takimiya

### Scheme 124. Ir-Catalyzed Borylation of Naphthodichalcogenophenes



et al. reported a convenient route to organic semiconducting polymers containing the naphthothiadiazole core by the diborylation of naphthothiadiazole (Scheme 125).<sup>270,271</sup>

### Scheme 125. Ir-Catalyzed Borylation of Naphthothiadiazoles

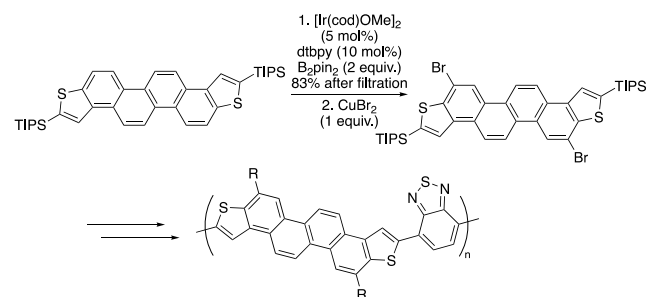


In 2021, Okamoto et al. used the borylation of chrysenodithiophene for the synthesis of conjugated polymers containing both chrysenodithiophene and benzothiadiazole units (Scheme 126).<sup>272</sup>

### 3.4. Transition-Metal-Catalyzed Borylation of C–H Bonds in Synthesis of Ligands

The late-stage modification of ligands for homogeneous catalysis is a final application of the borylation of C–H bonds constituting “late-stage” functionalization. These reactions can be divided into two types of functionalization: (1)

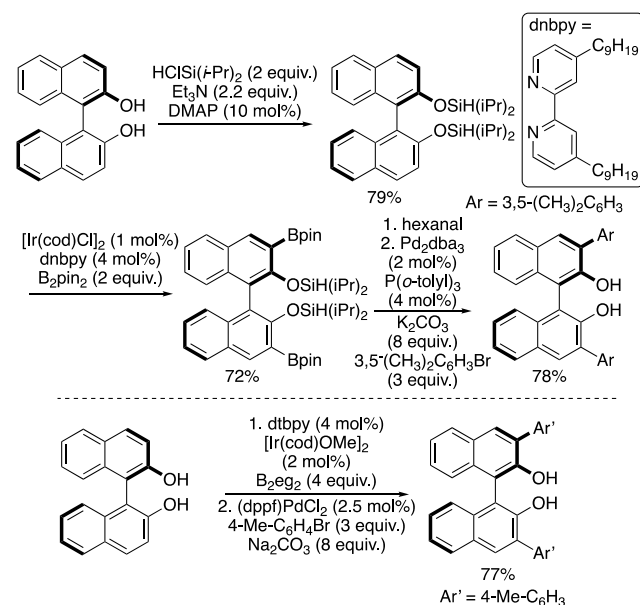
### Scheme 126. Ir-Catalyzed Borylation of Chrysenodithiophenes



the modification of common ligand cores by sequences comprising borylation and functionalization and (2) directed functionalizations in which the coordinating atom of the ligand precursor interacts with the transition metal catalyst and confers the desired site or stereoselectivity.

The binaphthalene core is a privileged structural class in enantioselective synthesis. In particular, the chiral binaphthol (BINOL) scaffold has been applied extensively in chiral Brønsted acid catalysis. Numerous theoretical and experimental studies have shown that aryl substituents at the 3- and 3'-positions strongly influence the selectivities of catalysts formed from these BINOL cores.<sup>273,274</sup> In 2014, Clark et al. demonstrated that silyl-directed borylation and subsequent Suzuki–Miyaura coupling introduces a wide variety of aryl substituents at the 3- and 3'-positions (Scheme 127).<sup>275</sup>

### Scheme 127. Borylation-Coupling Sequences for the Synthesis of 3- and 3'-Substituted BINOLs

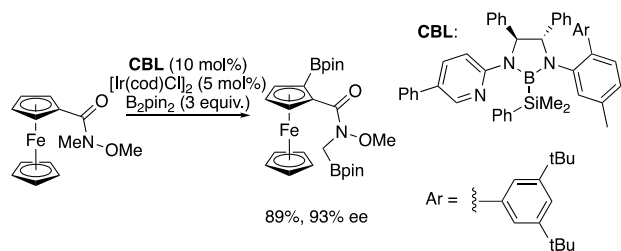


Chattopadhy et al. later showed in 2019 that the silyl directing group is not necessary if the diboron reagent is  $\text{B}_2\text{eg}_2$  (eg = ethylene glycolate) (Scheme 127). Noncovalent interactions between the phenol and Beg groups appear to direct the borylation to the *ortho* position.<sup>276</sup>

Ferrocenes are prevalent in ligands for homogeneous catalysis. Thus, methods to introduce substituents or even planar chirality to the ferrocene core are valuable for the synthesis of ferrocenyl-based ligands. The undirected bor-

ylation of ferrocenes was first investigated by Plenio et al. in 2004, but these reactions occurred in moderate yield.<sup>277</sup> In 2022, Xu et al. developed a chiral bidentate boryl ligand that enabled the enantioselective borylation of ferrocenes containing amide functionality (Scheme 128). The amide functionality

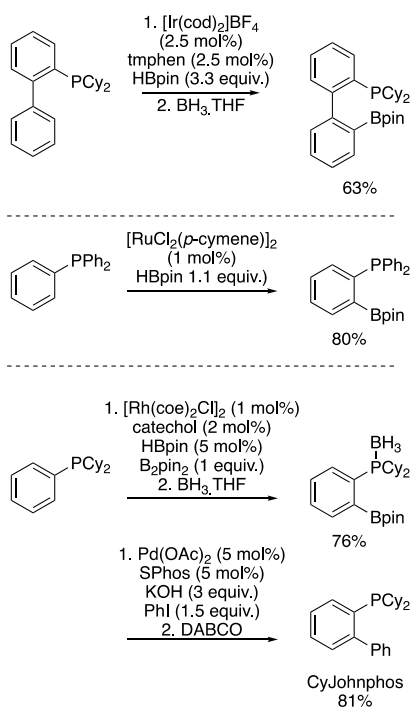
### Scheme 128. Enantioselective Borylation of Ferrocene Enabled by a Chiral Bidentate Boryl Ligand



is presumed to interact with a vacant binding site on the iridium catalyst, thereby directing the borylation to the C–H bond located *ortho* to the directing group.<sup>153</sup>

Phosphines are common supporting ligands in homogeneous catalysis. The coordination of phosphines to transition metal catalysts is a powerful avenue to direct the site of borylation. In 2014, Clark et al. showed that the combination of  $[\text{Ir}(\text{cod})_2]\text{BF}_4$  and tmphen catalyze the borylation of biaryl phosphines at the distal aryl group (Scheme 129). In 2019,

### Scheme 129. Phosphine-Directed *ortho*-Borylation of Arenes

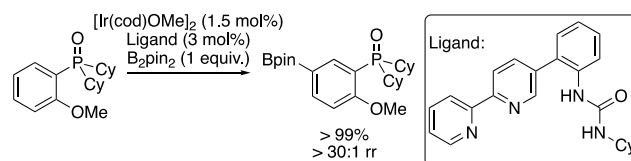


Clark et al. further showed that 2-methylaryl phosphines undergo borylation at the benzylic position in the presence of the cationic iridium complex  $[\text{Ir}(\text{cod})_2]\text{BF}_4$  with tmphen as ligand.<sup>278,279,291</sup> Similarly, Takeya et al. showed that aryl phosphines undergo highly *ortho*-selective borylation in the presence of  $[\text{RuCl}_2(\textit{p}\text{-cymene})]_2$  (Scheme 129).<sup>280</sup> Shi et al. showed that similar reactivity and selectivity was observed in

the presence of  $[\text{Rh}(\text{coe})_2\text{Cl}]_2$  and applied the *ortho*-selective borylation to a concise synthesis of CyJohnphos (Scheme 129).<sup>281</sup> In all these cases, the selectivity is postulated to arise from coordination of the phosphino group to the metal catalyst.

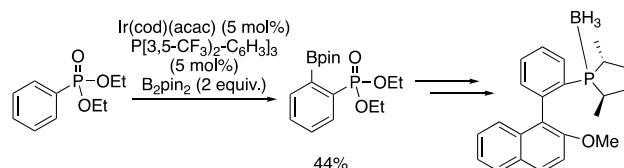
In 2015, Kanai et al. developed a bipyridine ligand with the capacity to participate in secondary hydrogen-bonding interactions with substrates. When combined with  $[\text{Ir}(\text{cod})\text{OMe}]_2$ , this ligand forms complexes that catalyze the *meta*-selective borylation of aryl phosphine oxides and phosphonate esters (Scheme 130).<sup>282,283</sup>

### Scheme 130. *meta*-Selective Borylation of Phosphine Oxides Enabled by a Hydrogen-Bonding Ligand



In 2020, Watson et al. showed that arylphosphonates also undergo *ortho*-selective borylation with cationic iridium catalysts formed from  $[\text{Ir}(\text{cod})(\text{acac})]$  and the electron-deficient ligand  $\text{P}[(3,5\text{-CF}_3)_2\text{-C}_6\text{H}_3]_3$  (Scheme 131). The

### Scheme 131. *ortho*-Selective Borylation of Arylphosphonates with Cationic Iridium Catalysts



authors noted that similar results were obtained with  $[\text{Ir}(\text{cod})_2]\text{BF}_4$ , but  $[\text{Ir}(\text{cod})(\text{acac})]$  was chosen as the precatalyst because of its bench stability and lower price. The resulting aryl boronic esters were then used in the synthesis of a biarylphosphine ligand.<sup>284</sup>

In 2020, Phipps et al. reported the desymmetrization of diaryl phosphinamides catalyzed by a complex that interacts with the substrate through an ion pair (Scheme 132). The phosphinamide is postulated to hydrogen bond to the sulfonate bipyridine, while the chiral cation confers enantioselectivity.<sup>285</sup> In 2021, Xu et al. reported the desymmetrization of diaryl phosphinates to synthesize phosphines in which phosphorus is a stereogenic center (Scheme 133).<sup>286</sup>

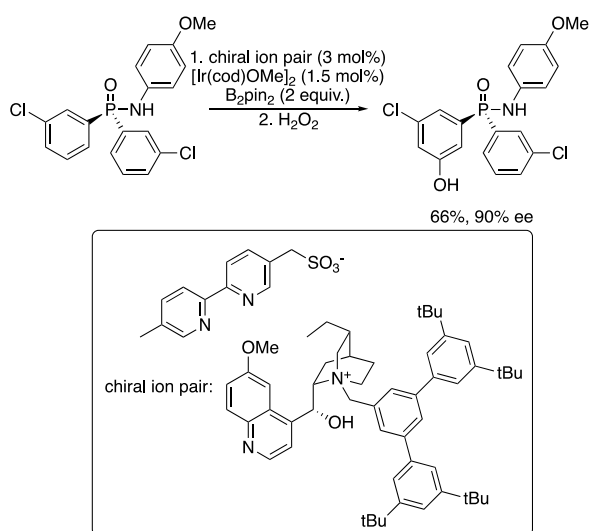
In 2019, Xu et al. demonstrated that the combination of a chiral bidentate boryl ligand and iridium catalyzes the desymmetrization of diarylaminomethanes. The resulting boronic ester was then used for the synthesis of an aminophosphine ligand (Scheme 134).<sup>287</sup>

Finally, the double borylation of a bipyridine enabled Segawa et al.'s 2017 synthesis of a bis-2-pyridylidene palladium complex (Scheme 135).<sup>288</sup>

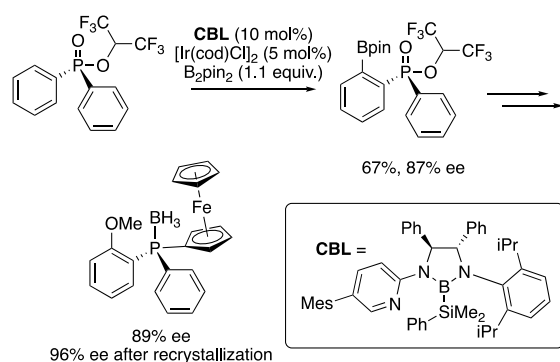
## 4. CONCLUSION AND OUTLOOK

C–H functionalization is a fast-growing field that has had and will continue to impact the many research areas of synthetic chemistry. Among methods for C–H functionalization, reactions to functionalize C–H bonds with boron and silicon

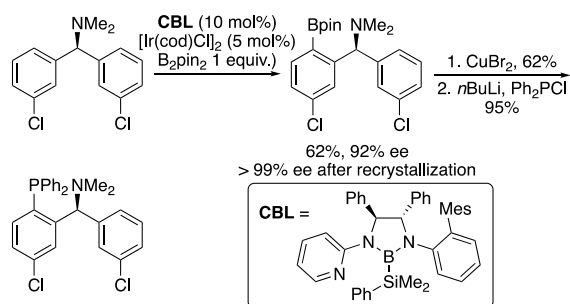
**Scheme 132. Desymmetrization of Diaryl Phosphinamides by Borylation of Aryl C–H Bonds with a Chiral, Ion-Pairing Strategy**



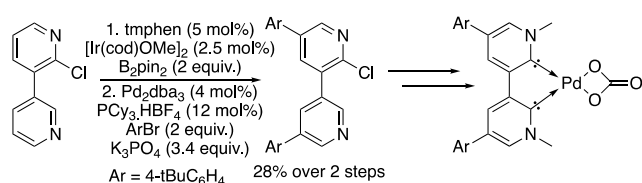
**Scheme 133. Desymmetrization of Diaryl Phosphinates by Borylation with a Chiral Bidentate Boryl Ligand**



**Scheme 134. Desymmetrization of Diaryl Aminomethanes by Borylation with a Chiral Bidentate Boryl Ligand**



**Scheme 135. Borylation-Coupling of a 3,3'-Bipyridine Enables the Synthesis of a Bis-2-pyridylidene Palladium Complex**



are particularly attractive because they occur with high regioselectivity and form products with boron- and silicon-based groups that can be transformed into a range of different functional groups. Because of these characteristics, the silylation and borylation of C–H bonds have been widely applied to the modification of many classes of complex molecules, including active pharmaceutical ingredients, natural products, intermediates in the synthesis of such compounds, organic materials, and ligands. This review has outlined such applications.

There are many similarities between the catalytic systems used for the silylation and borylation of C–H bonds. As such, both fields are well-developed in similar areas and require further development in others. For example, the silylation and borylation of aryl C–H bonds can occur under mild conditions in a general fashion that is suitable for synthetic applications, particularly undirected methods.

At the same time, the functionalization of alkyl C–H bonds, specifically with silicon, has been limited to intramolecular reactions. However, a major goal for future development is the intermolecular silylation and borylation of alkyl C–H bonds. For silicon, directed examples exist using trialkyl silanes, but further development of methods that incorporate silyl groups that contain at least one electronegative atom and, thereby, enable a wider range of subsequent derivatizations are needed. Undirected examples of the functionalization of alkyl C–H bonds with boron and silicon are the least developed. With the undirected borylation of alkyl C–H bonds reported recently under conditions with the substrate as limiting reagent, it is likely that further catalyst development and reaction designs will enable this class of borylation to occur in a practical fashion.

Although progress has been made toward creating catalysts that react with high activity and site selectivity, site-selective silylations and borylations of C–H bonds in molecules with multiple similarly active C–H bonds is an urgent unmet need. Although directing strategies exist, further developments of methods that exploit existing functionality to control site selectivity and do not require laborious installation and removal of directing groups are needed. More challenging is the development of methods with catalyst-controlled site selectivity. Such methods have the capability to expand the scope of borylation and silylation reactions and to enable a broader range of functionalization of complex molecules at a “late stage.”

## AUTHOR INFORMATION

### Corresponding Author

John F. Hartwig – Department of Chemistry, University of California, Berkeley, California 94720, United States;  
 orcid.org/0000-0002-4157-468X; Email: jhartwig@berkeley.edu

### Authors

Isaac F. Yu – Department of Chemistry, University of California, Berkeley, California 94720, United States;  
 orcid.org/0000-0001-9659-2204

Jake W. Wilson – Department of Chemistry, University of California, Berkeley, California 94720, United States;  
 orcid.org/0009-0007-9480-3291

Complete contact information is available at:  
<https://pubs.acs.org/10.1021/acs.chemrev.3c00207>

## Author Contributions

CRedit: **Isaac F. Yu** conceptualization, data curation, writing-original draft, writing-review & editing; **Jake W. Wilson** conceptualization, data curation, writing-original draft, writing-review & editing; **John F. Hartwig** conceptualization, data curation, writing-original draft, writing-review & editing.

## Notes

The authors declare no competing financial interest.

## Biographies

Isaac F. Yu was born and raised in Torrance, CA and Taipei, Taiwan. He received his B.S. in chemistry from the National Taiwan University in 2019, where he conducted research in the laboratory of Prof. Ching-Wen Chiu. Currently, he is a Ph.D. candidate in the laboratory of Prof. John Hartwig at the University of California, Berkeley. His research focuses on the mechanistic study and development of new catalysts for the undirected borylation of alkyl C–H bonds. Outside of the lab, Isaac enjoys volleyball, skiing, and spending quality time with friends.

Jake W. Wilson was born and raised in Lansing, MI. He received his B.S. in chemistry from the University of Michigan, Ann Arbor in 2019, where he conducted research in the laboratory of Prof. John Montgomery. Currently, he is a Ph.D. candidate in the laboratory of Prof. John Hartwig at the University of California, Berkeley. His research focuses on the development of new catalytic systems for the borylation and silylation of C–H bonds. Outside of the lab, Jake enjoys musical theater, golfing, and spending quality time with friends.

John F. Hartwig is the Henry Rapoport Professor of Chemistry at the University of California, Berkeley. The work in his laboratory has focused on revealing the fundamental principles that control metal-centered reactivity and creating catalysts and new catalytic reactions, including the functionalization of C–H bonds, using this information. For this work, he has received the Wolf Prize in Chemistry, the A.C. Cope Award, and he is a member of the National Academy of Sciences. He is the author of the textbook *Organotransition Metal Chemistry – From Bonding to Catalysis*. Outside the laboratory, he enjoys cycling, hiking, skiing, music, theater, cooking, and time with his wife and two daughters.

## ACKNOWLEDGMENTS

We thank the NSF (DGE 1752814) for funding.

## ABBREVIATIONS

bpy	2,2'-bipyridine
BQ	benzoquinone
coe	cyclooctene
cod	1,4-cyclooctadiene
2-CINQ	2-chlorobenzoquinone
dba	dibenzylideneacetone
DCM	dichloromethane
2,6-DiCIBQ	2,6-dichlorobenzoquinone
DMAP	4-dimethylaminopyridine
DMBQ	2,6-dimethoxybenzoquinone
DMP	Dess–Martin periodinane
dppf	1,1'-bis(diphenylphosphino)ferrocene
dtbpy	4,4'-ditert-butyl-2,2'-bipyridine
dtbpf	1,1'-bis(di-tert-butylphosphino)ferrocene
HFIP	1,1,1,3,3,3-hexafluoroisopropanol
nbd	norbornene
nbe	norbornadiene
NMP	N-methylpyrrolidone

MTBE	methyl tert-butyl ether
SPhos	dicyclohexyl(2',6'-dimethoxy[1,1'-biphenyl]-2-yl)phosphane
TBAF	tetrabutylammonium fluoride
TBHP	tert-butyl hydroperoxide
TBSCl	tert-butyltrimethylsilyl chloride
tBuDavePhos	2-ditert-butylphosphino-2'-(N,N-dimethylamino)biphenyl
THF	tetrahydrofuran
tmphen	3,4,7,8-tetramethyl-1,10-phenanthroline
TMSCl	trimethylsilyl chloride
XPhos	dicyclohexyl[2',4',6'-tris(propan-2-yl)[1,1'-biphenyl]-2-yl]phosphane

## REFERENCES

- Arndtsen, B. A.; Bergman, R. G.; Mobley, T. A.; Peterson, T. H. Selective Intermolecular Carbon-Hydrogen Bond Activation by Synthetic Metal Complexes in Homogeneous Solution. *Acc. Chem. Res.* **1995**, *28*, 154–162.
- Cernak, T.; Dykstra, K. D.; Tyagarajan, S.; Vachal, P.; Krska, S. W. The medicinal chemist's toolbox for late stage functionalization of drug-like molecules. *Chem. Soc. Rev.* **2016**, *45*, 546–576.
- Mkhalid, I. A. I.; Barnard, J. H.; Marder, T. B.; Murphy, J. M.; Hartwig, J. F. C–H Activation for the Construction of C–B Bonds. *Chem. Rev.* **2010**, *110*, 890–931.
- Cheng, C.; Hartwig, J. F. Catalytic Silylation of Unactivated C–H Bonds. *Chem. Rev.* **2015**, *115*, 8946–8975.
- Hartwig, J. F. Borylation and Silylation of C–H Bonds: A Platform for Diverse C–H Bond Functionalizations. *Acc. Chem. Res.* **2012**, *45*, 864–873.
- Gustavson, W. A.; Epstein, P. S.; Curtis, M. D. Homogeneous Activation of the Carbon-Hydrogen bond. Formation of Phenylsiloxanes from Benzene and Silicon Hydrides. *Organometallics* **1982**, *1*, 884–885.
- Ishikawa, M.; Sakamoto, H.; Okazaki, S.; Naka, A. Nickel-Catalyzed Reactions of 3,4-Benzo-1,1,2,2-tetraethyl-1,2-disilacyclobutene. *J. Organomet. Chem.* **1992**, *439*, 19–21.
- Uchimar, Y.; El Sayed, A. M. M.; Tanaka, M. Selective Arylation of a Silicon-Hydrogen Bond in o-Bis(dimethylsilyl)benzene via Carbon-Hydrogen Bond Activation of Arenes. *Organometallics* **1993**, *12*, 2065–2069.
- Tatsuo, I.; Kousaku, I.; Jun, T.; Norio, M. Palladium-Catalyzed Benzylic C–H Borylation of Alkylbenzenes with Bis(pinacolato)-diboron or Pinacolborane. *Chem. Lett.* **2001**, *30*, 1082–1083.
- Tsukada, N.; Hartwig, J. F. Intermolecular and Intramolecular, Platinum-Catalyzed, Acceptorless Dehydrogenative Coupling of Hydrosilanes with Aryl and Aliphatic Methyl C–H Bonds. *J. Am. Chem. Soc.* **2005**, *127*, 5022–5023.
- Miki, M.; Naoaki, F.; Jun-ichi, W.; Shinji, W.; Yuzuru, M. Platinum-Catalyzed Aromatic C–H Silylation of Arenes with 1,1,1,3,5,5,5-Heptamethyltrisiloxane. *Chem. Lett.* **2007**, *36*, 910–911.
- Ohmura, T.; Kijima, A.; Sugino, M. Synthesis of 1-Borylisoindoles via Palladium-Catalyzed Dehydrogenation/C–H Borylation of Isoindolines. *J. Am. Chem. Soc.* **2009**, *131*, 6070–6071.
- Takaya, J.; Ito, S.; Nomoto, H.; Saito, N.; Kirai, N.; Iwasawa, N. Fluorine-Controlled C–H Borylation of Arenes Catalyzed by a P<sub>2</sub>SiN-Pincer Platinum Complex. *Chem. Commun.* **2015**, *51*, 17662–17665.
- Furukawa, T.; Tobisu, M.; Chatani, N. C–H Functionalization at Sterically Congested Positions by the Platinum-Catalyzed Borylation of Arenes. *J. Am. Chem. Soc.* **2015**, *137*, 12211–12214.
- Furukawa, T.; Tobisu, M.; Chatani, N. Nickel-Catalyzed Borylation of Arenes and Indoles via C–H Bond Cleavage. *Chem. Commun.* **2015**, *51*, 6508–6511.
- Zhang, H.; Hagihara, S.; Itami, K. Aromatic C–H Borylation by Nickel Catalysis. *Chem. Lett.* **2015**, *44*, 779–781.

- (17) Yoshii, D.; Yatabe, T.; Yabe, T.; Yamaguchi, K. C(sp<sup>3</sup>)-H Selective Benzylic Borylation by In Situ Reduced Ultrasmall Ni Species on CeO<sub>2</sub>. *ACS Catal.* **2021**, *11*, 2150–2155.
- (18) Procopio, L. J.; Berry, D. H. Dehydrogenative Coupling of Trialkylsilanes Mediated by Ruthenium Phosphine Complexes: Catalytic Synthesis of Carbosilanes. *J. Am. Chem. Soc.* **1991**, *113*, 4039–4040.
- (19) Djurovich, P. I.; Dolich, A. R.; Berry, D. H. Transfer Dehydrogenative Coupling of Triethylsilane Catalysed by Ruthenium and Rhodium Complexes. A New Si-C Bond Forming Process. *J. Chem. Soc. Chem. Commun.* **1994**, 1897–1898.
- (20) Ezbiansky, K.; Djurovich, P. I.; LaForest, M.; Sinning, D. J.; Zayes, R.; Berry, D. H. Catalytic C-H Bond Functionalization: Synthesis of Arylsilanes by Dehydrogenative Transfer Coupling of Arenes and Triethylsilane. *Organometallics* **1998**, *17*, 1455–1457.
- (21) Murphy, J. M.; Lawrence, J. D.; Kawamura, K.; Incarvito, C.; Hartwig, J. F. Ruthenium-Catalyzed Regiospecific Borylation of Methyl C-H Bonds. *J. Am. Chem. Soc.* **2006**, *128*, 13684–13685.
- (22) Mazzacano, T. J.; Mankad, N. P. Base Metal Catalysts for Photochemical C-H Borylation That Utilize Metal-Metal Cooperativity. *J. Am. Chem. Soc.* **2013**, *135*, 17258–17261.
- (23) Sunada, Y.; Soejima, H.; Nagashima, H. Disilaferracycle Dicarboxyl Complex Containing Weakly Coordinated η<sup>2</sup>-(H-Si) Ligands: Application to C-H Functionalization of Indoles and Arenes. *Organometallics* **2014**, *33*, 5936–5939.
- (24) Dombay, T.; Werncke, C. G.; Jiang, S.; Grellier, M.; Vendier, L.; Bontemps, S.; Sortais, J.-B.; Sabo-Etienne, S.; Darcel, C. Iron-Catalyzed C-H Borylation of Arenes. *J. Am. Chem. Soc.* **2015**, *137*, 4062–4065.
- (25) Chen, H.; Hartwig, J. F. Catalytic, Regiospecific End-Functionalization of Alkanes: Rhenium-Catalyzed Borylation under Photochemical Conditions. *Angew. Chem., Int. Ed.* **1999**, *38*, 3391–3393.
- (26) Cheng, C.; Hartwig, J. F. Rhodium-Catalyzed Intermolecular C-H Silylation of Arenes with High Steric Regiocontrol. *Science* **2014**, *343*, 853–857.
- (27) Karmel, C.; Chen, Z.; Hartwig, J. F. Iridium-Catalyzed Silylation of C-H Bonds in Unactivated Arenes: A Sterically Encumbered Phenanthroline Ligand Accelerates Catalysis. *J. Am. Chem. Soc.* **2019**, *141*, 7063–7072.
- (28) Obligacion, J. V.; Semproni, S. P.; Chirik, P. J. Cobalt-Catalyzed C-H Borylation. *J. Am. Chem. Soc.* **2014**, *136*, 4133–4136.
- (29) Ishiyama, T.; Takagi, J.; Ishida, K.; Miyaura, N.; Anastasi, N.; Hartwig, J. F. Mild Iridium-Catalyzed Borylation of Arenes. High Turnover Numbers, Room Temperature Reactions, and Isolation of a Potential Intermediate. *J. Am. Chem. Soc.* **2002**, *124*, 390–391.
- (30) Preshlock, S. M.; Ghaffari, B.; Maligres, P. E.; Krska, S. W.; Maleczka, R. E., Jr; Smith, M. R., III High-Throughput Optimization of Ir-Catalyzed C-H Borylation: A Tutorial for Practical Applications. *J. Am. Chem. Soc.* **2013**, *135*, 7572–7582.
- (31) Larsen, M. A.; Hartwig, J. F. Iridium-Catalyzed C-H Borylation of Heteroarenes: Scope, Regioselectivity, Application to Late-Stage Functionalization, and Mechanism. *J. Am. Chem. Soc.* **2014**, *136*, 4287–4299.
- (32) Chen, H.; Schlecht, S.; Semple, T. C.; Hartwig, J. F. Thermal, Catalytic, Regiospecific Functionalization of Alkanes. *Science* **2000**, *287*, 1995–1997.
- (33) Obligacion, J. V.; Semproni, S. P.; Pappas, I.; Chirik, P. J. Cobalt-Catalyzed C(sp<sup>2</sup>)-H Borylation: Mechanistic Insights Inspire Catalyst Design. *J. Am. Chem. Soc.* **2016**, *138*, 10645–10653.
- (34) Boller, T. M.; Murphy, J. M.; Hapke, M.; Ishiyama, T.; Miyaura, N.; Hartwig, J. F. Mechanism of the Mild Functionalization of Arenes by Diboron Reagents Catalyzed by Iridium Complexes. Intermediacy and Chemistry of Bipyridine-Ligated Iridium Tris Boryl Complexes. *J. Am. Chem. Soc.* **2005**, *127*, 14263–14278.
- (35) Karmel, C.; Hartwig, J. F. Mechanism of the Iridium-Catalyzed Silylation of Aromatic C-H Bonds. *J. Am. Chem. Soc.* **2020**, *142*, 10494–10505.
- (36) Tamura, H.; Yamazaki, H.; Sato, H.; Sakaki, S. Iridium-Catalyzed Borylation of Benzene with Diboron. Theoretical Elucidation of Catalytic Cycle Including Unusual Iridium(V) Intermediate. *J. Am. Chem. Soc.* **2003**, *125*, 16114–16126.
- (37) Huang, G.; Kalek, M.; Liao, R.-Z.; Himo, F. Mechanism, Reactivity, and Selectivity of the Iridium-Catalyzed C(sp<sup>3</sup>)-H Borylation of Chlorosilanes. *Chem. Sci.* **2015**, *6*, 1735–1746.
- (38) Clot, E.; Mégret, C.; Eisenstein, O.; Perutz, R. N. Validation of the M-C/H-C Bond Enthalpy Relationship through Application of Density Functional Theory. *J. Am. Chem. Soc.* **2006**, *128*, 8350–8357.
- (39) Guilhaumé, J.; Clot, E.; Eisenstein, O.; Perutz, R. N. Importance of Palladium-Carbon Bond Energies in Direct Arylation of Polyfluorinated Benzenes. *Dalton Trans.* **2010**, *39*, 10510–10519.
- (40) Tajuddin, H.; Harrison, P.; Bitterlich, B.; Collings, J. C.; Sim, N.; Batsanov, A. S.; Cheung, M. S.; Kawamorita, S.; Maxwell, A. C.; Shukla, L.; Morris, J.; Lin, Z.; Marder, T. B.; Steel, P. G. Iridium-Catalyzed C-H Borylation of Quinolines and Unsymmetrical 1,2-Disubstituted Benzenes: Insights into Steric and Electronic Effects on Selectivity. *Chem. Sci.* **2012**, *3*, 3505–3515.
- (41) Wright, J. S.; Scott, P. J. H.; Steel, P. G. Iridium-Catalyzed C-H Borylation of Heteroarenes: Balancing Steric and Electronic Regiocontrol. *Angew. Chem., Int. Ed.* **2021**, *60*, 2796–2821.
- (42) Caldeweyher, E.; Elkin, M.; Gheibi, G.; Johansson, M.; Sködl, C.; Norrby, P.-O.; Hartwig, J. F. Hybrid Machine Learning Approach to Predict the Site Selectivity of Iridium-Catalyzed Arene Borylation. *J. Am. Chem. Soc.* **2023**, *145*, 17367–17376.
- (43) Rej, S.; Chatani, N. Regioselective Transition-Metal-Free C(sp<sup>2</sup>)-H Borylation: A Subject of Practical and Ongoing Interest in Synthetic Organic Chemistry. *Angew. Chem., Int. Ed.* **2022**, *61*, No. e202209539.
- (44) Bähr, S.; Oestreich, M. Electrophilic Aromatic Substitution with Silicon Electrophiles: Catalytic Friedel-Crafts C-H Silylation. *Angew. Chem., Int. Ed.* **2017**, *56*, 52–59.
- (45) Shu, C.; Noble, A.; Aggarwal, V. K. Metal-free photoinduced C(sp<sup>3</sup>)-H borylation of alkanes. *Nature* **2020**, *586*, 714–719.
- (46) Sarkar, S.; Wagulde, S.; Jia, X.; Gevorgyan, V. General and selective metal-free radical α-C-H borylation of aliphatic amines. *Chem.* **2022**, *8*, 3096–3108.
- (47) Tu, J.-L.; Hu, A.-M.; Guo, L.; Xia, W. Iron-Catalyzed C(sp<sup>3</sup>)-H Borylation, Thiolation, and Sulfinylation Enabled by Photoinduced Ligand-to-Metal Charge Transfer. *J. Am. Chem. Soc.* **2023**, *145*, 7600–7611.
- (48) Toutov, A. A.; Liu, W.-B.; Betz, K. N.; Fedorov, A.; Stoltz, B. M.; Grubbs, R. H. Silylation of C-H bonds in aromatic heterocycles by an Earth-abundant metal catalyst. *Nature* **2015**, *518*, 80–84.
- (49) Liu, S.; Pan, P.; Fan, H.; Li, H.; Wang, W.; Zhang, Y. Photocatalytic C-H silylation of heteroarenes by using trialkylhydrosilanes. *Chem. Sci.* **2019**, *10*, 3817–3825.
- (50) Rammal, F.; Gao, D.; Boujnah, S.; Hussein, A. A.; Lalevé, J.; Gaumont, A.-C.; Morlet-Savary, F.; Lakhdar, S. Photochemical C-H Silylation and Hydroxymethylation of Pyridines and Related Structures: Synthetic Scope and Mechanisms. *ACS Catal.* **2020**, *10*, 13710–13717.
- (51) Kim, J. H.; Constantin, T.; Simonetti, M.; Lloveria, J.; Sheikh, N. S.; Leonori, D. A Radical Approach for the Selective C-H Borylation of Azines. *Nature* **2021**, *595*, 677–683.
- (52) Du, W.; Kaskar, B.; Blumbergs, P.; Subramanian, P. K.; Curran, D. P. Semisynthesis of DB-67 and other Silatecans from Camptothecin by Thiol-Promoted Addition of Silyl Radicals. *Bioorg. Med. Chem.* **2003**, *11*, 451–458.
- (53) Leonori, D.; Aggarwal, V. K. Lithiation-Borylation Methodology and Its Application in Synthesis. *Acc. Chem. Res.* **2014**, *47*, 3174–3183.
- (54) Hartwig, J. F.; Romero, E. A. Iridium-Catalyzed Silylation of Unactivated C-H Bonds. *Tetrahedron* **2019**, *75*, 4059–4070.
- (55) Richter, S. C.; Oestreich, M. Emerging Strategies for C-H Silylation. *Trends Chem.* **2020**, *2*, 13–27.
- (56) Li, B.; Dixneuf, P. H. Metal-Catalyzed Silylation of sp<sup>3</sup> C-H Bonds. *Chem. Soc. Rev.* **2021**, *50*, 5062–5085.

- (57) Hua, Y.; Asgari, P.; Avullala, T.; Jeon, J. Catalytic Reductive ortho-C-H Silylation of Phenols with Traceless, Versatile Acetal Directing Groups and Synthetic Applications of Dioxasilines. *J. Am. Chem. Soc.* **2016**, *138*, 7982–7991.
- (58) Lin, Y.; Jiang, K.-Z.; Cao, J.; Zheng, Z.-J.; Xu, Z.; Cui, Y.-M.; Xu, L.-W. Iridium-Catalyzed Intramolecular C-H Silylation of Siloxane-Tethered Arene and Hydrosilane: Facile and Catalytic Synthesis of Cyclic Siloxanes. *Adv. Synth. Catal.* **2017**, *359*, 2247–2252.
- (59) Devaraj, K.; Sollert, C.; Juds, C.; Gates, P. J.; Pilarski, L. T. Ru-Catalyzed C-H Silylation of Unprotected Gramines, Tryptamines and Their Congeners. *Chem. Commun.* **2016**, *52*, 5868–5871.
- (60) Wang, D.; Li, M.; Chen, X.; Wang, M.; Liang, Y.; Zhao, Y.; Houk, K. N.; Shi, Z. Palladium-Catalyzed Silacyclization of (Hetero)-Arenes with a Tetrasilane Reagent through Twofold C-H Activation. *Angew. Chem., Int. Ed.* **2021**, *60*, 7066–7071.
- (61) Wang, D.; Chen, X.; Wong, J. J.; Jin, L.; Li, M.; Zhao, Y.; Houk, K. N.; Shi, Z. Phosphorus(III)-Assisted Regioselective C-H Silylation of Heteroarenes. *Nat. Commun.* **2021**, *12*, 524.
- (62) Modak, A.; Patra, T.; Chowdhury, R.; Raul, S.; Maiti, D. Palladium-Catalyzed Remote meta-Selective C-H Bond Silylation and Germanylation. *Organometallics* **2017**, *36*, 2418–2423.
- (63) Cheng, C.; Hartwig, J. F. Iridium-Catalyzed Silylation of Aryl C-H Bonds. *J. Am. Chem. Soc.* **2015**, *137*, 592–595.
- (64) Karmel, C.; Rubel, C. Z.; Kharitonova, E. V.; Hartwig, J. F. Iridium-Catalyzed Silylation of Five-Membered Heteroarenes: High Sterically Derived Selectivity from a Pyridyl-Imidazoline Ligand. *Angew. Chem., Int. Ed.* **2020**, *59*, 6074–6081.
- (65) Simmons, E. M.; Hartwig, J. F. Catalytic Functionalization of Unactivated Primary C-H Bonds Directed by an Alcohol. *Nature* **2012**, *483*, 70–73.
- (66) Bian, L.; Cao, S.; Cheng, L.; Nakazaki, A.; Nishikawa, T.; Qi, J. Semi-Synthesis and Structure-Activity Relationship of Neuritogenic Oleanene Derivatives. *Chem. Med. Chem.* **2018**, *13*, 1972–1977.
- (67) Li, B. J.; Driess, M.; Hartwig, J. F. Iridium-Catalyzed Regioselective Silylation of Secondary Alkyl C-H Bonds for the Synthesis of 1,3-Diols. *J. Am. Chem. Soc.* **2014**, *136*, 6586–6589.
- (68) Frihed, T. G.; Heuckendorff, M.; Pedersen, C. M.; Bols, M. Easy Access to L-Mannosides and L-Galactosides by Using C-H Activation of the Corresponding 6-Deoxysugars. *Angew. Chem., Int. Ed.* **2012**, *51*, 12285–12288.
- (69) Frihed, T. G.; Pedersen, C. M.; Bols, M. Synthesis of All Eight L-Glycopyranosyl Donors Using C-H Activation. *Angew. Chem., Int. Ed.* **2014**, *53*, 13889–13893.
- (70) Michaudel, Q.; Journot, G.; Regueiro-Ren, A.; Goswami, A.; Guo, Z.; Tully, T. P.; Zou, L.; Ramabhadran, R. O.; Houk, K. N.; Baran, P. S. Improving Physical Properties via C-H Oxidation: Chemical and Enzymatic Approaches. *Angew. Chem., Int. Ed.* **2014**, *53*, 12091–12096.
- (71) Ma, X.; Kucera, R.; Goethe, O. F.; Murphy, S. K.; Herzon, S. B. Directed C-H Bond Oxidation of (+)-Pleuromutilin. *J. Org. Chem.* **2018**, *83*, 6843–6892.
- (72) Hung, K.; Condakes, M. L.; Novaes, L. F. T.; Harwood, S. J.; Morikawa, T.; Yang, Z.; Maimone, T. J. Development of a Terpene Feedstock-Based Oxidative Synthetic Approach to the Illicium Sesquiterpenes. *J. Am. Chem. Soc.* **2019**, *141*, 3083–3099.
- (73) Leger, P. R.; Kuroda, Y.; Chang, S.; Jurczyk, J.; Sarpong, R. C-C Bond Cleavage Approach to Complex Terpenoids: Development of a Unified Total Synthesis of the Phomactins. *J. Am. Chem. Soc.* **2020**, *142*, 15536–15547.
- (74) Zeng, Z.-Y.; Liao, J.-X.; Hu, Z.-N.; Liu, D.-Y.; Zhang, Q.-J.; Sun, J.-S. Chemical Synthesis of Quillaic Acid, the Aglycone of QS-21. *Org. Chem. Front.* **2021**, *8*, 748–753.
- (75) Chen, J.; Shi, Z.; Lu, P. Enantioselective Synthesis of Indanes with a Quaternary Stereocenter via Diastereoselective C(sp<sup>3</sup>)-H Functionalization. *Org. Lett.* **2021**, *23*, 7359–7363.
- (76) Lusi, R. F.; Sennari, G.; Sarpong, R. Total Synthesis of Nine Longiborneol Sesquiterpenoids Using a Functionalized Camphor Strategy. *Nat. Chem.* **2022**, *14*, 450–456.
- (77) Ghavtadze, N.; Melkonyan, F. S.; Gulevich, A. V.; Huang, C.; Gevorgyan, V. Conversion of 1-Alkenes into 1,4-Diols Through an Auxiliary-Mediated Formal Homoallylic C-H Oxidation. *Nat. Chem.* **2014**, *6*, 122–125.
- (78) Karmel, C.; Li, B.; Hartwig, J. F. Rhodium-Catalyzed Regioselective Silylation of Alkyl C-H Bonds for the Synthesis of 1,4-Diols. *J. Am. Chem. Soc.* **2018**, *140*, 1460–1470.
- (79) Su, B.; Hartwig, J. F. Ir-Catalyzed Enantioselective, Intramolecular Silylation of Methyl C-H Bonds. *J. Am. Chem. Soc.* **2017**, *139*, 12137–12140.
- (80) Yang, B.; Yang, W.; Guo, Y.; You, L.; He, C. Enantioselective Silylation of Aliphatic C-H Bonds for the Synthesis of Silicon-Stereogenic Dihydrobenzosiloles. *Angew. Chem., Int. Ed.* **2020**, *59*, 22217–22222.
- (81) Bunescu, A.; Butcher, T. W.; Hartwig, J. F. Traceless Silylation of  $\beta$ -C(sp<sup>3</sup>)-H Bonds of Alcohols via Perfluorinated Acetals. *J. Am. Chem. Soc.* **2018**, *140*, 1502–1507.
- (82) Su, B.; Lee, T.; Hartwig, J. F. Iridium-Catalyzed,  $\beta$ -Selective C(sp<sup>3</sup>)-H Silylation of Aliphatic Amines To Form Silapyrrolidines and 1,2-Amino Alcohols. *J. Am. Chem. Soc.* **2018**, *140*, 18032–18038.
- (83) Pan, J.-L.; Li, Q.-Z.; Zhang, T.-Y.; Hou, S.-H.; Kang, J.-C.; Zhang, S.-Y. Palladium-Catalyzed Direct Intermolecular Silylation of Remote Unactivated C(sp<sup>3</sup>)-H Bonds. *Chem. Commun.* **2016**, *52*, 13151–13154.
- (84) Liu, Y.-J.; Liu, Y.-H.; Zhang, Z.-Z.; Yan, S.-Y.; Chen, K.; Shi, B.-F. Divergent and Stereoselective Synthesis of  $\beta$ -Silyl- $\alpha$ -Amino Acids through Palladium-Catalyzed Intermolecular Silylation of Unactivated Primary and Secondary C-H Bonds. *Angew. Chem., Int. Ed.* **2016**, *55*, 13859–13862.
- (85) Zhan, B.-B.; Fan, J.; Jin, L.; Shi, B.-F. Divergent Synthesis of Silicon-Containing Peptides via Pd-Catalyzed Post-Assembly  $\gamma$ -C(sp<sup>3</sup>)-H Silylation. *ACS Catal.* **2019**, *9*, 3298–3303.
- (86) Li, J.; Jiang, C. Palladium-Catalyzed C-H Silylation of Aliphatic Ketones Using an Aminooxyamide Auxiliary. *Org. Lett.* **2021**, *23*, 5359–5362.
- (87) Miyaura, N.; Suzuki, A. Palladium-Catalyzed Cross-Coupling Reactions of Organoboron Compounds. *Chem. Rev.* **1995**, *95*, 2457–2483.
- (88) Suzuki, A. Cross-Coupling Reactions Of Organoboranes: An Easy Way To Construct C-C Bonds (Nobel Lecture). *Angew. Chem., Int. Ed.* **2011**, *50*, 6722–6737.
- (89) Beck, E. M.; Hatley, R.; Gaunt, M. J. Synthesis of Rhazinicine by a Metal-Catalyzed C-H Bond Functionalization Strategy. *Angew. Chem., Int. Ed.* **2008**, *47*, 3004–3007.
- (90) Kholod, I.; Vallat, O.; Buciumas, A.-M.; Neels, A.; Neier, R. Synthetic Strategies for the Synthesis and Transformation of Rhazinilam Analogues. *Eur. J. Org. Chem.* **2014**, *2014*, 7865–7877.
- (91) Kikuchi, T.; Takagi, J.; Isou, H.; Ishiyama, T.; Miyaura, N. Vinyl C-H Borylation of Cyclic Vinyl Ethers with Bis(pinacolato)-diboron Catalyzed by an Iridium(I)-dtbpy Complex. *Chem.—Asian J.* **2008**, *3*, 2082–2090.
- (92) Fischer, D. F.; Sarpong, R. Total Synthesis of (+)-Complanidine A Using an Iridium-Catalyzed Pyridine C-H Functionalization. *J. Am. Chem. Soc.* **2010**, *132*, 5926–5927.
- (93) Robbins, D. W.; Boebel, T. A.; Hartwig, J. F. Iridium-Catalyzed, Silyl-Directed Borylation of Nitrogen-Containing Heterocycles. *J. Am. Chem. Soc.* **2010**, *132*, 4068–4069.
- (94) Liskey, C. W.; Liao, X. B.; Hartwig, J. F. Cyanation of Arenes via Iridium-Catalyzed Borylation. *J. Am. Chem. Soc.* **2010**, *132*, 11389–11391.
- (95) Sumida, Y.; Harada, R.; Kato-Sumida, T.; Johmoto, K.; Uekusa, H.; Hosoya, T. Boron-Selective Biaryl Coupling Approach to Versatile Dibenzoxaborins and Application to Concise Synthesis of Defucogilvocarcin M. *Org. Lett.* **2014**, *16*, 6240–6243.
- (96) Han, S.; Movassaghi, M. Concise Total Synthesis and Stereochemical Revision of all (–)-Trigonoliumins. *J. Am. Chem. Soc.* **2011**, *133*, 10768–10771.

- (97) Liu, F.; Movassaghi, M. Electrophilic Carbonyl Activation: Competing Condensative Cyclizations of Tryptamine Derivatives. *Tetrahedron Lett.* **2015**, *56*, 2995–3000.
- (98) Schwaben, J.; Cordes, J.; Harms, K.; Koert, U. Total Syntheses of (+)-Pestaphthalide A and (–)-Pestaphthalide B. *Synthesis* **2011**, *2011*, 2929–2934.
- (99) Bartholomäus, R.; Dommershausen, F.; Thiele, M.; Karanjule, N. S.; Harms, K.; Koert, U. Total Synthesis of the Postulated Structure of Fulicineroside. *Eur. J. Chem.* **2013**, *19*, 7423–7436.
- (100) López-Rodríguez, R.; Ros, A.; Fernández, R.; Lassaletta, J. M. Pinacolborane as the Boron Source in Nitrogen-Directed Borylations of Aromatic N,N-Dimethylhydrazones. *J. Org. Chem.* **2012**, *77*, 9915–9920.
- (101) Filipiński, K. J.; Guzman-Perez, A.; Bian, J.; Perreault, C.; Aspnes, G. E.; Didiuk, M. T.; Dow, R. L.; Hank, R. F.; Jones, C. S.; Maguire, R. J.; Tu, M.; Zeng, D.; Liu, S.; Knafels, J. D.; Litchfield, J.; Atkinson, K.; Derksen, D. R.; Bourbonnais, F.; Gajiwala, K. S.; Hickey, M.; Johnson, T. O.; Humphries, P. S.; Pfeifferkorn, J. A. Pyrimidone-Based Series of Glucokinase Activators with Alternative Donor-Acceptor Motif. *Bioorg. Med. Chem. Lett.* **2013**, *23*, 4571–4578.
- (102) Seechurn, C. C. C. J.; Sivakumar, V.; Satoskar, D.; Colacot, T. J. Iridium-Catalyzed C–H Borylation of Heterocycles Using an Overlooked 1,10-Phenanthroline Ligand: Reinventing the Catalytic Activity by Understanding the Solvent-Assisted Neutral to Cationic Switch. *Organometallics* **2014**, *33*, 3514–3522.
- (103) Kallepalli, V. A.; Shi, F.; Paul, S.; Onyeozili, E. N.; Maleczka, R. E.; Smith, M. R. I. Boc Groups as Protectors and Directors for Ir-Catalyzed C–H Borylation of Heterocycles. *J. Org. Chem.* **2009**, *74*, 9199–9201.
- (104) Shockley, S. E.; Holder, J. C.; Stoltz, B. M. A Catalytic, Enantioselective Formal Synthesis of (+)-Dichroanone and (+)-Taiwaniquinone H. *Org. Lett.* **2014**, *16*, 6362–6365.
- (105) Pitts, A. K.; O'Hara, F.; Snell, R. H.; Gaunt, M. J. A Concise and Scalable Strategy for the Total Synthesis of Dictyodendrin B Based on Sequential C–H Functionalization. *Angew. Chem., Int. Ed.* **2015**, *54*, 5451–5455.
- (106) Li, H. L.; Kuninobu, Y.; Kanai, M. Lewis Acid-Base Interaction-Controlled ortho-Selective C–H Borylation of Aryl Sulfides. *Angew. Chem., Int. Ed.* **2017**, *56*, 1495–1499.
- (107) Li, H.-L.; Kanai, M.; Kuninobu, Y. Iridium/Bipyridine-Catalyzed ortho-Selective C–H Borylation of Phenol and Aniline Derivatives. *Org. Lett.* **2017**, *19*, 5944–5947.
- (108) Obligacion, J. V.; Bezdek, M. J.; Chirik, P. J. C(sp<sup>2</sup>)-H Borylation of Fluorinated Arenes Using an Air-Stable Cobalt Precatalyst: Electronically Enhanced Site Selectivity Enables Synthetic Opportunities. *J. Am. Chem. Soc.* **2017**, *139*, 2825–2832.
- (109) Cao, B.-C.; Wu, G.-J.; Yu, F.; He, Y.-P.; Han, F.-S. A Total Synthesis of (–)-Hamigeran B and (–)-4-Bromohamigeran B. *Org. Lett.* **2018**, *20*, 3687–3690.
- (110) Shi, Y.; Yang, Y.; Xu, S. Iridium-Catalyzed Enantioselective C(sp<sup>3</sup>)-H Borylation of Aminocyclopropanes. *Angew. Chem., Int. Ed.* **2022**, *61*, No. e202201463.
- (111) Marcos-Atanes, D.; Vidal, C.; Navo, C. D.; Peccati, F.; Jiménez-Osés, G.; Mascareñas, J. L. Iridium-Catalyzed ortho-Selective Borylation of Aromatic Amides Enabled by 5-Trifluoromethylated Bipyridine Ligands. *Angew. Chem., Int. Ed.* **2023**, *62*, e202214510.
- (112) Miller, J. F.; Chong, P. Y.; Shotwell, J. B.; Catalano, J. G.; Tai, V. W. F.; Fang, J.; Banka, A. L.; Roberts, C. D.; Youngman, M.; Zhang, H.; Xiong, Z.; Mathis, A.; Pouliot, J. J.; Hamatake, R. K.; Price, D. J.; Seal, J. W., III; Stroup, L. L.; Creech, K. L.; Carballo, L. H.; Todd, D.; Spaltenstein, A.; Furst, S.; Hong, Z.; Peat, A. J. Hepatitis C Replication Inhibitors That Target the Viral NS4B Protein. *J. Med. Chem.* **2014**, *57*, 2107–2120.
- (113) Campeau, L.-C.; Chen, Q.; Gauvreau, D.; Girardin, M.; Belyk, K.; Maligres, P.; Zhou, G.; Gu, C.; Zhang, W.; Tan, L.; O'Shea, P. D. A Robust Kilo-Scale Synthesis of Doravirine. *Org. Process Res. Dev.* **2016**, *20*, 1476–1481.
- (114) Murphy, J. M.; Liao, X.; Hartwig, J. F. Meta Halogenation of 1,3-Disubstituted Arenes via Iridium-Catalyzed Arene Borylation. *J. Am. Chem. Soc.* **2007**, *129*, 15434–15435.
- (115) Cordes, J.; Wessel, C.; Harms, K.; Koert, U. meta-Selective Aromatic Borylation as Key Step in the Synthesis of Poipuol. *Synthesis* **2008**, *2008*, 2217–2220.
- (116) Zhao, L.; Tsukano, C.; Kwon, E.; Takemoto, Y.; Hiram, M. Total Syntheses of Complanadines A and B. *Angew. Chem., Int. Ed.* **2013**, *52*, 1722–1725.
- (117) Zhao, L.; Tsukano, C.; Kwon, E.; Shirakawa, H.; Kaneko, S.; Takemoto, Y.; Hiram, M. Competent Route to Unsymmetric Dimer Architectures: Total Syntheses of (–)-Lycodine and (–)-Complanadines A and B, and Evaluation of Their Neurite Outgrowth Activities. *Eur. J. Chem.* **2017**, *23*, 802–812.
- (118) Sieser, J. E.; Maloney, M. T.; Chisowa, E.; Brenek, S. J.; Monfette, S.; Salisbury, J. J.; Do, N. M.; Singer, R. A. Ir-Catalyzed Borylation as an Efficient Route to a Nicotine Hapten. *Org. Process Res. Dev.* **2018**, *22*, 527–534.
- (119) Robinson, H.; Stillibrand, J.; Simelis, K.; Macdonald, S. J. F.; Nortcliffe, A. Iridium-catalysed C–H borylation of  $\beta$ -aryl-amino-propionic acids. *Org. Biomol. Chem.* **2020**, *18*, 6696–6701.
- (120) Srinivasan, R.; Coyne, A. G.; Abell, C. Regioselective Conversion of Arenes to N-aryl-1,2,3-triazoles Using C–H Borylation. *Eur. J. Chem.* **2014**, *20*, 11680–11684.
- (121) Li, X.; Deng, X.; Coyne, A. G.; Srinivasan, R. meta-Nitration of Arenes Bearing ortho/para Directing Group(s) Using C–H Borylation. *Chem.—Eur. J.* **2019**, *25*, 8018–8023.
- (122) Loach, R. P.; Fenton, O. S.; Amaike, K.; Siegel, D. S.; Ozkal, E.; Movassaghi, M. C7-Derivatization of C3-Alkylindoles Including Tryptophans and Tryptamines. *J. Org. Chem.* **2014**, *79*, 11254–11263.
- (123) Kallepalli, V. A.; Gore, K. A.; Shi, F.; Sanchez, L.; Chotana, G. A.; Miller, S. L.; Maleczka, R. E.; Smith, M. R. Harnessing C–H Borylation/Deborylation for Selective Deuteration, Synthesis of Boronate Esters, and Late Stage Functionalization. *J. Org. Chem.* **2015**, *80*, 8341–8353.
- (124) Meyer, F.-M.; Liras, S.; Guzman-Perez, A.; Perreault, C.; Bian, J.; James, K. Functionalization of Aromatic Amino Acids via Direct C–H Activation: Generation of Versatile Building Blocks for Accessing Novel Peptide Space. *Org. Lett.* **2010**, *12*, 3870–3873.
- (125) Hananya, N.; Eldar Boock, A.; Bauer, C. R.; Satchi-Fainaro, R.; Shabat, D. Remarkable Enhancement of Chemiluminescent Signal by Dioxetane-Fluorophore Conjugates: Turn-ON Chemiluminescence Probes with Color Modulation for Sensing and Imaging. *J. Am. Chem. Soc.* **2016**, *138*, 13438–13446.
- (126) Miura, W.; Hirano, K.; Miura, M. Iridium-Catalyzed Site-Selective C–H Borylation of 2-Pyridones. *Synthesis* **2017**, *49*, 4745–4752.
- (127) Fischer, D. F.; Sarpong, R. Total Synthesis of (+)-Complanadine A Using an Iridium-Catalyzed Pyridine C–H Functionalization. *J. Am. Chem. Soc.* **2010**, *132*, 5926–5927.
- (128) Antropow, A. H.; Garcia, N. R.; White, K. L.; Movassaghi, M. Enantioselective Synthesis of (–)-Vallesine: Late-Stage C17-Oxidation via Complex Indole Boronation. *Org. Lett.* **2018**, *20*, 3647–3650.
- (129) Myeong, I.-S.; Avci, N. H.; Movassaghi, M. Total Synthesis of (–)-Kopsifoline A and (+)-Kopsifoline E. *Org. Lett.* **2021**, *23*, 9118–9122.
- (130) Gao, P.; Szostak, M. Highly Selective and Divergent Acyl and Aryl Cross-Couplings of Amides via Ir-Catalyzed C–H Borylation/N–C(O) Activation. *Org. Lett.* **2020**, *22*, 6010–6015.
- (131) Wright, J. S.; Sharninghausen, L. S.; Preshlock, S.; Brooks, A. F.; Sanford, M. S.; Scott, P. J. H. Sequential Ir/Cu-Mediated Method for the Meta-Selective C–H Radiofluorination of (Hetero)Arenes. *J. Am. Chem. Soc.* **2021**, *143*, 6915–6921.
- (132) Brooks, A. F.; Topczewski, J. J.; Ichiishi, N.; Sanford, M. S.; Scott, P. J. H. Late-Stage [18F]Fluorination: New Solutions to Old Problems. *Chem. Sci.* **2014**, *5*, 4545–4553.
- (133) Gayler, K. M.; Kong, K.; Reisenauer, K.; Taube, J. H.; Wood, J. L. Staurosporine Analogs Via C–H Borylation. *ACS Med. Chem. Lett.* **2020**, *11*, 2441–2445.



- (134) Bream, R. N.; Clark, H.; Edney, D.; Harsanyi, A.; Hayler, J.; Ironmonger, A.; Mc Cleary, N.; Phillips, N.; Priestley, C.; Roberts, A.; Rushworth, P.; Szeto, P.; Webb, M. R.; Wheelhouse, K. Application of C-H Functionalization in the Development of a Concise and Convergent Route to the Phosphatidylinositol-3-kinase Delta Inhibitor Nemiralisib. *Org. Process Res. Dev.* **2021**, *25*, 529–540.
- (135) Saito, Y.; Segawa, Y.; Itami, K. para-C-H Borylation of Benzene Derivatives by a Bulky Iridium Catalyst. *J. Am. Chem. Soc.* **2015**, *137*, 5193–5198.
- (136) Saito, Y.; Yamanoue, K.; Segawa, Y.; Itami, K. Selective Transformation of Strychnine and 1,2-Disubstituted Benzenes by C-H Borylation. *Chem.* **2020**, *6*, 985–993.
- (137) Hoque, M. E.; Bisht, R.; Unnikrishnan, A.; Dey, S.; Mahamudul Hassan, M. M.; Guria, S.; Rai, R. N.; Sunoj, R. B.; Chattopadhyay, B. Iridium-Catalyzed Ligand-Controlled Remote para-Selective C-H Activation and Borylation of Twisted Aromatic Amides. *Angew. Chem., Int. Ed.* **2022**, *61*, No. e202203539.
- (138) Kuleshova, O.; Asako, S.; Ilies, L. Ligand-Enabled, Iridium-Catalyzed ortho-Borylation of Fluoroarenes. *ACS Catal.* **2021**, *11*, 5968–5973.
- (139) Ramadoss, B.; Jin, Y.; Asako, S.; Ilies, L. Remote Steric Control for Undirected meta-Selective C-H Activation of Arenes. *Science* **2022**, *375*, 658–663.
- (140) Marcos-Atanes, D.; Vidal, C.; Navo, C. D.; Peccati, F.; Jiménez-Osés, G.; Mascareñas, J. L. Iridium-Catalyzed ortho-Selective Borylation of Aromatic Amides Enabled by 5-Trifluoromethylated Bipyridine Ligands. *Angew. Chem., Int. Ed.* **2023**, *62*, No. e202214510.
- (141) Scott, J. S.; Moss, T. A.; Barlaam, B.; Davey, P. R. J.; Fairley, G.; Gangl, E. T.; Greenwood, R. D. R.; Hatoum-Mokdad, H.; Lister, A. S.; Longmire, D.; Polanski, R.; Stokes, S.; Tucker, M. J.; Varnes, J. G.; Yang, B. Addition of Fluorine and a Late-Stage Functionalization (LSF) of the Oral SERD AZD9833. *ACS Med. Chem. Lett.* **2020**, *11*, 2519–2525.
- (142) Mahamudul Hassan, M. M.; Mondal, B.; Singh, S.; Haldar, C.; Chaturvedi, J.; Bisht, R.; Sunoj, R. B.; Chattopadhyay, B. Ir-Catalyzed Ligand-Free Directed C-H Borylation of Arenes and Pharmaceuticals: Detailed Mechanistic Understanding. *J. Org. Chem.* **2022**, *87*, 4360–4375.
- (143) Hoque, M. E.; Hassan, M. M. M.; Chattopadhyay, B. Remarkably Efficient Iridium Catalysts for Directed C(sp<sup>2</sup>)-H and C(sp<sup>3</sup>)-H Borylation of Diverse Classes of Substrates. *J. Am. Chem. Soc.* **2021**, *143*, 5022–5037.
- (144) Oeschger, R.; Su, B.; Yu, I.; Ehinger, C.; Romero, E.; He, S.; Hartwig, J. Diverse functionalization of strong alkyl C-H bonds by undirected borylation. *Science* **2020**, *368*, 736–741.
- (145) Zhang, L. S.; Chen, G. H.; Wang, X.; Guo, Q. Y.; Zhang, X. S.; Pan, F.; Chen, K.; Shi, Z. J. Direct Borylation of Primary C-H Bonds in Functionalized Molecules by Palladium Catalysis. *Angew. Chem., Int. Ed.* **2014**, *53*, 3899–3903.
- (146) Chandrashekar, H. B.; Dolui, P.; Li, B.; Mandal, A.; Liu, H.; Guin, S.; Ge, H.; Maiti, D. Ligand-Enabled  $\delta$ -C(sp<sup>3</sup>)-H Borylation of Aliphatic Amines. *Angew. Chem., Int. Ed.* **2021**, *60*, 18194–18200.
- (147) He, J.; Jiang, H.; Takise, R.; Zhu, R.-Y.; Chen, G.; Dai, H.-X.; Dhar, T. G. M.; Shi, J.; Zhang, H.; Cheng, P. T. W.; Yu, J.-Q. Ligand-Promoted Borylation of C(sp<sup>3</sup>)-H Bonds with Palladium(II) Catalysts. *Angew. Chem., Int. Ed.* **2016**, *55*, 785–789.
- (148) Shi, Y.; Gao, Q.; Xu, S. Chiral Bidentate Boryl Ligand Enabled Iridium-Catalyzed Enantioselective C(sp<sup>3</sup>)-H Borylation of Cyclopropanes. *J. Am. Chem. Soc.* **2019**, *141*, 10599–10604.
- (149) Gao, Q.; Xu, S. Site- and Stereoselective C(sp<sup>3</sup>)-H Borylation of Strained (Hetero)Cycloalkanes Enabled by Iridium Catalysis. *Angew. Chem., Int. Ed.* **2023**, *62*, No. e202218025.
- (150) Yang, Y.; Chen, L.; Xu, S. Iridium-Catalyzed Enantioselective Unbiased Methylene C(sp<sup>3</sup>)-H Borylation of Acyclic Amides. *Angew. Chem., Int. Ed.* **2021**, *60*, 3524–3528.
- (151) Chen, L.; Yang, Y.; Liu, L.; Gao, Q.; Xu, S. Iridium-Catalyzed Enantioselective  $\alpha$ -C(sp<sup>3</sup>)-H Borylation of Azacycles. *J. Am. Chem. Soc.* **2020**, *142*, 12062–12068.
- (152) Du, R.; Liu, L.; Xu, S. Iridium-Catalyzed Regio- and Enantioselective Borylation of Unbiased Methylene C(sp<sup>3</sup>)-H Bonds at the Position  $\beta$  to a Nitrogen Center. *Angew. Chem., Int. Ed.* **2021**, *60*, 5843–5847.
- (153) Zou, X.; Li, Y.; Ke, Z.; Xu, S. Chiral Bidentate Boryl Ligand-Enabled Iridium-Catalyzed Enantioselective Dual C-H Borylation of Ferrocenes: Reaction Development and Mechanistic Insights. *ACS Catal.* **2022**, *12*, 1830–1840.
- (154) Bruch, A.; Fukazawa, A.; Yamaguchi, E.; Yamaguchi, S.; Studer, A. Bis(phosphoryl)-Bridged Biphenyls by Radical Phosphorylation: Synthesis and Photophysical and Electrochemical Properties. *Angew. Chem., Int. Ed.* **2011**, *50*, 12094–12098.
- (155) Rauch, F.; Fuchs, S.; Friedrich, A.; Sieh, D.; Krummenacher, I.; Braunschweig, H.; Finze, M.; Marder, T. B. Highly Stable, Readily Reducible, Fluorescent, Trifluoromethylated 9-Borafluorenes. *Eur. J. Chem.* **2020**, *26*, 12794–12808.
- (156) Narsaria, A. K.; Rauch, F.; Krebs, J.; Endres, P.; Friedrich, A.; Krummenacher, I.; Braunschweig, H.; Finze, M.; Nitsch, J.; Bickelhaupt, F. M.; Marder, T. B. Computationally Guided Molecular Design to Minimize the LE/CT Gap in D- $\pi$ -A Fluorinated Triarylboranes for Efficient TADF via D and  $\pi$ -Bridge Tuning. *Adv. Funct. Mater.* **2020**, *30*, 2002064.
- (157) Rauch, F.; Krebs, J.; Günther, J.; Friedrich, A.; Hähnel, M.; Krummenacher, I.; Braunschweig, H.; Finze, M.; Marder, T. B. Electronically Driven Regioselective Iridium-Catalyzed C-H Borylation of Donor- $\pi$ -Acceptor Chromophores Containing Triarylboron Acceptors. *Eur. J. Chem.* **2020**, *26*, 10626–10633.
- (158) Kurotobi, K.; Miyauchi, M.; Takakura, K.; Murafuji, T.; Sugihara, Y. Direct Introduction of a Boryl Substituent into the 2-Position of Azulene: Application of the Miyaura and Smith Methods to Azulene. *Eur. J. Org. Chem.* **2003**, *2003*, 3663–3665.
- (159) Fujinaga, M.; Murafuji, T.; Kurotobi, K.; Sugihara, Y. Polyborylation of azulenes. *Tetrahedron* **2009**, *65*, 7115–7121.
- (160) Nishimura, H.; Eliseeva, M. N.; Wakamiya, A.; Scott, L. T. 1,3,5,7-Tetra(Bpin)azulene by Exhaustive Direct Borylation of Azulene and 5,7-Di(Bpin)azulene by Selective Subsequent Deborylation. *Synlett* **2015**, *26*, 1578–1580.
- (161) Nishimura, H.; Ishida, N.; Shimazaki, A.; Wakamiya, A.; Saeki, A.; Scott, L. T.; Murata, Y. Hole-Transporting Materials with a Two-Dimensionally Expanded  $\pi$ -System around an Azulene Core for Efficient Perovskite Solar Cells. *J. Am. Chem. Soc.* **2015**, *137*, 15656–15659.
- (162) Ryota, O.; Kenji, Y.; Kenji, K. 2,7-Diborylanthracene as a Useful Building Block for Extended  $\pi$ -Conjugated Aromatics. *Chem. Lett.* **2011**, *40*, 941–943.
- (163) Takaki, Y.; Yoza, K.; Kobayashi, K. Fourfold C-H Borylation of Anthracene: 1,3,5,7-Tetraborylanthracene and Its Application to 1,3,5,7-Tetraarylanthracenes. *Chem. Lett.* **2017**, *46*, 655–658.
- (164) Kimoto, T.; Tanaka, K.; Sakai, Y.; Ohno, A.; Yoza, K.; Kobayashi, K. 2,8- and 2,9-Diboryltetracenes as Useful Building Blocks for Extended  $\pi$ -Conjugated Tetracenes. *Org. Lett.* **2009**, *11*, 3658–3661.
- (165) Hitosugi, S.; Nakamura, Y.; Matsuno, T.; Nakanishi, W.; Isobe, H. Iridium-Catalyzed Direct Borylation of Phenacenes. *Tetrahedron Lett.* **2012**, *53*, 1180–1182.
- (166) Figueira-Duarte, T. M.; Müllen, K. Pyrene-Based Materials for Organic Electronics. *Chem. Rev.* **2011**, *111*, 7260–7314.
- (167) Coventry, D. N.; Batsanov, A. S.; Goeta, A. E.; Howard, J. A. K.; Marder, T. B.; Perutz, R. N. Selective Ir-Catalyzed Borylation of Polycyclic Aromatic Hydrocarbons: Structures of Naphthalene-2,6-bis(boronate), Pyrene-2,7-bis(boronate) and Perylene-2,5,8,11-tetra(boronate) Esters. *Chem. Commun.* **2005**, 2172–2174.
- (168) Crawford, A. G.; Liu, Z.; Mkhaliid, I. A. I.; Thibault, M.-H.; Schwarz, N.; Alcaraz, G.; Steffen, A.; Collings, J. C.; Batsanov, A. S.; Howard, J. A. K.; Marder, T. B. Synthesis of 2- and 2,7-Functionalized Pyrene Derivatives: An Application of Selective C-H Borylation. *Eur. J. Chem.* **2012**, *18*, 5022–5035.

- (169) Ji, L.; Fucke, K.; Bose, S. K.; Marder, T. B. Iridium-Catalyzed Borylation of Pyrene: Irreversibility and the Influence of Ligand on Selectivity. *J. Org. Chem.* **2015**, *80*, 661–665.
- (170) Kano, H.; Uehara, K.; Matsuo, K.; Hayashi, H.; Yamada, H.; Aratani, N. Direct borylation of terrylene and quaterrylene. *Beilstein J. Org. Chem.* **2020**, *16*, 621–627.
- (171) Zhang, G.; Rominger, F.; Zschieschang, U.; Klauk, H.; Mastalerz, M. Facile Synthetic Approach to a Large Variety of Soluble Diarenoperylene. *Eur. J. Chem.* **2016**, *22*, 14840–14845.
- (172) Li, T.-Y.; Lin, Y.-C.; Song, Y.-H.; Lu, H.-F.; Chao, I.; Lin, C.-H. Synthesis and Physical Study of Perylene and Anthracene Polynitrile as Electron Acceptors. *Org. Lett.* **2019**, *21*, 5397–5401.
- (173) Würthner, F. Perylene Bisimide Dyes as Versatile Building Blocks for Functional Supramolecular Architectures. *Chem. Commun.* **2004**, 1564–1579.
- (174) Teraoka, T.; Hiroto, S.; Shinokubo, H. Iridium-Catalyzed Direct Tetraborylation of Perylene Bisimides. *Org. Lett.* **2011**, *13*, 2532–2535.
- (175) Battagliarin, G.; Li, C.; Enkelmann, V.; Müllen, K. 2,5,8,11-Tetraboronic Ester Perylenediimides: A Next Generation Building Block for Dye-Stuff Synthesis. *Org. Lett.* **2011**, *13*, 3012–3015.
- (176) Ito, S.; Hiroto, S.; Shinokubo, H. Facile Synthesis of Nitrogen-containing Polycyclic Aromatic Hydrocarbons from Perylene Bisimides. *Chem. Lett.* **2014**, *43*, 1309–1311.
- (177) García-Calvo, V.; Cuevas, J. V.; Barbero, H.; Ferrero, S.; Álvarez, C. M.; González, J. A.; Díaz de Greñu, B.; García-Calvo, J.; Torroba, T. Synthesis of a Tetracorannulene-perylenediimide That Acts as a Selective Receptor for C60 over C70. *Org. Lett.* **2019**, *21*, 5803–5807.
- (178) Fan, Y.; Ziabrev, K.; Zhang, S.; Lin, B.; Barlow, S.; Marder, S. R. Comparison of the Optical and Electrochemical Properties of Bi(perylenediimide)s Linked through Ortho and Bay Positions. *ACS Omega* **2017**, *2*, 377–385.
- (179) Tajima, K.; Fukui, N.; Shinokubo, H. Aggregation-Induced Emission of Nitrogen-Bridged Naphthalene Monoimide Dimers. *Org. Lett.* **2019**, *21*, 9516–9520.
- (180) Kaiser, R. P.; Ulč, J.; Čisářová, I.; Nečas, D. Direct regioselective C-H borylation of [5]helicene. *RSC Adv.* **2018**, *8*, 580–583.
- (181) Nečas, D.; Kaiser, R. P.; Ulč, J. Selective Borylation of [4]helicene. *Eur. J. Org. Chem.* **2016**, *2016*, 5647–5652.
- (182) Noguchi, H.; Hirose, T.; Yokoyama, S.; Matsuda, K. Fluorescence Behavior of 2,6,10-Trisubstituted 4,8,12-Triazatriangulene Cations in Solution and in the Solid State. *CrystEngComm* **2016**, *18*, 7377–7383.
- (183) Frédéric, L.; Fabri, B.; Guénée, L.; Zinna, F.; Di Bari, L.; Lacour, J. Triple Regioselective Functionalization of Cationic [4]helicenes via Iridium-Catalyzed Borylation and Suzuki Cross-Coupling Reactivity. *Eur. J. Chem.* **2022**, *28*, No. e202201853.
- (184) Peurifoy, S. R.; Castro, E.; Liu, F.; Zhu, X. Y.; Ng, F.; Jockusch, S.; Steigerwald, M. L.; Echegoyen, L.; Nuckolls, C.; Sisto, T. J. Three-Dimensional Graphene Nanostructures. *J. Am. Chem. Soc.* **2018**, *140*, 9341–9345.
- (185) Eliseeva, M. N.; Scott, L. T. Pushing the Ir-Catalyzed C-H Polyborylation of Aromatic Compounds to Maximum Capacity by Exploiting Reversibility. *J. Am. Chem. Soc.* **2012**, *134*, 15169–15172.
- (186) Kawasumi, K.; Zhang, Q.; Segawa, Y.; Scott, L. T.; Itami, K. A Grossly Warped Nanographene and the Consequences of Multiple Odd-Membered-Ring Defects. *Nat. Chem.* **2013**, *5*, 739–744.
- (187) Nagano, T.; Nakamura, K.; Tokimaru, Y.; Ito, S.; Miyajima, D.; Aida, T.; Nozaki, K. Functionalization of Azapentabenzocorannulenes by Fivefold C-H Borylation and Cross-Coupling Arylation: Application to Columnar Liquid-Crystalline Materials. *Eur. J. Chem.* **2018**, *24*, 14075–14078.
- (188) Kise, K.; Ooi, S.; Osuka, A.; Tanaka, T. Five-fold-symmetric Pentabromo- and Penta-iodo-corannulenes: Useful Precursors of Heteroatom-substituted Corannulenes. *Asian J. Org. Chem.* **2021**, *10*, 537–540.
- (189) Lin, H.-A.; Sato, Y.; Segawa, Y.; Nishihara, T.; Sugimoto, N.; Scott, L. T.; Higashiyama, T.; Itami, K. A Water-Soluble Warped Nanographene: Synthesis and Applications for Photoinduced Cell Death. *Angew. Chem., Int. Ed.* **2018**, *57*, 2874–2878.
- (190) Kato, K.; Lin, H.-A.; Kuwayama, M.; Nagase, M.; Segawa, Y.; Scott, L. T.; Itami, K. Two-Step Synthesis of a Red-Emissive Warped Nanographene Derivative via a Ten-Fold C-H Borylation. *Chem. Sci.* **2019**, *10*, 9038–9041.
- (191) Chiu, C.-Y.; Kim, B.; Gorodetsky, A. A.; Sattler, W.; Wei, S.; Sattler, A.; Steigerwald, M.; Nuckolls, C. Shape-shifting in contorted dibenzotetrathienocoronenes. *Chem. Sci.* **2011**, *2*, 1480–1486.
- (192) Yamaguchi, R.; Hiroto, S.; Shinokubo, H. Synthesis of Oxygen-Substituted Hexa-peri-hexabenzocoronenes through Ir-Catalyzed Direct Borylation. *Org. Lett.* **2012**, *14*, 2472–2475.
- (193) Yamaguchi, R.; Ito, S.; Lee, B. S.; Hiroto, S.; Kim, D.; Shinokubo, H. Functionalization of Hexa-peri-hexabenzocoronenes: Investigation of the Substituent Effects on a Superbenzene. *Chem.—Asian J.* **2013**, *8*, 178–190.
- (194) Oda, K.; Hiroto, S.; Hisaki, I.; Shinokubo, H. Synthesis of Bright Red-Emissive Dicyanoetheno-Bridged Hexa-Peri-Hexabenzocoronene Dimers. *Org. Biomol. Chem.* **2017**, *15*, 1426–1434.
- (195) Nagase, M.; Kato, K.; Yagi, A.; Segawa, Y.; Itami, K. Six-Fold C-H Borylation of Hexa-Peri-Hexabenzocoronene. *Beilstein J. Org. Chem.* **2020**, *16*, 391–397.
- (196) Plunkett, K. N.; Godula, K.; Nuckolls, C.; Tremblay, N.; Whalley, A. C.; Xiao, S. Expedient Synthesis of Contorted Hexabenzocoronenes. *Org. Lett.* **2009**, *11*, 2225–2228.
- (197) Kato, S.; Serizawa, Y.; Sakamaki, D.; Seki, S.; Miyake, Y.; Shinokubo, H. Diversity-Oriented Synthesis of Tetrathia[8]circulenes by Sequential C-H Borylation and Annulation. *Chem. Commun.* **2015**, *51*, 16944–16947.
- (198) Kato, S.; Akahori, S.; Serizawa, Y.; Lin, X.; Yamauchi, M.; Yagai, S.; Sakurai, T.; Matsuda, W.; Seki, S.; Shinokubo, H.; Miyake, Y. Systematic Synthesis of Tetrathia[8]circulenes: The Influence of Peripheral Substituents on the Structures and Properties in Solution and Solid States. *J. Org. Chem.* **2020**, *85*, 62–69.
- (199) Ikemoto, K.; Yoshii, A.; Izumi, T.; Taka, H.; Kita, H.; Xue, J. Y.; Kobayashi, R.; Sato, S.; Isobe, H. Modular Synthesis of Aromatic Hydrocarbon Macrocycles for Simplified, Single-Layer Organic Light-Emitting Devices. *J. Org. Chem.* **2016**, *81*, 662–666.
- (200) Ikemoto, K.; Kobayashi, R.; Sato, S.; Isobe, H. Synthesis and Bowl-in-Bowl Assembly of a Geodesic Phenylene Bowl. *Angew. Chem., Int. Ed.* **2017**, *56*, 6511–6514.
- (201) Ikemoto, K.; Lin, J.; Kobayashi, R.; Sato, S.; Isobe, H. Fluctuating Carbonaceous Networks with a Persistent Molecular Shape: A Saddle-Shaped Geodesic Framework of 1,3,5-Trisubstituted Benzene (Phenine). *Angew. Chem., Int. Ed.* **2018**, *57*, 8555–8559.
- (202) Sun, Z.; Mio, T.; Ikemoto, K.; Sato, S.; Isobe, H. Synthesis, Structures, and Assembly of Geodesic Phenine Frameworks with Isoreticular Networks of [n]Cyclo-para-phenylenes. *J. Org. Chem.* **2019**, *84*, 3500–3507.
- (203) Ikemoto, K.; Akiyoshi, M.; Mio, T.; Nishioka, K.; Sato, S.; Isobe, H. Synthesis of a Negatively Curved Nanocarbon Molecule with an Octagonal Omphalos via Design-of-Experiments Optimizations Supplemented by Machine Learning. *Angew. Chem., Int. Ed.* **2022**, *61*, No. e202204035.
- (204) Zhang, G.; Rominger, F.; Mastalerz, M. Fused  $\pi$ -Extended Truxenes via a Threefold Borylation as the Key Step. *Eur. J. Chem.* **2016**, *22*, 3084–3093.
- (205) Wagner, P.; Rominger, F.; Mastalerz, M. Switching the Statistical C3/C1 Ratio in the Threefold Aromatic Substitution of Tribenzotriquinacenes towards the C3 Isomer. *Angew. Chem., Int. Ed.* **2018**, *57*, 11321–11324.
- (206) Tomalia, D. A.; Baker, H.; Dewald, J.; Hall, M.; Kallos, G.; Martin, S.; Roeck, J.; Ryder, J.; Smith, P. A New Class of Polymers: Starburst-Dendritic Macromolecules. *Polym. J.* **1985**, *17*, 117–132.
- (207) Astruc, D.; Boisselier, E.; Ornelas, C. Dendrimers Designed for Functions: From Physical, Photophysical, and Supramolecular Properties to Applications in Sensing, Catalysis, Molecular Elec-

- tronics, Photonics, and Nanomedicine. *Chem. Rev.* **2010**, *110*, 1857–1959.
- (208) Burn, P. L.; Lo, S.-C.; Samuel, I. D. W. The Development of Light-Emitting Dendrimers for Displays. *Adv. Mater.* **2007**, *19*, 1675–1688.
- (209) Finke, A. D.; Moore, J. S. Iterative Synthesis of 1,3,5-Polyphenylene Dendrons via C-H Activation. *Org. Lett.* **2008**, *10*, 4851–4854.
- (210) Iwade, N.; Suginome, M. Synthesis of Masked Haloareneboronic Acids via Iridium-Catalyzed Aromatic C-H Borylation with 1,8-Naphthalenediaminoborane (danBH). *J. Organomet. Chem.* **2009**, *694*, 1713–1717.
- (211) Rauch, F.; Endres, P.; Friedrich, A.; Sieh, D.; Hähnel, M.; Krummenacher, I.; Braunschweig, H.; Finze, M.; Ji, L.; Marder, T. B. An Iterative Divergent Approach to Conjugated Starburst Borane Dendrimers. *Eur. J. Chem.* **2020**, *26*, 12951–12963.
- (212) Masuda, R.; Kuwano, S.; Goto, K. Late-Stage Functionalization of the Periphery of Oligophenylene Dendrimers with Various Arene Units via Fourfold C-H Borylation. *J. Org. Chem.* **2021**, *86*, 14433–14443.
- (213) Kondo, Y.; García-Cuadrado, D.; Hartwig, J. F.; Boalen, N. K.; Wagner, N. L.; Hillmyer, M. A. Rhodium-Catalyzed, Regiospecific Functionalization of Polyolefins in the Melt. *J. Am. Chem. Soc.* **2002**, *124*, 1164–1165.
- (214) Bae, C.; Hartwig, J. F.; Boalen Harris, N. K.; Long, R. O.; Anderson, K. S.; Hillmyer, M. A. Catalytic Hydroxylation of Polypropylenes. *J. Am. Chem. Soc.* **2005**, *127*, 767–776.
- (215) Bae, C. S.; Hartwig, J. F.; Chung, H. Y.; Harris, N. K.; Switek, K. A.; Hillmyer, M. A. Regiospecific Side-Chain Functionalization of Linear Low-Density Polyethylene with Polar Groups. *Angew. Chem., Int. Ed.* **2005**, *44*, 6410–6413.
- (216) Shin, J.; Jensen, S. M.; Ju, J.; Lee, S.; Xue, Z.; Noh, S. K.; Bae, C. Controlled Functionalization of Crystalline Polystyrenes via Activation of Aromatic C-H Bonds. *Macromolecules* **2007**, *40*, 8600–8608.
- (217) Shin, J.; Chang, A. Y.; Brownell, L. V.; Racoma, I. O.; Ozawa, C. H.; Chung, H.-Y.; Peng, S.; Bae, C. Hydrophilic graft modification of a commercial crystalline polyolefin. *J. Polym. Sci., Part A: Polym. Chem.* **2008**, *46*, 3533–3545.
- (218) Jo, T. S.; Kim, S. H.; Shin, J.; Bae, C. Highly Efficient Incorporation of Functional Groups into Aromatic Main-Chain Polymer Using Iridium-Catalyzed C-H Activation and Suzuki-Miyaura Reaction. *J. Am. Chem. Soc.* **2009**, *131*, 1656–1657.
- (219) Chang, Y.; Lee, H. H.; Kim, S. H.; Jo, T. S.; Bae, C. Scope and Regioselectivity of Iridium-Catalyzed C-H Borylation of Aromatic Main-Chain Polymers. *Macromolecules* **2013**, *46*, 1754–1764.
- (220) Varnado, C. D.; Zhao, X.; Ortiz, M.; Zuo, Z.; Jiang, Z.; Manthiram, A.; Bielawski, C. W. Pyridine- and Pyrimidine-Functionalized Poly(sulfone)s: Performance-Enhancing Crosslinkers for Acid/Base Blend Proton Exchange Membranes Used in Direct Methanol Fuel Cells. *ACS Adv.* **2013**, *4*, 2167–2176.
- (221) Feng, D.; Mishra, S.; Munyaneza, N. E.; Kundu, S.; Scott, C. N. Facile Transformation of Poly(phenyl ether) by C-H Borylation: A Viable Method to New Aromatic Materials. *Eur. Polym. J.* **2021**, *158*, 110687.
- (222) Loudet, A.; Burgess, K. BODIPY Dyes and Their Derivatives: Syntheses and Spectroscopic Properties. *Chem. Rev.* **2007**, *107*, 4891–4932.
- (223) Ulrich, G.; Ziesel, R.; Harriman, A. The Chemistry of Fluorescent Bodipy Dyes: Versatility Unsurpassed. *Angew. Chem., Int. Ed.* **2008**, *47*, 1184–1201.
- (224) Chen, J.; Mizumura, M.; Shinokubo, H.; Osuka, A. Functionalization of Boron Dipyrin (BODIPY) Dyes through Iridium and Rhodium Catalysis: A Complementary Approach to  $\alpha$ - and  $\beta$ -Substituted BODIPYs. *Eur. J. Chem.* **2009**, *15*, 5942–5949.
- (225) Kadish, K.; Smith, K. M.; Guillard, R. *The Porphyrin Handbook*, Vol. 3; Elsevier, 2000.
- (226) Hata, H.; Shinokubo, H.; Osuka, A. Highly Regioselective Ir-Catalyzed  $\beta$ -Borylation of Porphyrins via C-H Bond Activation and Construction of  $\beta$ - $\beta$ -Linked Diporphyrin. *J. Am. Chem. Soc.* **2005**, *127*, 8264–8265.
- (227) Baba, H.; Chen, J.; Shinokubo, H.; Osuka, A. Efficient Rhodium-Catalyzed Installation of Unsaturated Ester Functions onto Porphyrins: Site-Specific Heck-Type Addition versus Conjugate Addition. *Eur. J. Chem.* **2008**, *14*, 4256–4262.
- (228) Chen, J.; Aratani, N.; Shinokubo, H.; Osuka, A. Post-Modification of meso-meso-Linked Porphyrin Arrays by Iridium and Rhodium Catalysts for Tuning of Energy Gap. *Chem.—Asian J.* **2009**, *4*, 1126–1133.
- (229) Hisaki, I.; Hiroto, S.; Kim, K. S.; Noh, S. B.; Kim, D.; Shinokubo, H.; Osuka, A. Synthesis of Doubly  $\beta$ -to- $\beta$  1,3-Butadiyne-Bridged Diporphyrins: Enforced Planar Structures and Large Two-Photon Absorption Cross Sections. *Angew. Chem., Int. Ed.* **2007**, *46*, 5125–5128.
- (230) Song, J.; Jang, S. Y.; Yamaguchi, S.; Sankar, J.; Hiroto, S.; Aratani, N.; Shin, J.-Y.; Easwaramoorthi, S.; Kim, K. S.; Kim, D.; Shinokubo, H.; Osuka, A. 2,5-Thienylene-Bridged Triangular and Linear Porphyrin Trimers. *Angew. Chem., Int. Ed.* **2008**, *47*, 6004–6007.
- (231) Park, J. K.; Lee, H. R.; Chen, J.; Shinokubo, H.; Osuka, A.; Kim, D. Photoelectrochemical Properties of Doubly  $\beta$ -Functionalized Porphyrin Sensitizers for Dye-Sensitized Nanocrystalline-TiO<sub>2</sub> Solar Cells. *J. Phys. Chem. C* **2008**, *112*, 16691–16699.
- (232) Park, J. K.; Chen, J.; Lee, H. R.; Park, S. W.; Shinokubo, H.; Osuka, A.; Kim, D. Doubly  $\beta$ -Functionalized Meso-Meso Directly Linked Porphyrin Dimer Sensitizers for Photovoltaics. *J. Phys. Chem. C* **2009**, *113*, 21956–21963.
- (233) Song, J.; Aratani, N.; Kim, P.; Kim, D.; Shinokubo, H.; Osuka, A. Porphyrin “Lego Block” Strategy To Construct Directly meso- $\beta$  Doubly Linked Porphyrin Rings. *Angew. Chem., Int. Ed.* **2010**, *49*, 3617–3620.
- (234) Song, J.; Kim, P.; Aratani, N.; Kim, D.; Shinokubo, H.; Osuka, A. Strategic Synthesis of 2,6-Pyridylene-Bridged  $\beta$ -to- $\beta$  Porphyrin Nanorings through Cross-Coupling. *Eur. J. Chem.* **2010**, *16*, 3009–3012.
- (235) Song, J.; Aratani, N.; Shinokubo, H.; Osuka, A. A  $\beta$ -to- $\beta$  2,5-Thienylene-Bridged Cyclic Porphyrin Tetramer: its Rational Synthesis and 1:2 Binding Mode with C60. *Chem. Sci.* **2011**, *2*, 748–751.
- (236) Song, J.; Aratani, N.; Shinokubo, H.; Osuka, A. A Porphyrin Nanobarrel That Encapsulates C60. *J. Am. Chem. Soc.* **2010**, *132*, 16356–16357.
- (237) Wang, K.; Liu, P.; Zhang, F.; Xu, L.; Zhou, M.; Nakai, A.; Kato, K.; Furukawa, K.; Tanaka, T.; Osuka, A.; Song, J. A Robust Porphyrin-Stabilized Triplet Carbon Diradical. *Angew. Chem., Int. Ed.* **2021**, *60*, 7002–7006.
- (238) Fukui, N.; Kim, T.; Kim, D.; Osuka, A. Porphyrin Arch-Tapes: Synthesis, Contorted Structures, and Full Conjugation. *J. Am. Chem. Soc.* **2017**, *139*, 9075–9088.
- (239) Yamaguchi, S.; Katoh, T.; Shinokubo, H.; Osuka, A. Porphyrin Pincer Complexes: Peripherally Cyclometalated Porphyrins and Their Catalytic Activities Controlled by Central Metals. *J. Am. Chem. Soc.* **2007**, *129*, 6392–6393.
- (240) Song, J.; Aratani, N.; Heo, J. H.; Kim, D.; Shinokubo, H.; Osuka, A. Directly Pd(II)-Bridged Porphyrin Belts with Remarkable Curvatures. *J. Am. Chem. Soc.* **2010**, *132*, 11868–11869.
- (241) Yamaguchi, S.; Katoh, T.; Shinokubo, H.; Osuka, A. Pt(II)- and Pt(IV)-Bridged Cofacial Diporphyrins via Carbon-Transition Metal  $\sigma$ -Bonds. *J. Am. Chem. Soc.* **2008**, *130*, 14440–14441.
- (242) Yamaguchi, S.; Shinokubo, H.; Osuka, A. Double Cleavage of sp<sup>2</sup> C-H and sp<sup>3</sup> C-H Bonds on One Metal Center: DMF-Appended Cyclometalated Platinum(II) and -(IV) Porphyrins. *Inorg. Chem.* **2009**, *48*, 795–797.
- (243) Yamaguchi, S.; Shinokubo, H.; Osuka, A.  $\eta^2$ -Porphyrin Ru(II)  $\pi$  Complexes. *J. Am. Chem. Soc.* **2010**, *132*, 9992–9993.
- (244) Yoshida, K.; Yamaguchi, S.; Osuka, A.; Shinokubo, H. Platinum(II) and Platinum(IV) Porphyrin Pincer Complexes: Synthesis, Structures, and Reactivity. *Organometallics* **2010**, *29*, 3997–4000.

- (245) Yamamoto, J.; Shimizu, T.; Yamaguchi, S.; Aratani, N.; Shinokubo, H.; Osuka, A. Synthesis of a Diimidazolylporphyrin Pincer Palladium Complex. *J. Porphyr. Phthalocyanines* **2011**, *15*, 534–538.
- (246) Hiroto, S.; Hisaki, I.; Shinokubo, H.; Osuka, A. Synthesis of Directly and Doubly Linked Dioxoisobacteriochlorin Dimers. *J. Am. Chem. Soc.* **2008**, *130*, 16172–16173.
- (247) Hata, H.; Yamaguchi, S.; Mori, G.; Nakazono, S.; Katoh, T.; Takatsu, K.; Hiroto, S.; Shinokubo, H.; Osuka, A. Regioselective Borylation of Porphyrins by C-H Bond Activation under Iridium Catalysis to Afford Useful Building Blocks for Porphyrin Assemblies. *Chem.—Asian J.* **2007**, *2*, 849–859.
- (248) Ghosh, A.; Steene, E. High-Valent Transition Metal Centers Versus Noninnocent Ligands in Metalloporphyrins: Insights from Electrochemistry and Implications for High-Valent Heme Protein Intermediates. *J. Inorg. Biochem.* **2002**, *91*, 423–436.
- (249) Aviv-Harel, I.; Gross, Z. Aura of Corroles. *Eur. J. Chem.* **2009**, *15*, 8382–8394.
- (250) Hiroto, S.; Hisaki, I.; Shinokubo, H.; Osuka, A. Synthesis of Corrole Derivatives through Regioselective Ir-Catalyzed Direct Borylation. *Angew. Chem., Int. Ed.* **2005**, *44*, 6763–6766.
- (251) Hiroto, S.; Furukawa, K.; Shinokubo, H.; Osuka, A. Synthesis and Biradicaloid Character of Doubly Linked Corrole Dimers. *J. Am. Chem. Soc.* **2006**, *128*, 12380–12381.
- (252) Cho, S.; Lim, J. M.; Hiroto, S.; Kim, P.; Shinokubo, H.; Osuka, A.; Kim, D. Unusual Interchromophoric Interactions in  $\beta,\beta'$  Directly and Doubly Linked Corrole Dimers: Prohibited Electronic Communication and Abnormal Singlet Ground States. *J. Am. Chem. Soc.* **2009**, *131*, 6412–6420.
- (253) Claessens, C. G.; González-Rodríguez, D.; Rodríguez-Morgade, M. S.; Medina, A.; Torres, T. Subphthalocyanines, Subporphyrins, and Subporphyrins: Singular Nonplanar Aromatic Systems. *Chem. Rev.* **2014**, *114*, 2192–2277.
- (254) Shimizu, S. Recent Advances in Subporphyrins and Triphyrin Analogues: Contracted Porphyrins Comprising Three Pyrrole Rings. *Chem. Rev.* **2017**, *117*, 2730–2784.
- (255) Kitano, M.; Okuda, Y.; Tsurumaki, E.; Tanaka, T.; Yorimitsu, H.; Osuka, A.  $\beta,\beta'$ -Diborylated Subporphyrinato Boron(III) Complexes as Useful Synthetic Precursors. *Angew. Chem., Int. Ed.* **2015**, *54*, 9275–9279.
- (256) Morimoto, Y.; Osuka, A.; Tanaka, T. Synthesis, Properties and Reactivity of an ortho-Phenylene-Cyclopentene-Bridged Tetrapyrrole. *J. Porphyr. Phthalocyanines* **2021**, *25*, 937–943.
- (257) Morimoto, Y.; Chen, F.; Matsuo, Y.; Kise, K.; Tanaka, T.; Osuka, A. Improved Synthesis of ortho-Phenylene-bridged Cyclic Tetrapyrroles and Oxidative Fusion Reactions Toward Substituted Tetraaza[8]circulenes. *Chem.—Asian J.* **2021**, *16*, 648–655.
- (258) Matsuo, Y.; Kise, K.; Morimoto, Y.; Osuka, A.; Tanaka, T. Fold-in Synthesis of a Pentabenzopentaaza[10]circulene. *Angew. Chem., Int. Ed.* **2022**, *61*, No. e202116789.
- (259) Rao, Y.; Kim, T.; Park, K. H.; Peng, F.; Liu, L.; Liu, Y.; Wen, B.; Liu, S.; Kirk, S. R.; Wu, L.; Chen, B.; Ma, M.; Zhou, M.; Yin, B.; Zhang, Y.; Kim, D.; Song, J.  $\pi$ -Extended “Earring” Porphyrins with Multiple Cavities and Near-Infrared Absorption. *Angew. Chem., Int. Ed.* **2016**, *55*, 6438–6442.
- (260) Wu, L.; Li, F.; Rao, Y.; Wen, B.; Xu, L.; Zhou, M.; Tanaka, T.; Osuka, A.; Song, J. Synthesis, Structures, and Near-IR Absorption of Heterole-Fused Earring Porphyrins. *Angew. Chem., Int. Ed.* **2019**, *58*, 8124–8128.
- (261) Mori, G.; Shinokubo, H.; Osuka, A. Highly Selective Ir-Catalyzed Direct Sixfold Borylation of Peripheral Aromatic Substituents on Hexakisaryl-Substituted [28]Hexaphyrin(1.1.1.1.1.1). *Tetrahedron Lett.* **2008**, *49*, 2170–2172.
- (262) Nakamura, S.; Hiroto, S.; Shinokubo, H. Synthesis and oxidation of cyclic tetraindole. *Chem. Sci.* **2012**, *3*, 524–527.
- (263) Nakamura, S.; Kondo, T.; Hiroto, S.; Shinokubo, H. Porphyrin Analogues That Consist of Indole, Benzofuran, and Benzothiophene Subunits. *Asian J. Org. Chem.* **2013**, *2*, 312–319.
- (264) *Handbook of Thiophene-Based Materials*; Perepichka, I. F., Perepichka, D. F., Eds.; Wiley, 2009.
- (265) Maegawa, Y.; Inagaki, S. Iridium-Bipyridine Periodic Mesoporous Organosilica Catalyzed Direct C-H Borylation using a Pinacolborane. *Dalton Trans.* **2015**, *44*, 13007–13016.
- (266) Osaka, I.; Abe, T.; Mori, H.; Saito, M.; Takemura, N.; Koganezawa, T.; Takimiya, K. Small band gap polymers incorporating a strong acceptor, thieno[3,2-b]thiophene-2,5-dione, with p-channel and bipolar charge transport characteristics. *J. Mater. Chem. C* **2014**, *2*, 2307–2312.
- (267) Nakano, M.; Shinamura, S.; Sugimoto, R.; Osaka, I.; Miyazaki, E.; Takimiya, K. Borylation on Benzo[1,2-b:4,5-b']- and Naphtho[1,2-b:5,6-b']dichalcogenophenes: Different Chalcogen Atom Effects on Borylation Reaction Depending on Fused Ring Structure. *Org. Lett.* **2012**, *14*, 5448–5451.
- (268) Shinamura, S.; Sugimoto, R.; Yanai, N.; Takemura, N.; Kashiki, T.; Osaka, I.; Miyazaki, E.; Takimiya, K. Orthogonally Functionalized Naphthodithiophenes: Selective Protection and Borylation. *Org. Lett.* **2012**, *14*, 4718–4721.
- (269) Osaka, I.; Komatsu, K.; Koganezawa, T.; Takimiya, K. 5,10-Linked Naphthodithiophenes as the Building Block for Semiconducting Polymers. *Sci. Technol. Adv. Mater.* **2014**, *15*, 024201.
- (270) Kawashima, K.; Miyazaki, E.; Shimawaki, M.; Inoue, Y.; Mori, H.; Takemura, N.; Osaka, I.; Takimiya, K. 5,10-Diborylated Naphtho[1,2-c:5,6-c']bis[1,2,5]thiadiazole: a Ready-to-use Precursor for the Synthesis of High-Performance Semiconducting Polymers. *Polym. Chem.* **2013**, *4*, 5224–5227.
- (271) Osaka, I.; Takimiya, K. Naphthobischalcogenadiazole Conjugated Polymers: Emerging Materials for Organic Electronics. *Adv. Mater.* **2017**, *29*, 1605218.
- (272) Kurosawa, T.; Okamoto, T.; Cen, D.; Ikeda, D.; Ishii, H.; Takeya, J. Chrysenodithiophene-Based Conjugated Polymer: An Elongated Fused  $\pi$ -Electronic Backbone with a Unique Orbital Structure Toward Efficient Intermolecular Carrier Transport. *Macromolecules* **2021**, *54*, 2113–2123.
- (273) Chen, Y.; Yekta, S.; Yudin, A. K. Modified BINOL Ligands in Asymmetric Catalysis. *Chem. Rev.* **2003**, *103*, 3155–3212.
- (274) Brunel, J. M. BINOL: A Versatile Chiral Reagent. *Chem. Rev.* **2005**, *105*, 857–898.
- (275) Ahmed, I.; Clark, D. A. Rapid Synthesis of 3,3' Bis-Arylated BINOL Derivatives Using a C-H Borylation in Situ Suzuki-Miyaura Coupling Sequence. *Org. Lett.* **2014**, *16*, 4332–4335.
- (276) Bisht, R.; Chaturvedi, J.; Pandey, G.; Chattopadhyay, B. Double-Fold Ortho and Remote C-H Bond Activation/Borylation of BINOL: A Unified Strategy for Arylation of BINOL. *Org. Lett.* **2019**, *21*, 6476–6480.
- (277) Datta, A.; Köllhofer, A.; Plenio, H. Ir-Catalyzed C-H Activation in the Synthesis of Borylated Ferrocenes and Half-Sandwich Compounds. *Chem. Commun.* **2004**, 1508–1509.
- (278) Wright, S. E.; Richardson-Solorzano, S.; Stewart, T. N.; Miller, C. D.; Morris, K. C.; Daley, C. J. A.; Clark, T. B. Accessing Amphiphilic Phosphine Boronates through C-H Borylation by an Unforeseen Cationic Iridium Complex. *Angew. Chem., Int. Ed.* **2019**, *58*, 2834–2838.
- (279) Morris, K. C.; Wright, S. E.; Meyer, G. F.; Clark, T. B. Phosphine-Directed  $sp^3$  C-H, C-O, and C-N Borylation. *J. Org. Chem.* **2020**, *85*, 14795–14801.
- (280) Fukuda, K.; Iwasawa, N.; Takaya, J. Ruthenium-Catalyzed ortho C-H Borylation of Arylphosphines. *Angew. Chem., Int. Ed.* **2019**, *58*, 2850–2853.
- (281) Wen, J.; Wang, D.; Qian, J.; Wang, D.; Zhu, C.; Zhao, Y.; Shi, Z. Rhodium-Catalyzed PIII-Directed ortho-C-H Borylation of Arylphosphines. *Angew. Chem., Int. Ed.* **2019**, *58*, 2078–2082.
- (282) Kuninobu, Y.; Ida, H.; Nishi, M.; Kanai, M. A meta-selective C-H borylation directed by a secondary interaction between ligand and substrate. *Nat. Chem.* **2015**, *7*, 712–717.
- (283) Wang, J.; Torigoe, T.; Kuninobu, Y. Hydrogen-Bond-Controlled Formal meta-Selective C-H Transformations and Regioselective Synthesis of Multisubstituted Aromatic Compounds. *Org. Lett.* **2019**, *21*, 1342–1346.

(284) Xu, F.; Duke, O. M.; Rojas, D.; Eichelberger, H. M.; Kim, R. S.; Clark, T. B.; Watson, D. A. Arylphosphonate-Directed Ortho C-H Borylation: Rapid Entry into Highly-Substituted Phosphoarenes. *J. Am. Chem. Soc.* **2020**, *142*, 11988–11992.

(285) Genov, G. R.; Douthwaite, J. L.; Lahdenperä, A. S. K.; Gibson, D. C.; Phipps, R. J. Enantioselective Remote C-H Activation Directed by a Chiral Cation. *Science* **2020**, *367*, 1246–1251.

(286) Song, S.-Y.; Li, Y.; Ke, Z.; Xu, S. Iridium-Catalyzed Enantioselective C-H Borylation of Diarylphosphinates. *ACS Catal.* **2021**, *11*, 13445–13451.

(287) Zou, X.; Zhao, H.; Li, Y.; Gao, Q.; Ke, Z.; Xu, S. Chiral Bidentate Boryl Ligand Enabled Iridium-Catalyzed Asymmetric C(sp<sup>2</sup>)-H Borylation of Diarylmethylamines. *J. Am. Chem. Soc.* **2019**, *141*, 5334–5342.

(288) Yoshidomi, T.; Fukushima, T.; Itami, K.; Segawa, Y. Synthesis, Structure, and Electrochemical Property of a Bimetallic Bis-2-pyridylidene Palladium Acetate Complex. *Chem. Lett.* **2017**, *46*, 587–590.

(289) Feng, Y.; Holte, D.; Zoller, J.; Umemiya, S.; Simke, L. R.; Baran, P. S. Total Synthesis of Verruculogen and Fumitremorgin A Enabled by Ligand-Controlled C–H Borylation. *J. Am. Chem. Soc.* **2015**, *137* (32), 10160–10163.

(290) Liao, X.; Stanley, L. M.; Hartwig, J. F. Enantioselective Total Syntheses of (–)-Taiwaniaquinone H and (–)-Taiwaniaquinol B by Iridium-Catalyzed Borylation and Palladium-Catalyzed Asymmetric  $\alpha$ -Arylation. *J. Am. Chem. Soc.* **2011**, *133* (7), 2088–2091.

(291) Crawford, K. M.; Ramseyer, T. R.; Daley, C. J. A.; Clark, T. B. Phosphine-Directed C–H Borylation Reactions: Facile and Selective Access to Ambiphilic Phosphine Boronate Esters. *Angew. Chem. Int. Ed.* **2014**, *53*, 7589–7593.